

Electrocatalytic reduction of CO₂ to CO by a Series of organometallic Re(I)-tpy complexes

*Shriya Saha^a, Thomas Doughty^b, Dibyendu Banerjee^c, Sunil K. Patel^a, Dibyendu Mallick^{*c}, E. Siva Subramaniam Iyer^a, Souvik Roy^{*b}, Raja Mitra^{*a}*

^a*School of Chemical and Materials Sciences, Indian Institute of Technology Goa, Farmagudi, Goa 403401, India. Email: rajamitra@iitgoa.ac.in*

^b*School of Chemistry, University of Lincoln, Green Lane, Lincoln, Lincolnshire, LN6 7DL, UK. Email: sroy@lincoln.ac.uk*

^c*Department of Chemistry, Presidency University, Kolkata 700073, India. Email: dibyendu.chem@presiuniv.ac.in*

Table of content:

Topics	Page number
<i>Characterisation of L2</i>	S3-S5
<i>Characterisation of L3</i>	S6-S8
<i>Characterisation of L4</i>	S9-S11
<i>Characterisation of L5</i>	S12-S14
<i>Characterisation of Re1</i>	S15-S18
<i>Characterisation of Re2</i>	S19-S22
<i>Characterisation of Re3</i>	S23-S26
<i>Characterisation of Re4</i>	S27-S30
<i>Characterisation of Re5</i>	S31-S37
<i>ATR-IR comparison study</i>	S38
<i>Stability of the metal complexes in acetonitrile monitored by UV-Vis</i>	S39
<i>TD-DFT study of Re1-5</i>	S40-S44
<i>Transient Absorption studies of Re1-5 and L5</i>	S45-S49
<i>Scan rate-dependent Cyclic Voltammograms of Re1-5</i>	S49-S51
<i>Diffusion coefficients for Re1-5 and Re7</i>	S52
<i>Fast scan rate-dependent Cyclic Voltammograms of Re1-5 and Re7</i>	S53
<i>Catalytic Cyclic Voltammograms of Re1-5 and Re7 in absence and presence of trifluoroethanol</i>	S53
<i>Catalytic Cyclic Voltammograms of Re1-5 at fast scan rates</i>	S54
<i>Representative Cyclic Voltammogram of Re2 for i_{cat} and i_p determination</i>	S54
<i>Cyclic Voltammogram of Re2 under different scan rates</i>	S55
<i>Cyclic Voltammogram of Re3 and Re4 showing effect of water on electrocatalysis</i>	S55
<i>Cyclic Voltammogram of Re2 under N_2 and CO_2 with varying amount of trifluoroethanol</i>	S56
<i>Fast scan Cyclic Voltammograms of Re2 with varying amount of trifluoroethanol</i>	S56
<i>Controlled potential electrolysis (CPE) of Re1-5 in CO_2</i>	S57
<i>Stability studies after CPE Re5, Re1 and Re2 by UV-Vis</i>	S57-58
<i>Rinse test</i>	S59
<i>References</i>	S59
<i>Cartesian coordinates for L1-5 and Re1-5</i>	S60-S69

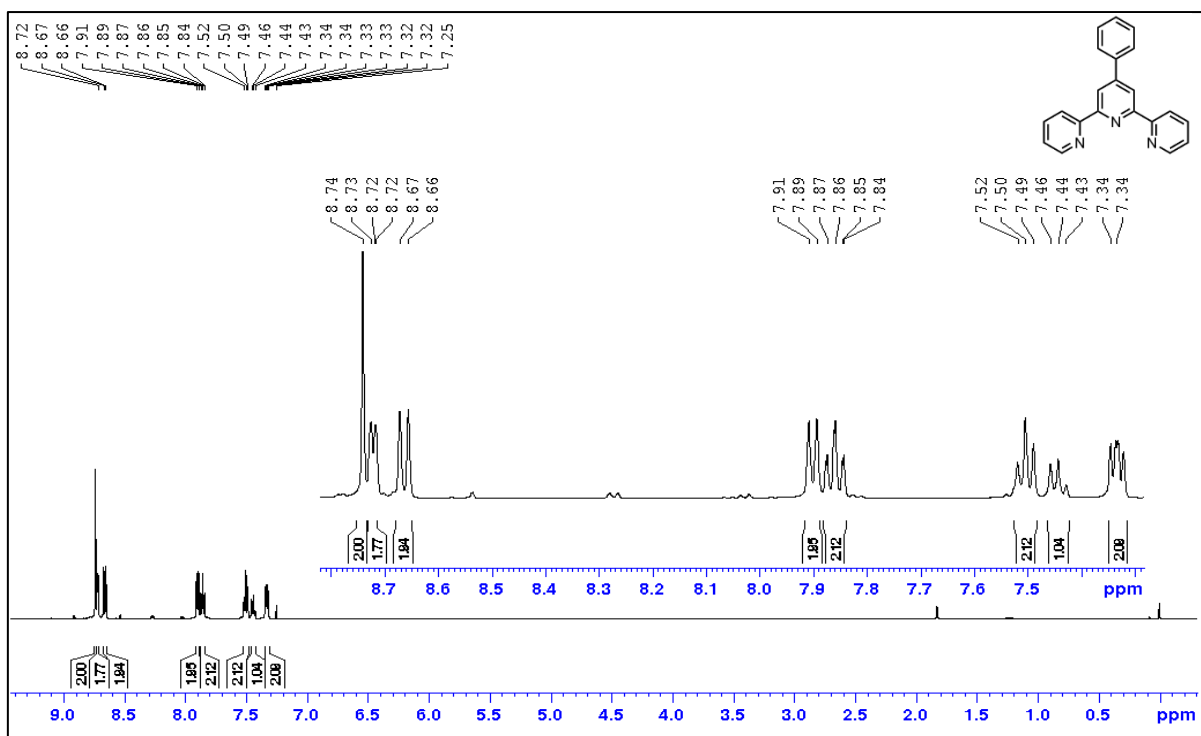


Figure S1a: ^1H NMR spectrum of L2 (500 MHz, CDCl_3).

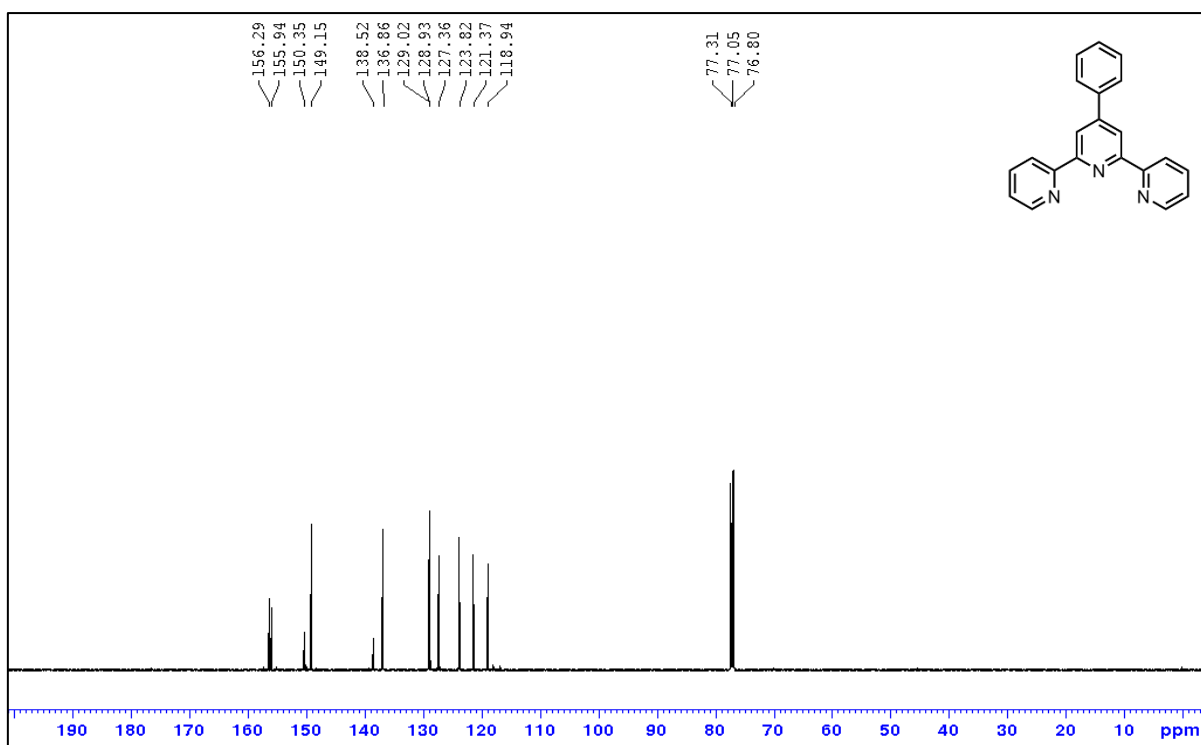


Figure S1b: $^{13}\text{C}\{^1\text{H}\}$ NMR spectrum of L2 (125 MHz, CDCl_3).

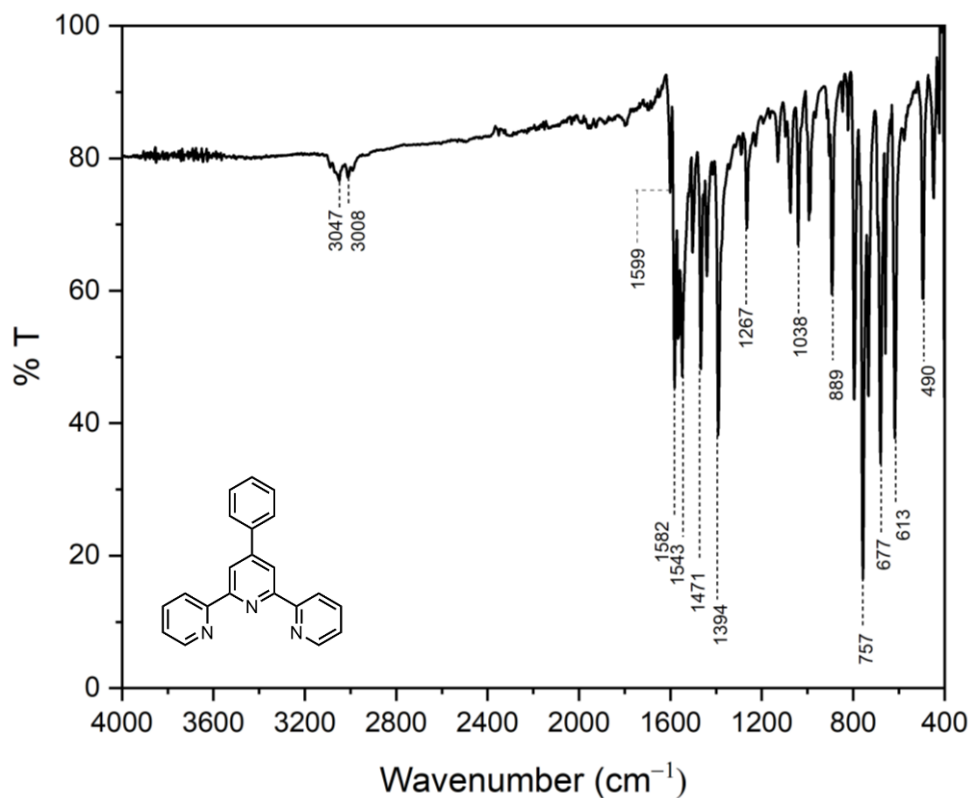


Figure S1c: ATR-IR spectrum of L2.

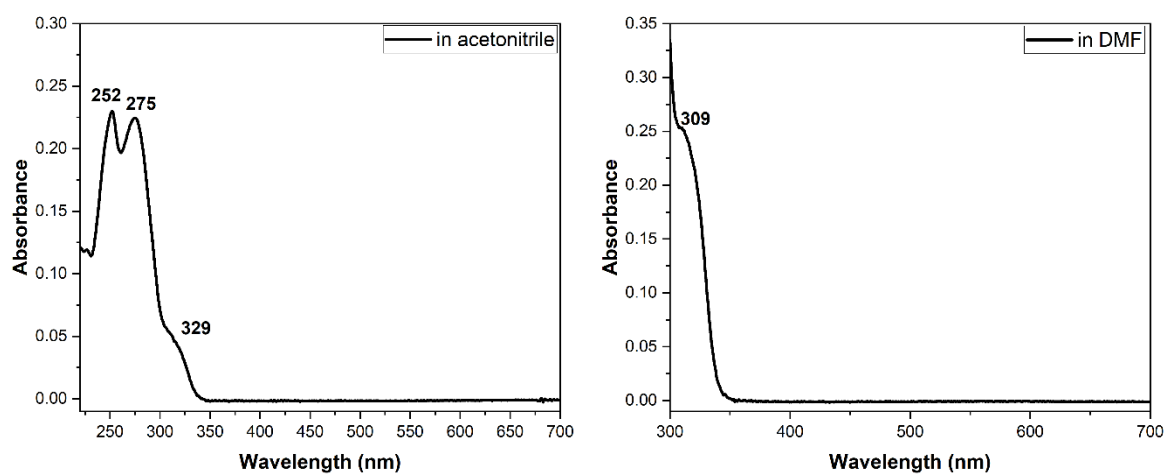


Figure S1d: Absorbance spectra of L2 (0.01 mM) in acetonitrile and DMF.

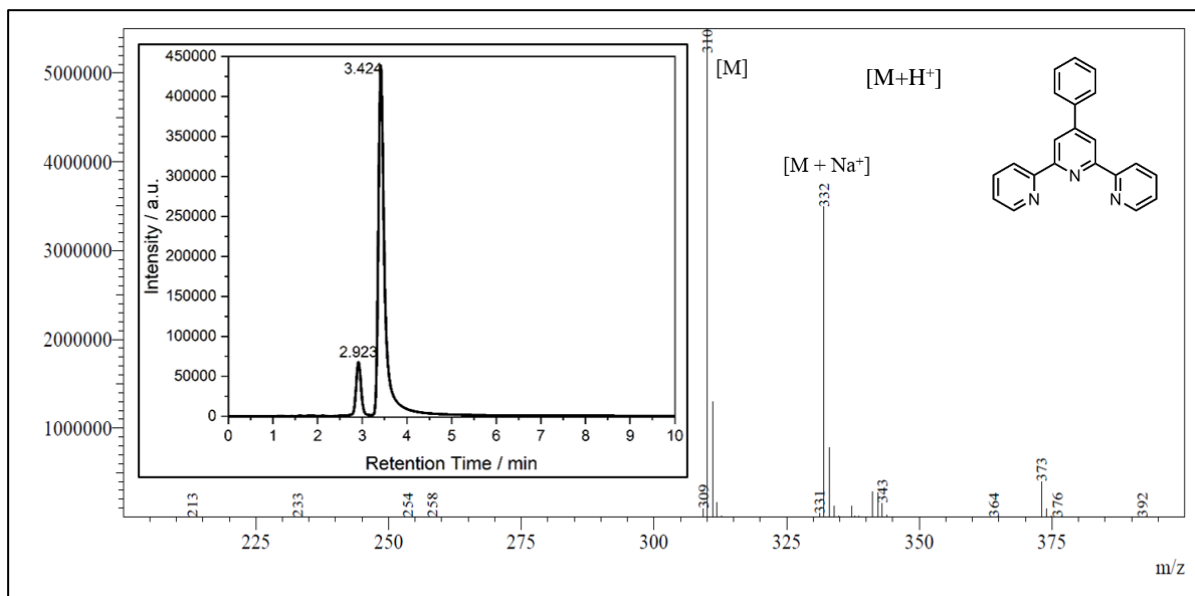


Figure S1e: LC-MS spectrum of **L2**, mass values shown at 3.424 min; Mass fragmentation pattern for **L2** [$C_{21}H_{15}N_3 = M$]; $m/z = 310$ [$M+H$]⁺ ($C_{21}H_{16}N_3$), $m/z = 332$ [$M+Na$]⁺ ($C_{21}H_{16}N_3Na$).

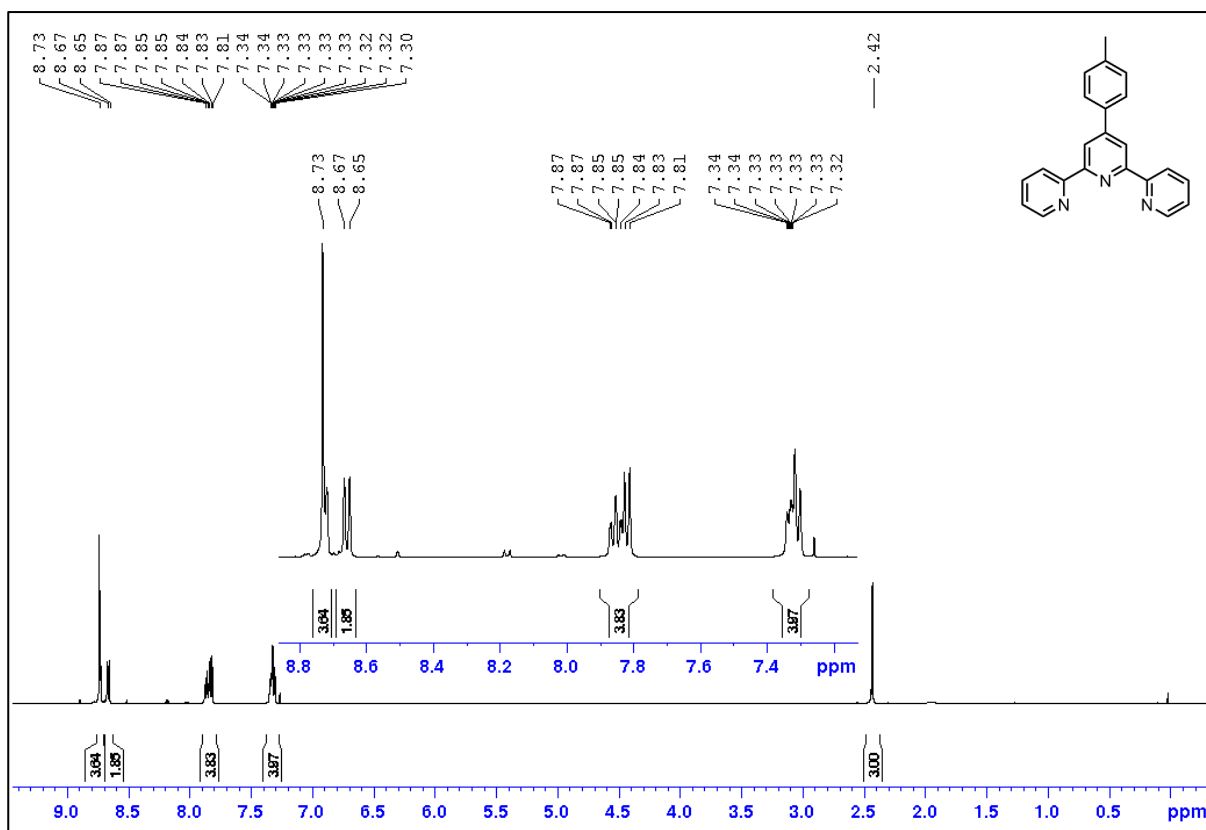


Figure S2a: ^1H NMR spectrum of **L3** (500 MHz, CDCl_3).

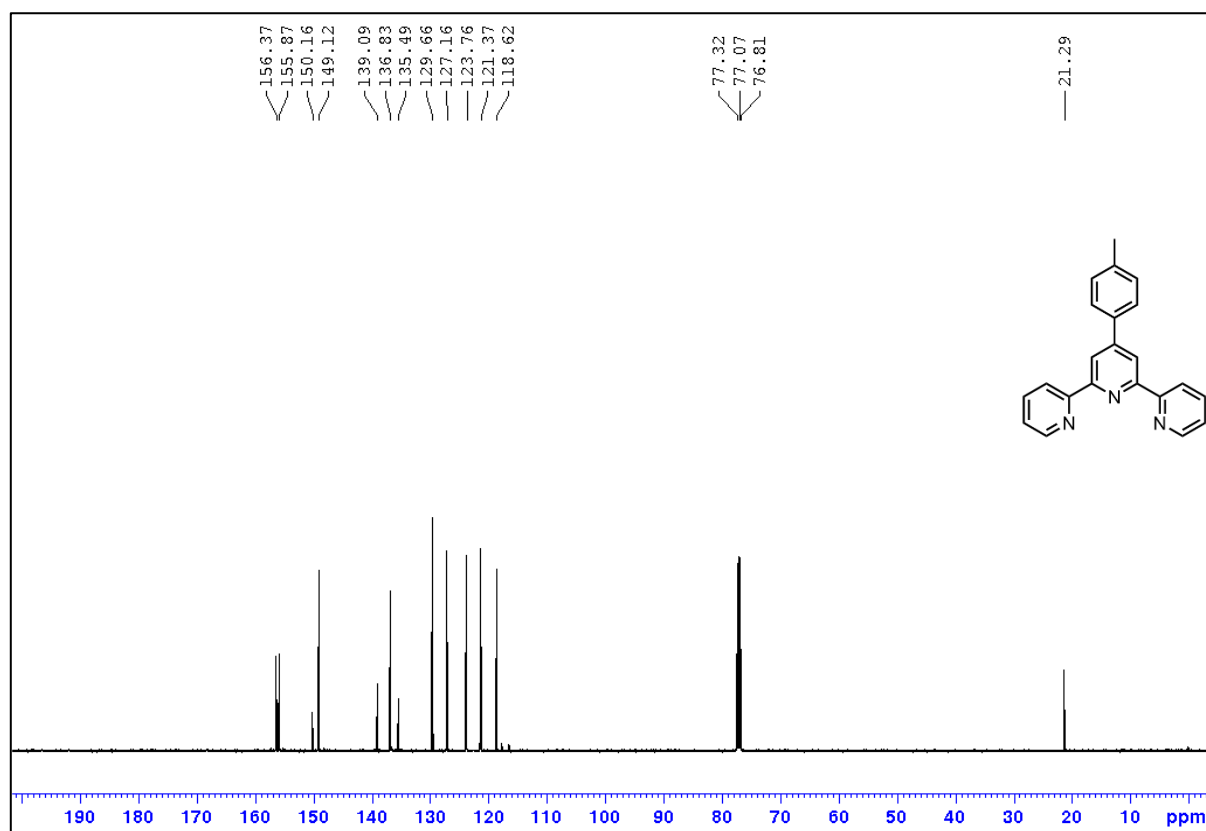


Figure S2b: $^{13}\text{C}\{^1\text{H}\}$ NMR spectrum of **L3** (125 MHz, CDCl_3).

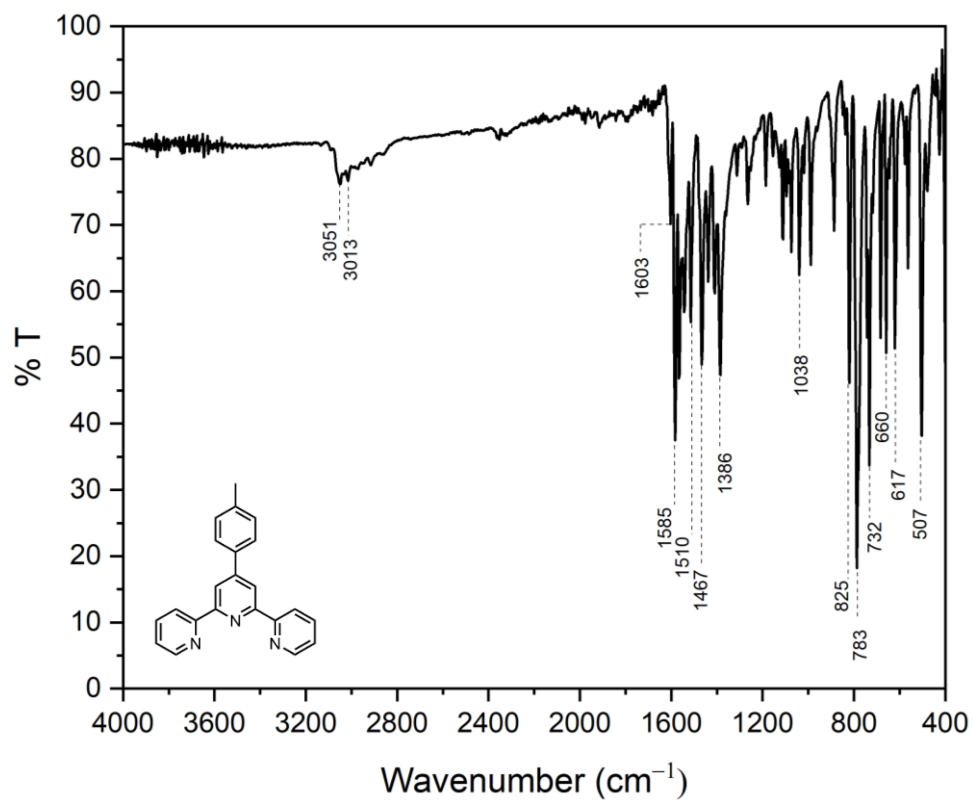


Figure S2c: ATR-IR spectrum of L3.

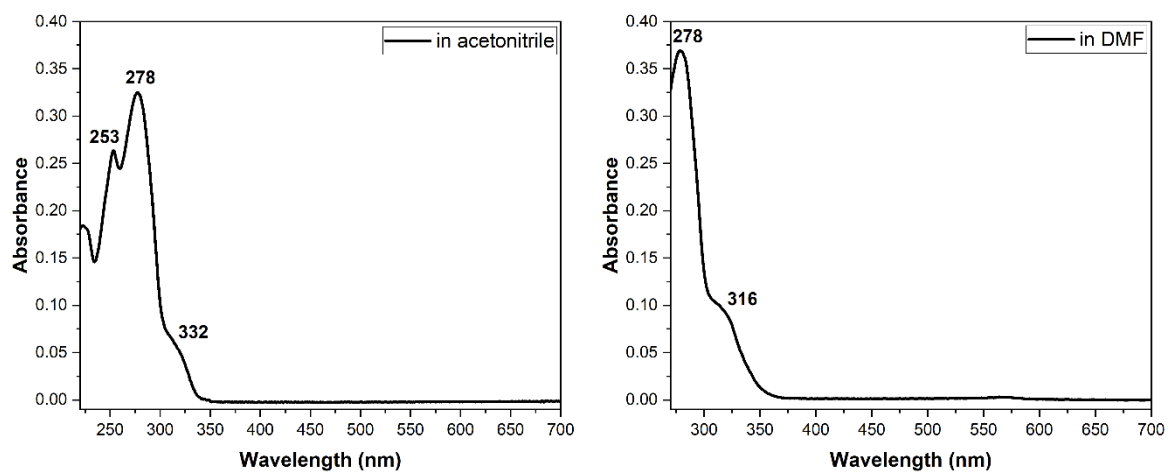


Figure S2d: Absorbance spectra of L3 (0.01 mM) in acetonitrile and DMF.

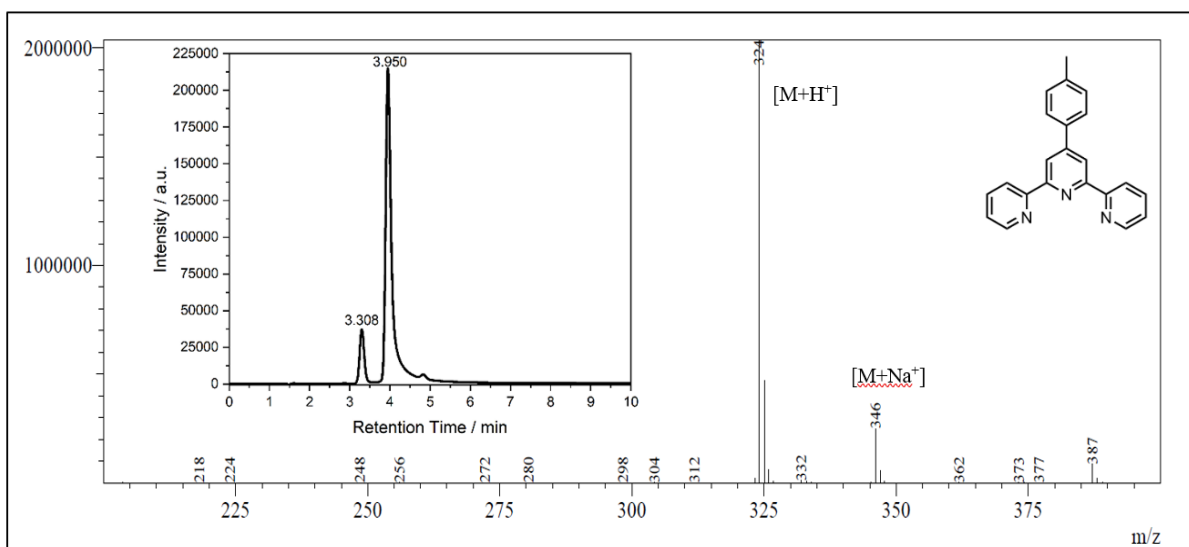


Figure S2e: LC-MS spectrum of **L3**, mass values shown at 3.950 min; Mass fragmentation pattern for **L3** [$C_{22}H_{17}N_3 = M$]; $m/z = 324$ $[M+H]^+$ ($C_{22}H_{18}N_3$), $m/z = 346$ $[M+Na]^+$ ($C_{22}H_{18}N_3Na$).

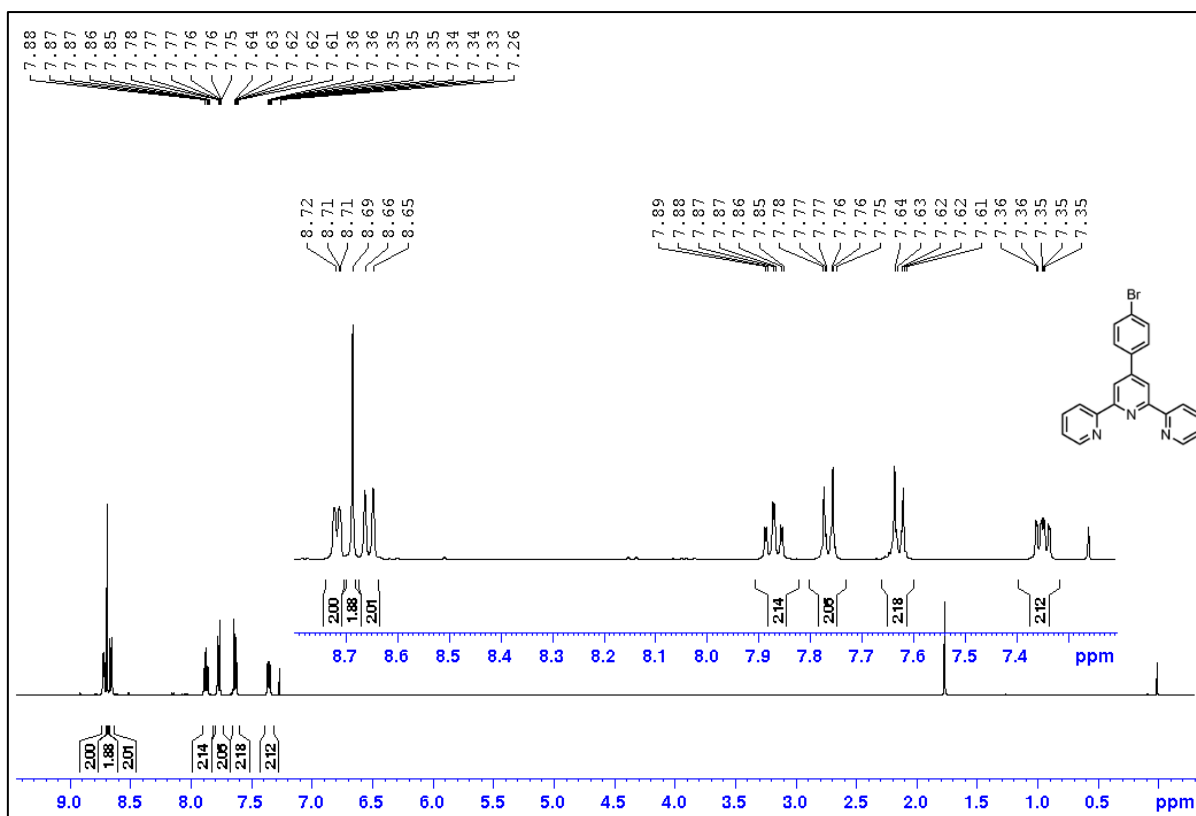


Figure S3a: ^1H NMR spectrum of **L4** (500 MHz, CDCl_3) (water peak at 1.6 ppm).

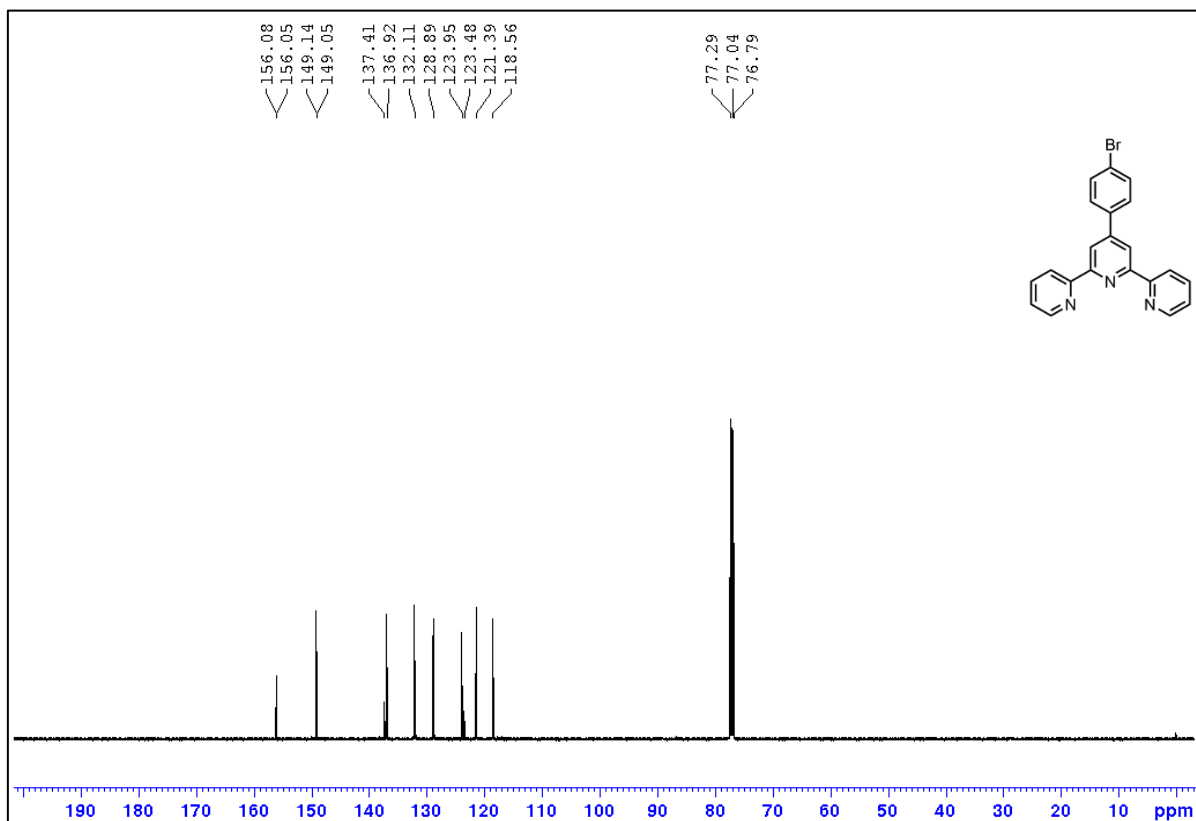


Figure S3b: $^{13}\text{C}\{^1\text{H}\}$ NMR spectrum of **L4** (125 MHz, CDCl_3).

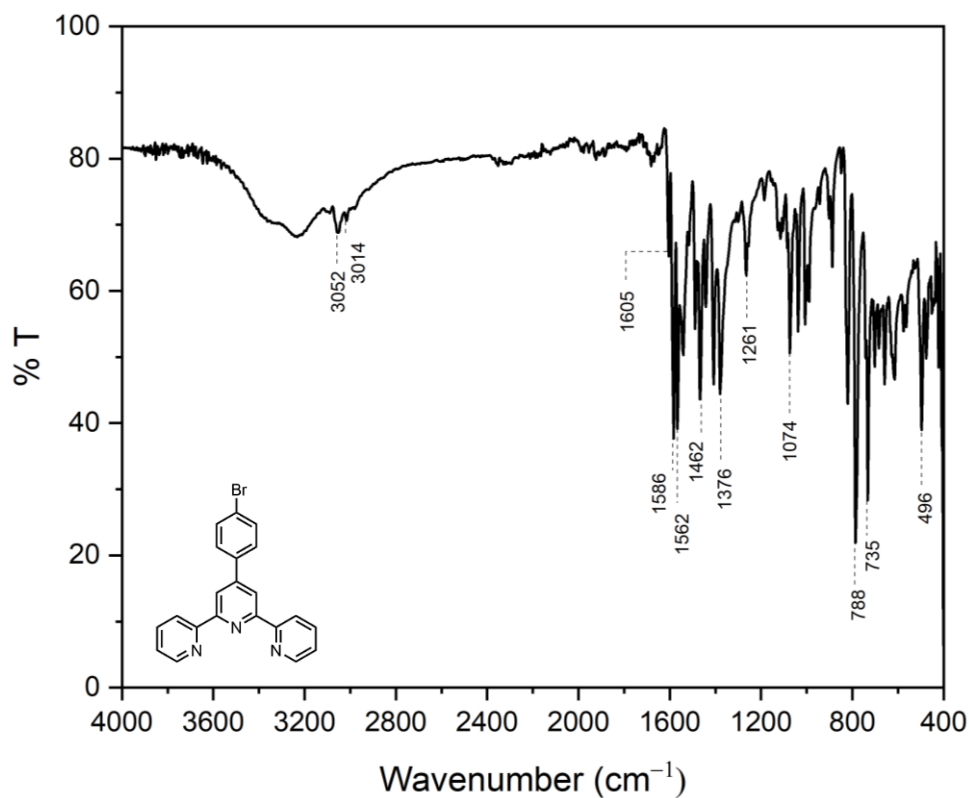


Figure S3c: ATR-IR spectrum of **L4**.

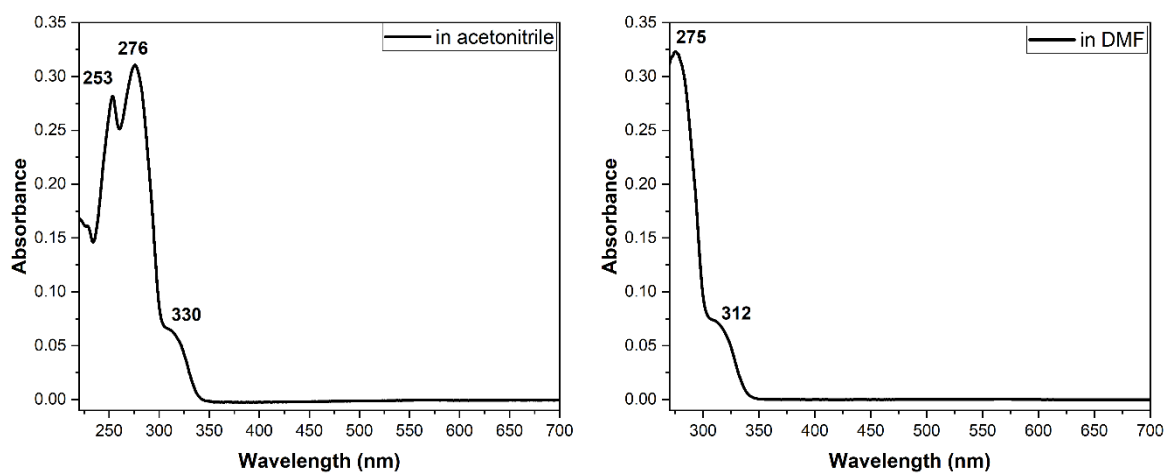


Figure S3d: Absorbance spectra of **L4** (0.01 mM) in acetonitrile and DMF.

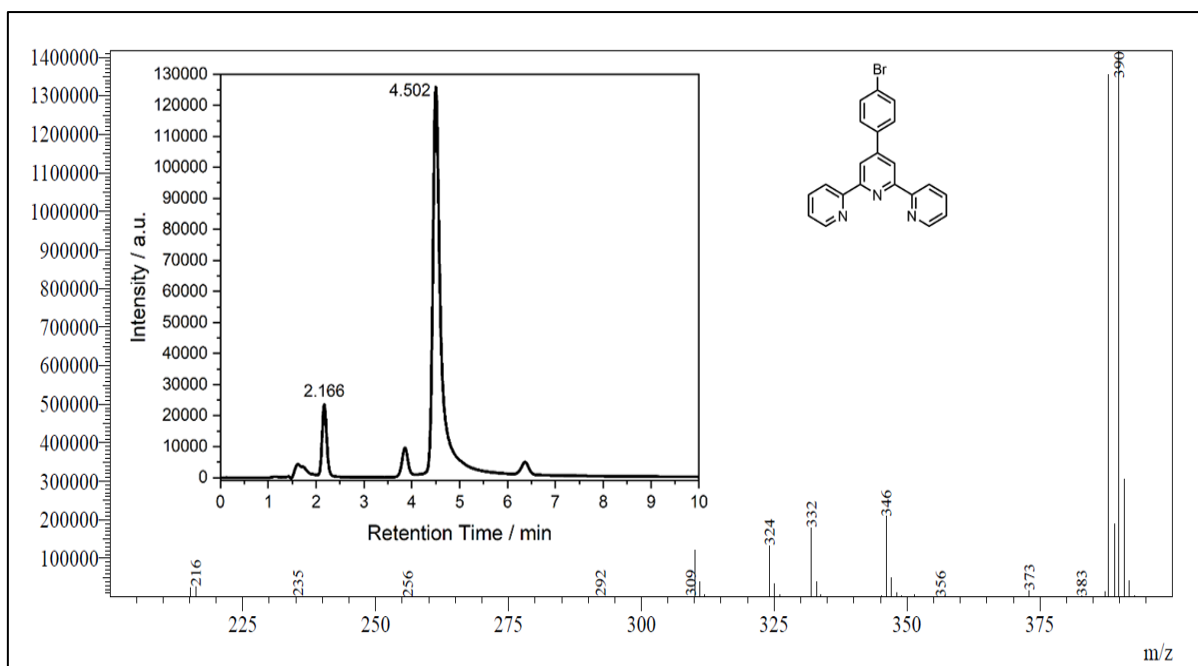


Figure S3e: LC-MS spectrum of **L4**, mass values shown at 4.502 min; Mass fragmentation pattern for **L4** [$C_{21}H_{14}BrN_3 = M$]; $m/z = 388 [M+H]^+$ ($C_{21}H_{15}^{79}BrN_3$); $m/z = 390 [M+H]^+$ ($C_{21}H_{15}^{81}BrN_3$).

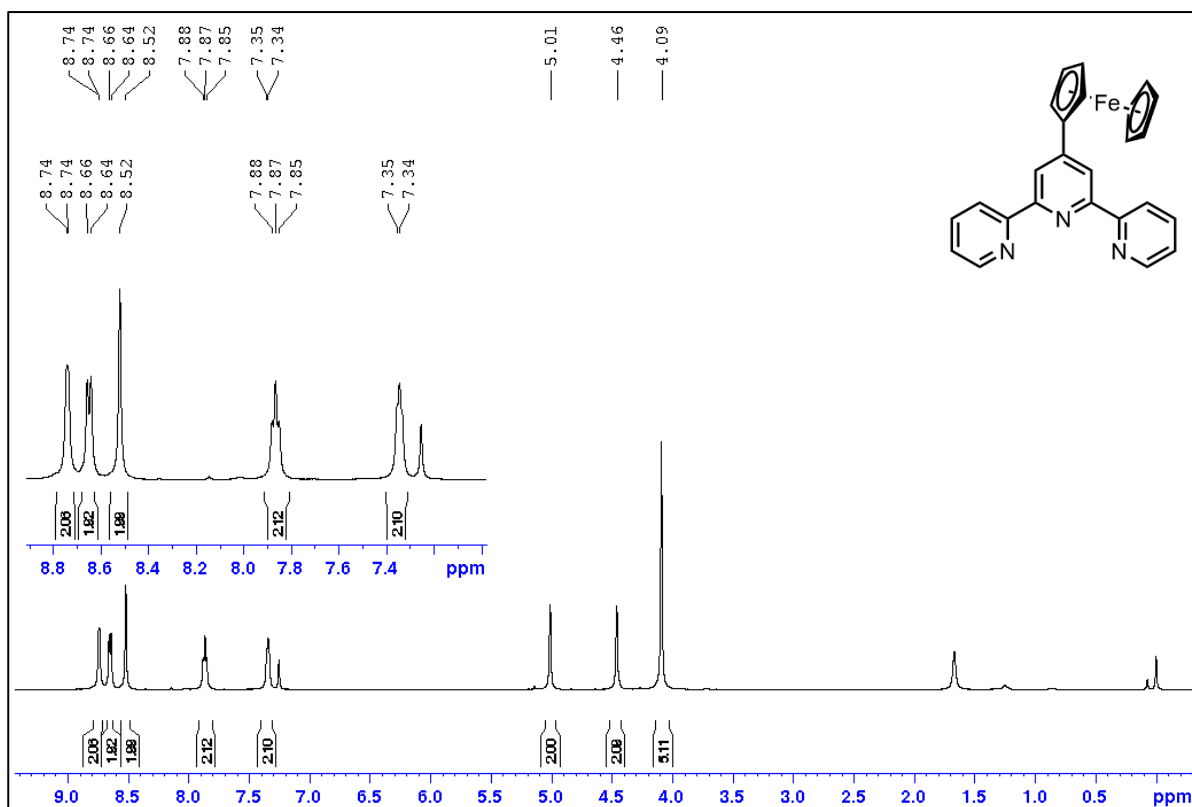


Figure S4a: ^1H NMR spectrum of L5 (500 MHz, CDCl_3) (water peak at 1.6 ppm).

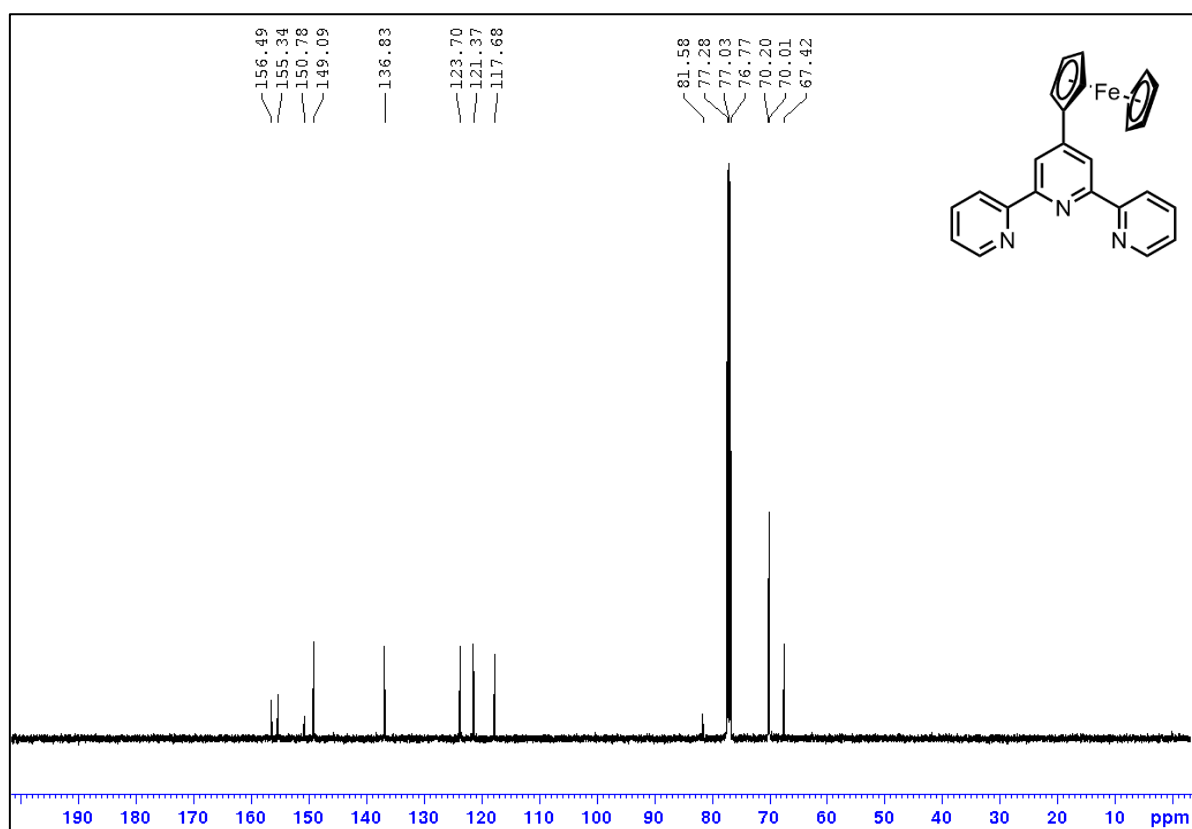


Figure S4b: $^{13}\text{C}\{^1\text{H}\}$ NMR spectrum of L5 (125 MHz, CDCl_3).

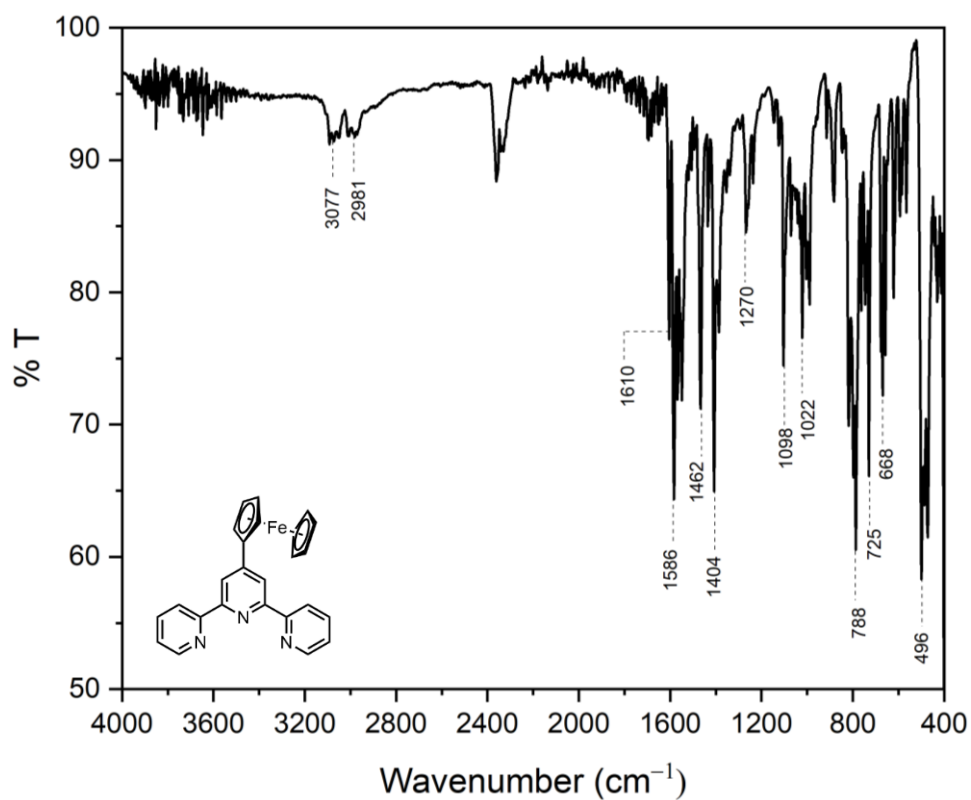


Figure S4c: ATR-IR spectrum of L5.

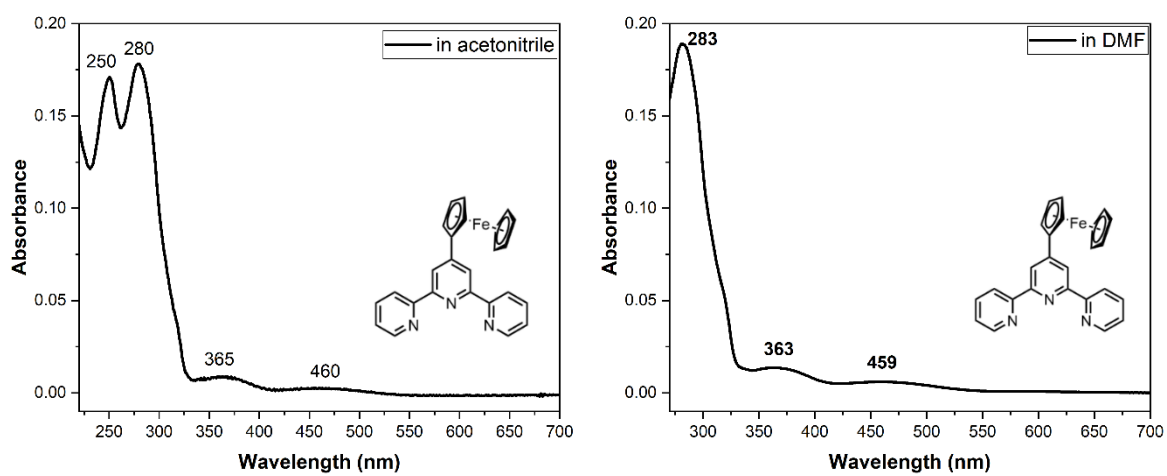


Figure S4d: Absorbance spectra of L5 (0.01 mM) in acetonitrile and DMF.

<Sample Information>

Sample Name	: L5	Sample Type	: Unknown
Sample ID	: L5	Acquired by	: IIT GOA
Data Filename	: L5_25-03-2023.lcd	Processed by	: IIT GOA
Method Filename	: C_95_D_5_10_min_0.2ml_min.lcm		
Batch Filename	: 25032023.lcb		
Vial #	: 1-91		
Injection Volume	: 1 uL		
Date Acquired	: 3/25/2023 12:42:27 PM		
Date Processed	: 3/25/2023 12:58:21 PM		

<Chromatogram>

mAU

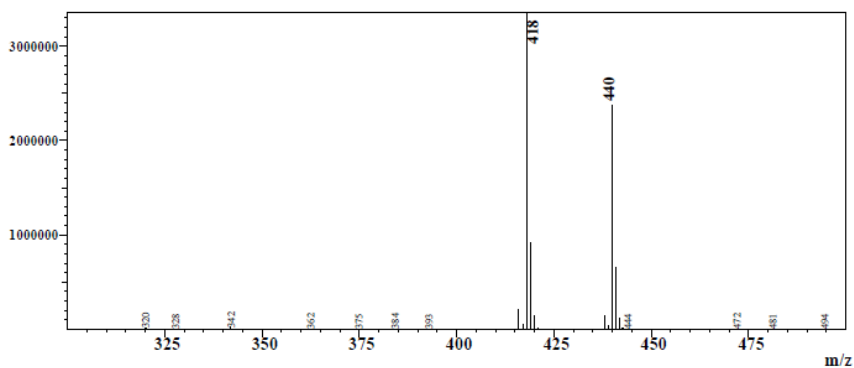
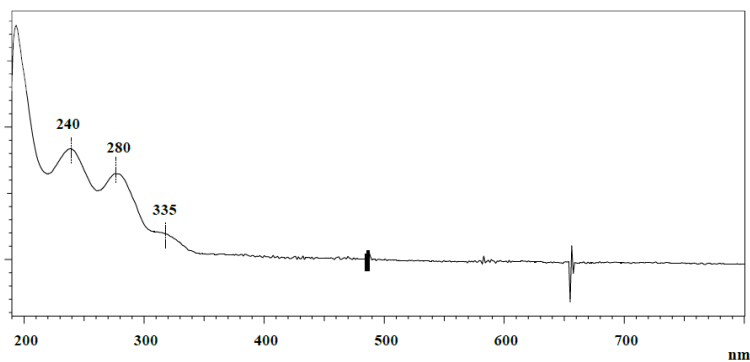
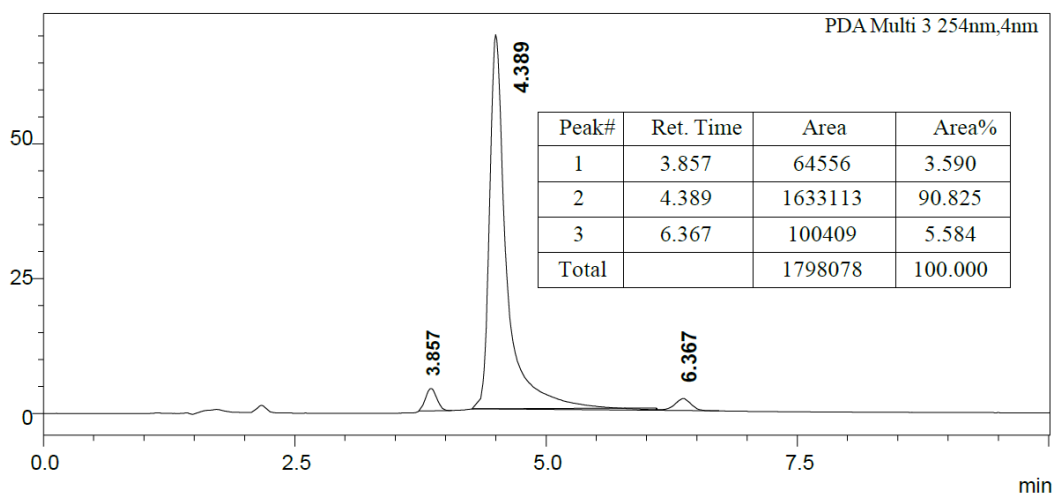


Figure S4e: RP-HPLC-MS and corresponding UV-Vis spectra of **L5** at $t_R = 4.389$ min; HPLC purity 90%; m/z values for $t_R = 3.857, 4.389$ & 6.367 min shows same m/z : fragmentation pattern at 4.389 min [$C_{25}H_{19}FeN_3 = M$]; $m/z = 418$ [$M+H$] $^+$ ($C_{25}H_{20}FeN_3^+$), $m/z = 440$ [$M+Na$] $^+$ ($C_{25}H_{20}FeN_3Na^+$).

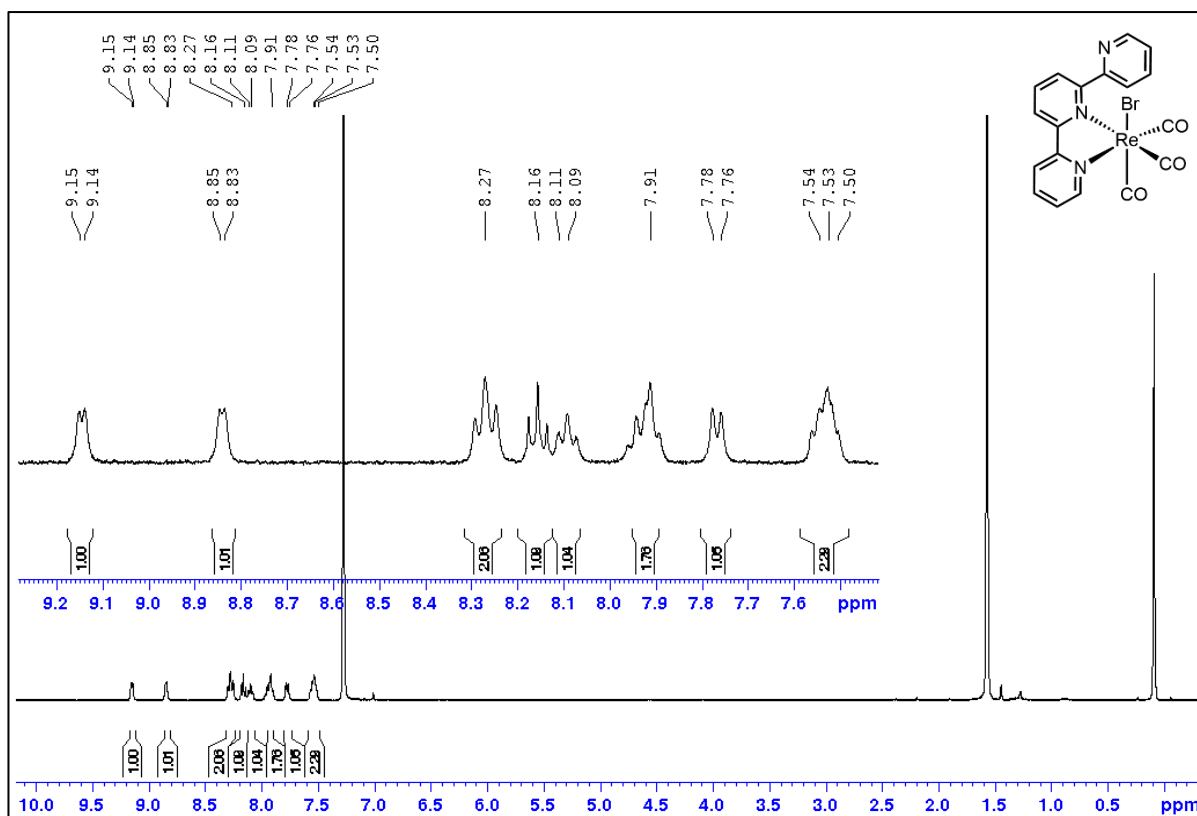


Figure S5a: ^1H NMR spectrum of **Re1** (400 MHz, CDCl_3) (water peak at 1.6 ppm).

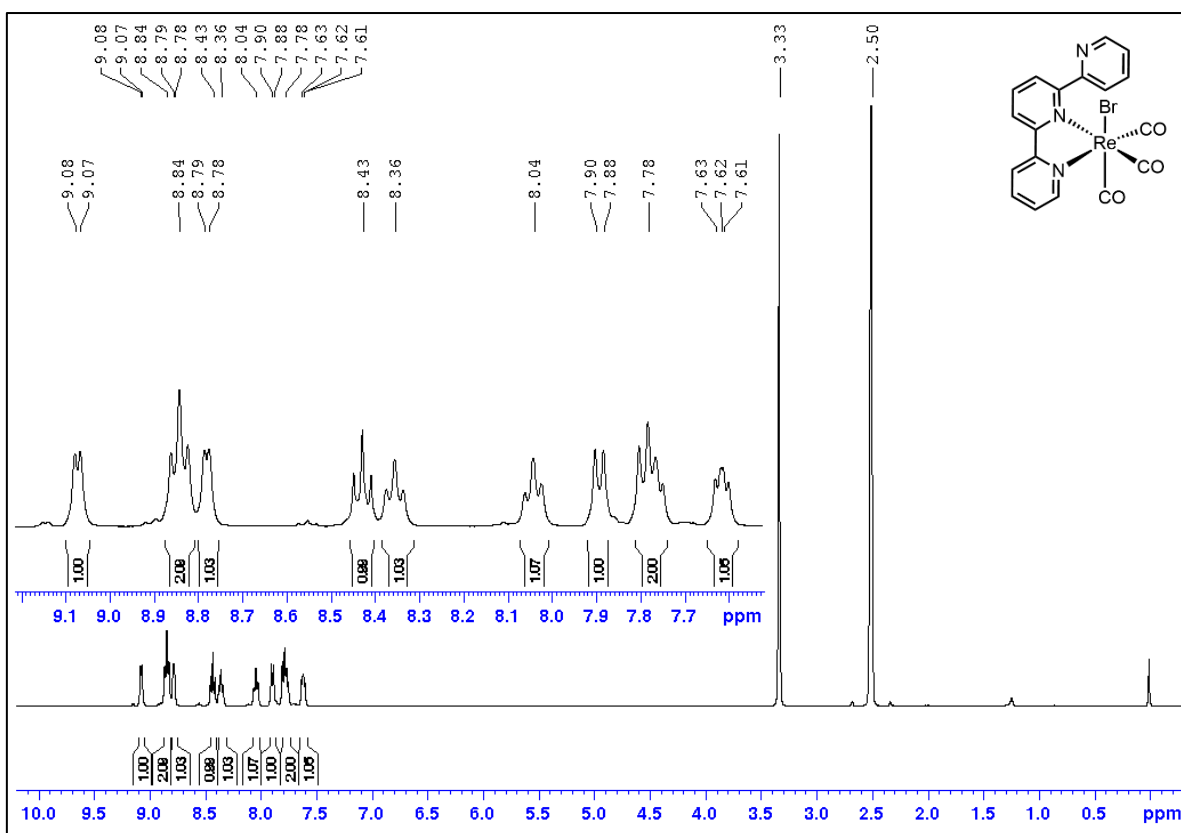


Figure S5b: ^1H NMR spectrum of **Re1** (400 MHz, DMSO-d_6) (water peak at 3.33 ppm).

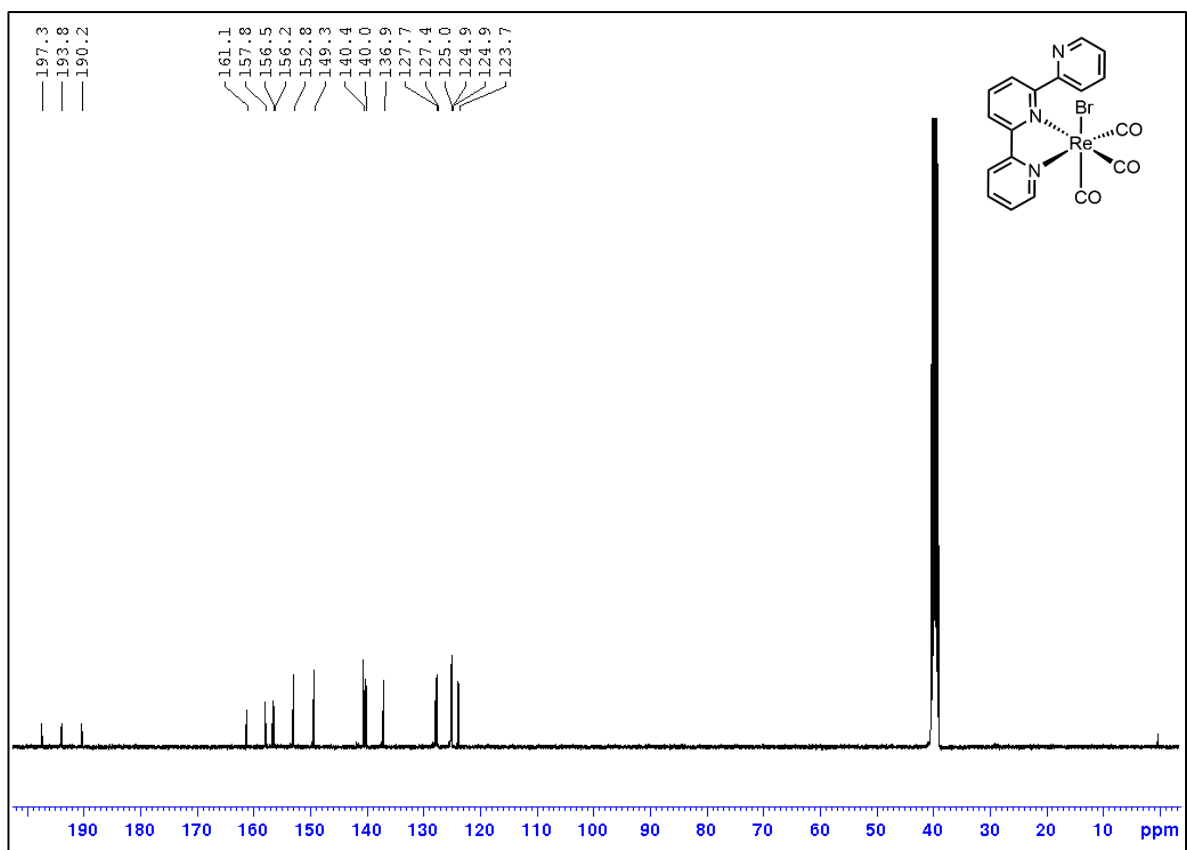


Figure S5c: $^{13}\text{C}\{^1\text{H}\}$ NMR spectrum of **Re1** (101 MHz, $\text{DMSO-}d_6$) with 16405 scans.

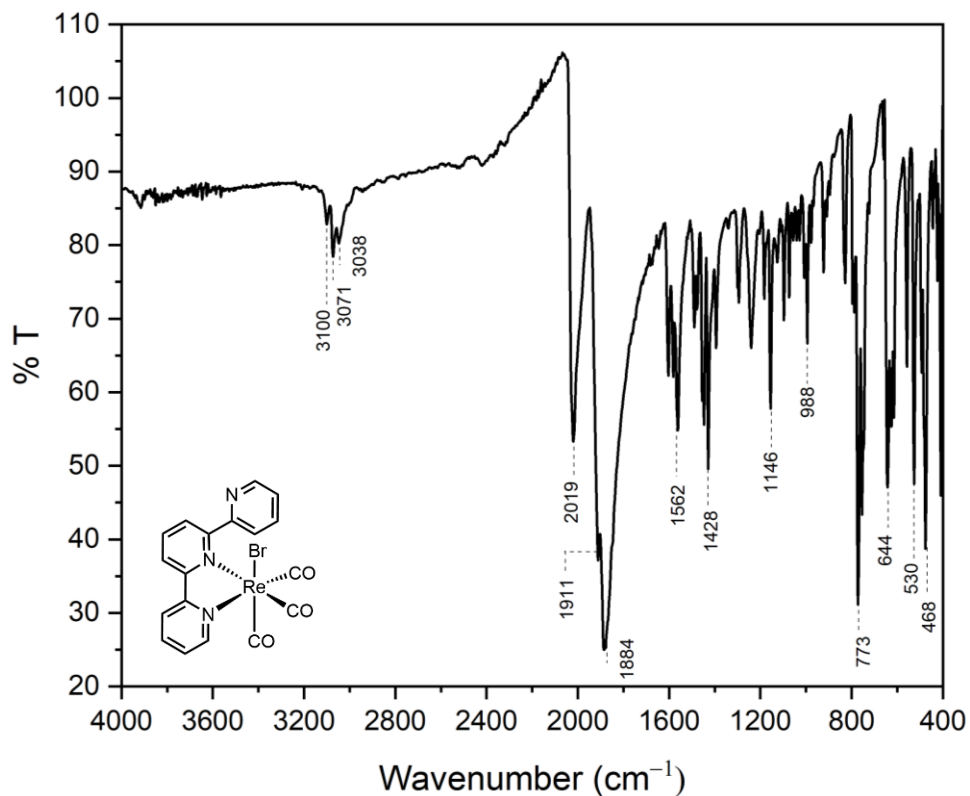


Figure S5d: ATR-IR spectrum of **Re1**.

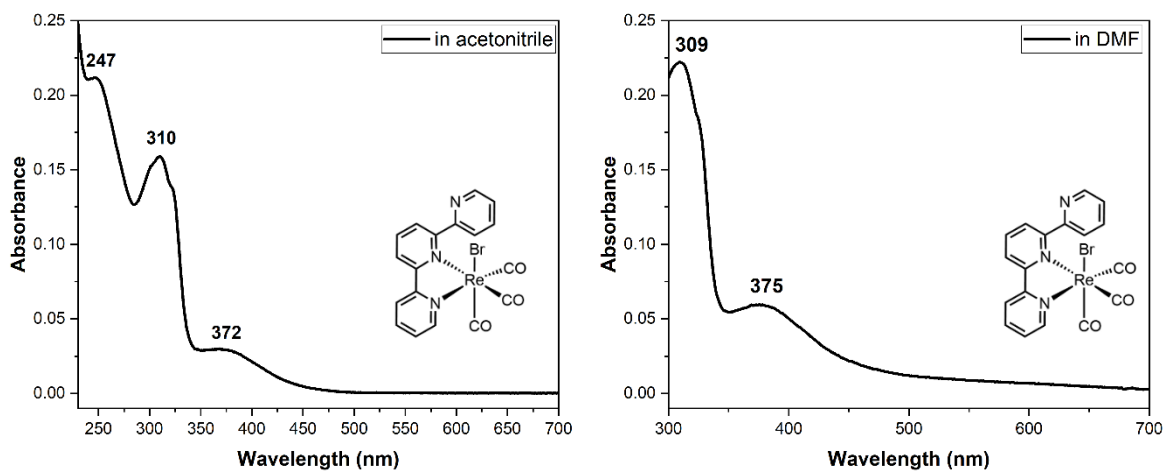


Figure S5e: Absorbance spectra of **Re1** (0.01 mM) in acetonitrile and DMF.

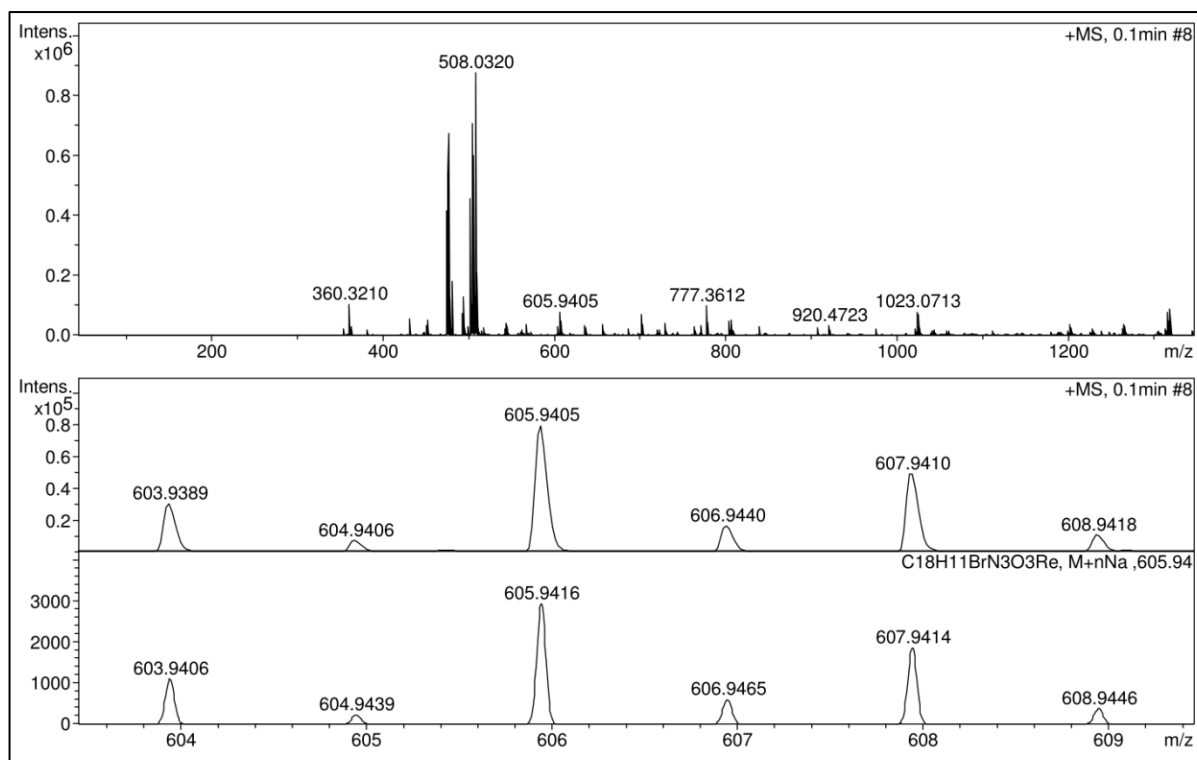
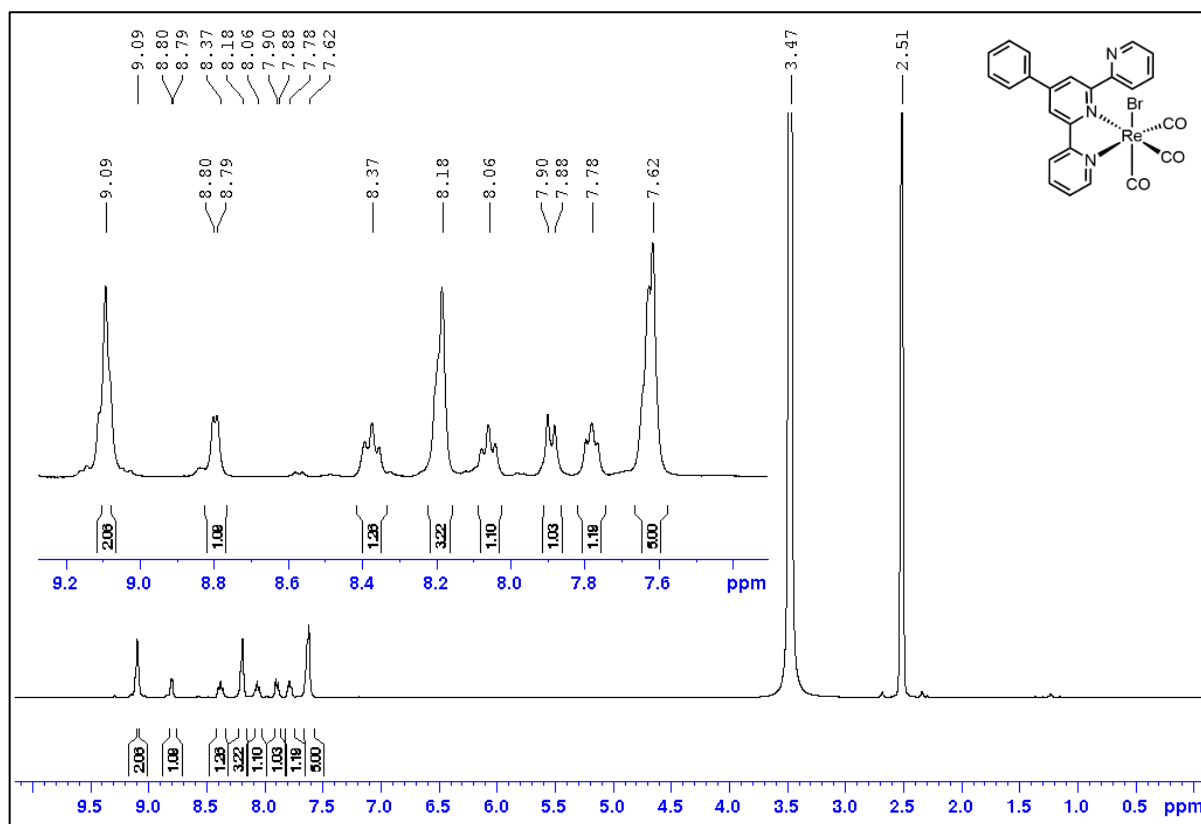
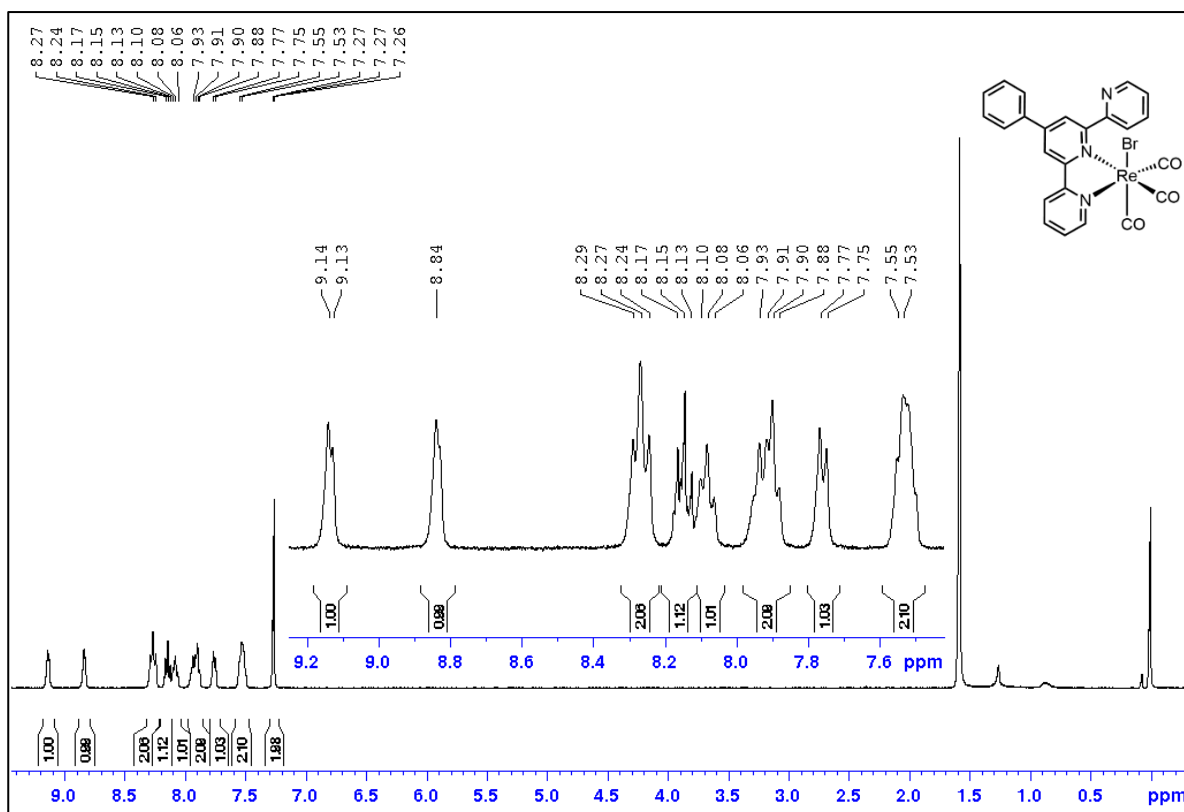


Figure S5e: HRMS for **Re1** [$C_{18}H_{11}BrN_3O_3Re = M$] Calcd for $[M+Na^+]$ m/z 605.9416 found m/z 605.9405; Calcd for $[(M-CO-Br)^+ + MeOH]$ m/z 508.0631 found m/z 508.0320.



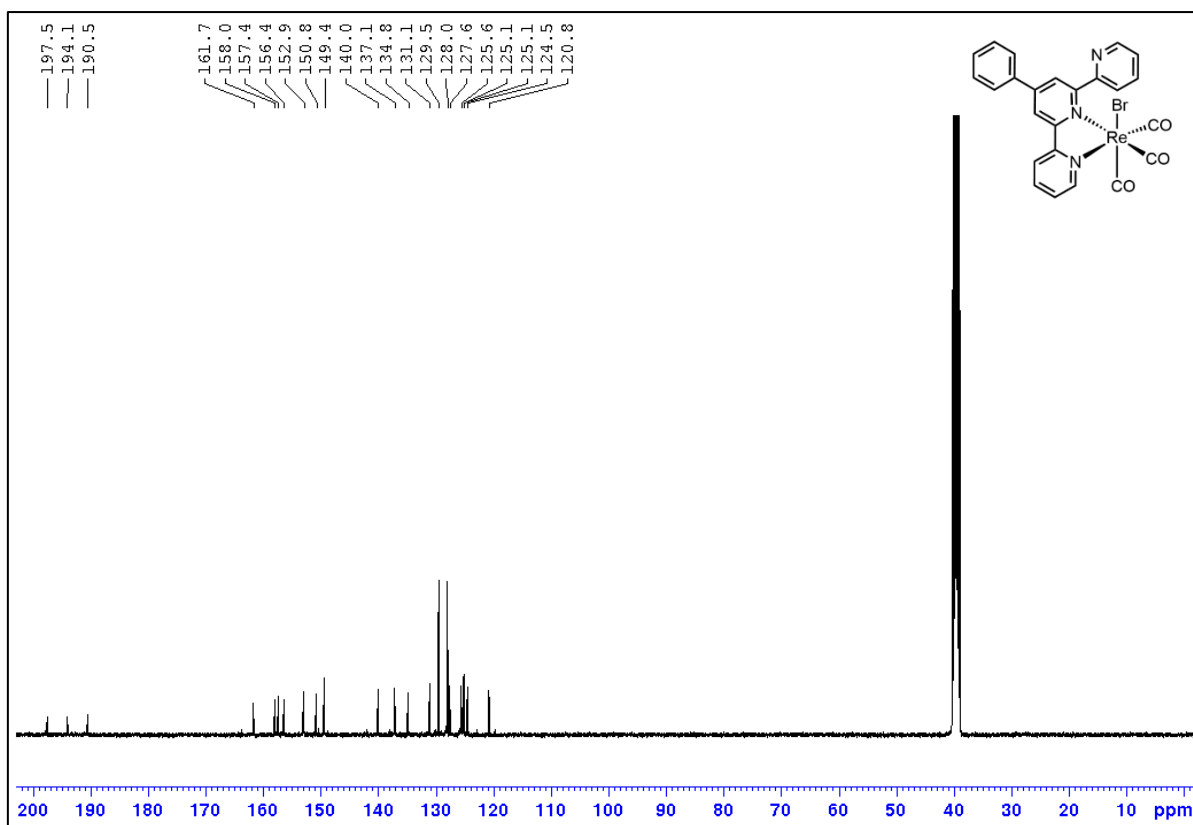


Figure S6c: $^{13}\text{C}\{^1\text{H}\}$ NMR spectrum of **Re2** (101 MHz, DMSO-d_6) with 13678 scans.

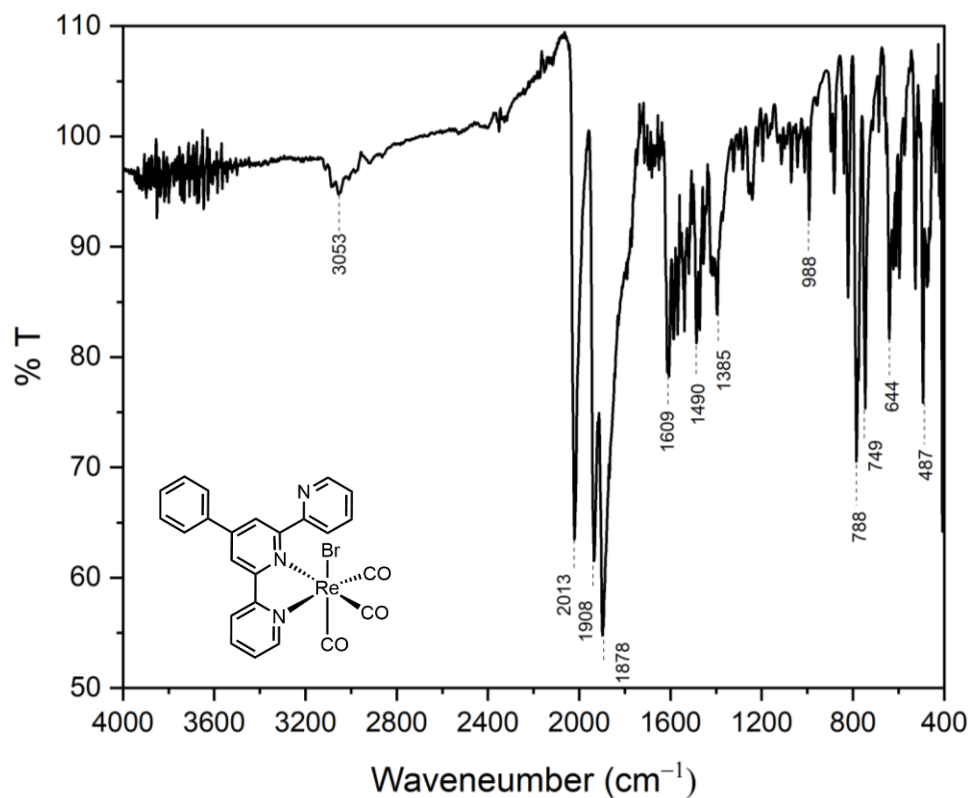


Figure S6d: ATR-IR spectrum of **Re2**.

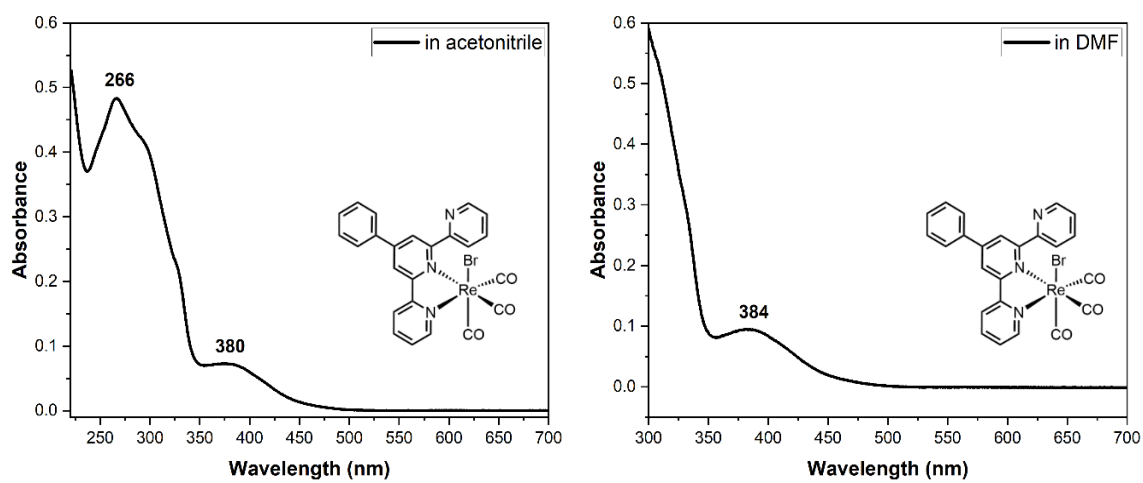


Figure S6e: Absorbance spectra of **Re2** (0.01 mM) in acetonitrile and DMF.

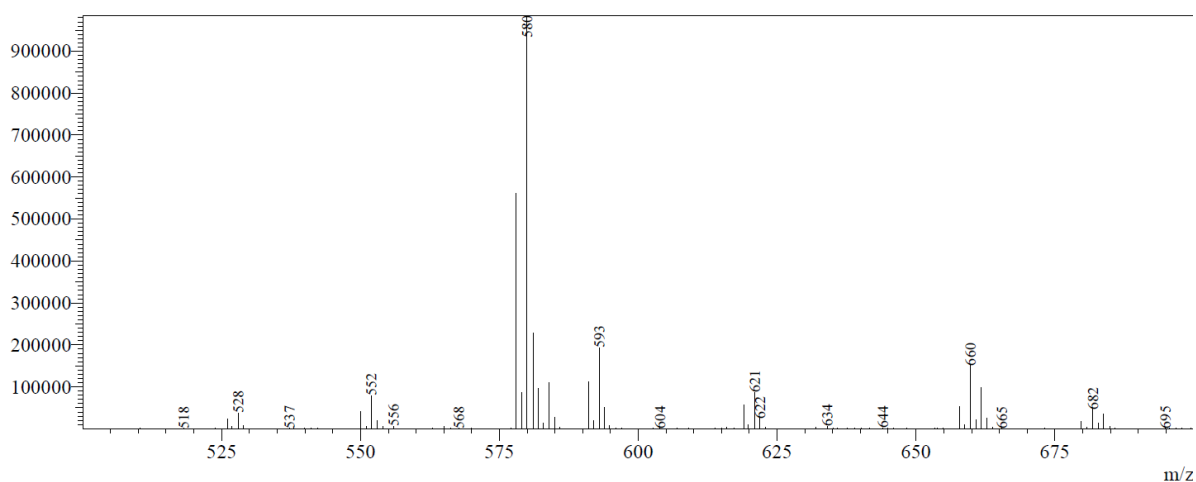


Figure S6f: Mass fragmentation pattern and isotopic distribution for **Re2** [$C_{24}H_{15}BrN_3O_3Re = M$]; $m/z = 660 [M+H]^+$ ($C_{24}H_{16}BrN_3O_3Re$); $m/z = 580 [M-Br]^+$ ($C_{24}H_{16}N_3O_3Re$).

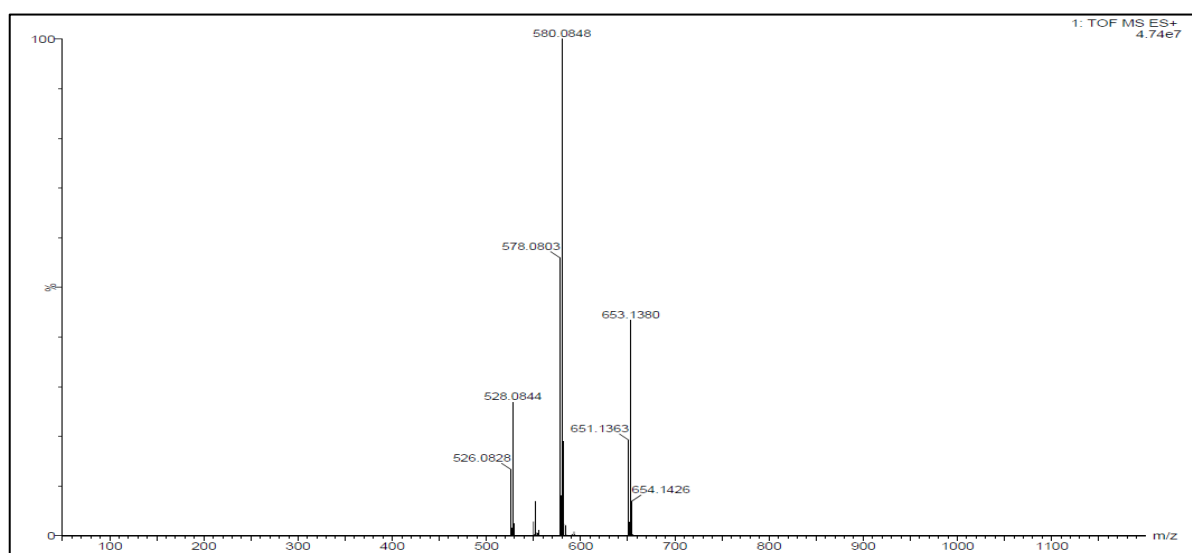


Figure S6g: HRMS for **Re2** [$C_{24}H_{15}BrN_3O_3Re = M$]; Calcd for $[M-CO+Na]^+$ m/z 653.9775 found m/z 653.1380; Calcd for $[M-Br]^+$ m/z 580.0643 found m/z 580.0848.

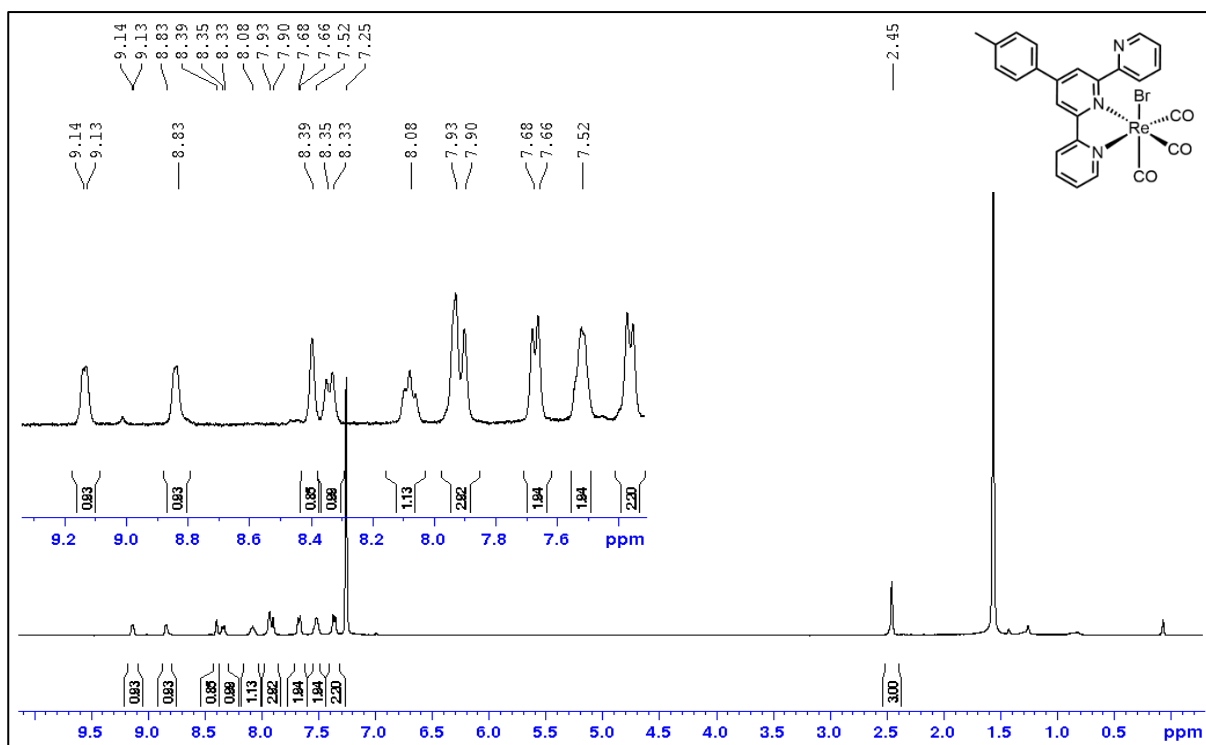


Figure S7a: ^1H NMR spectrum of **Re3** (400 MHz, CDCl_3) (water peak at 1.6 ppm).

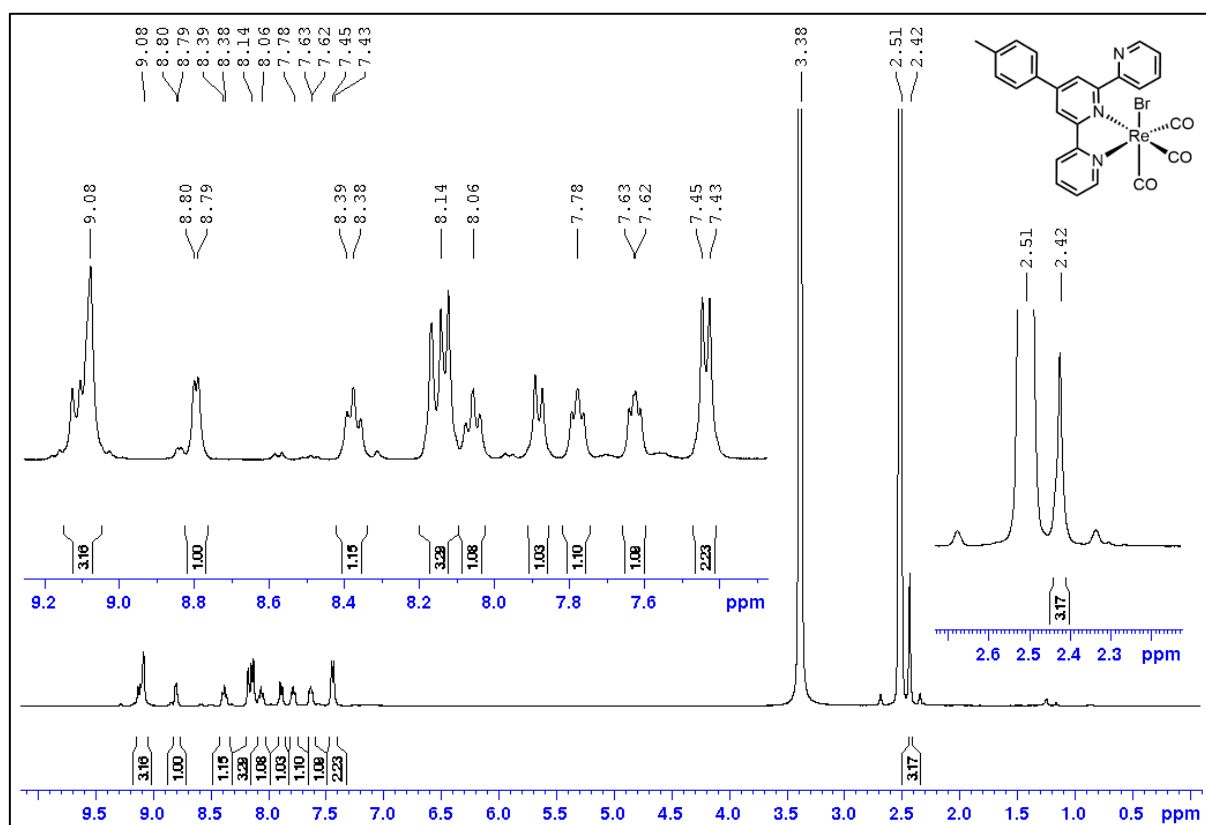


Figure S7b: ^1H NMR spectrum of **Re3** (400 MHz, $\text{DMSO}-d_6$) (water peak at 3.38 ppm).

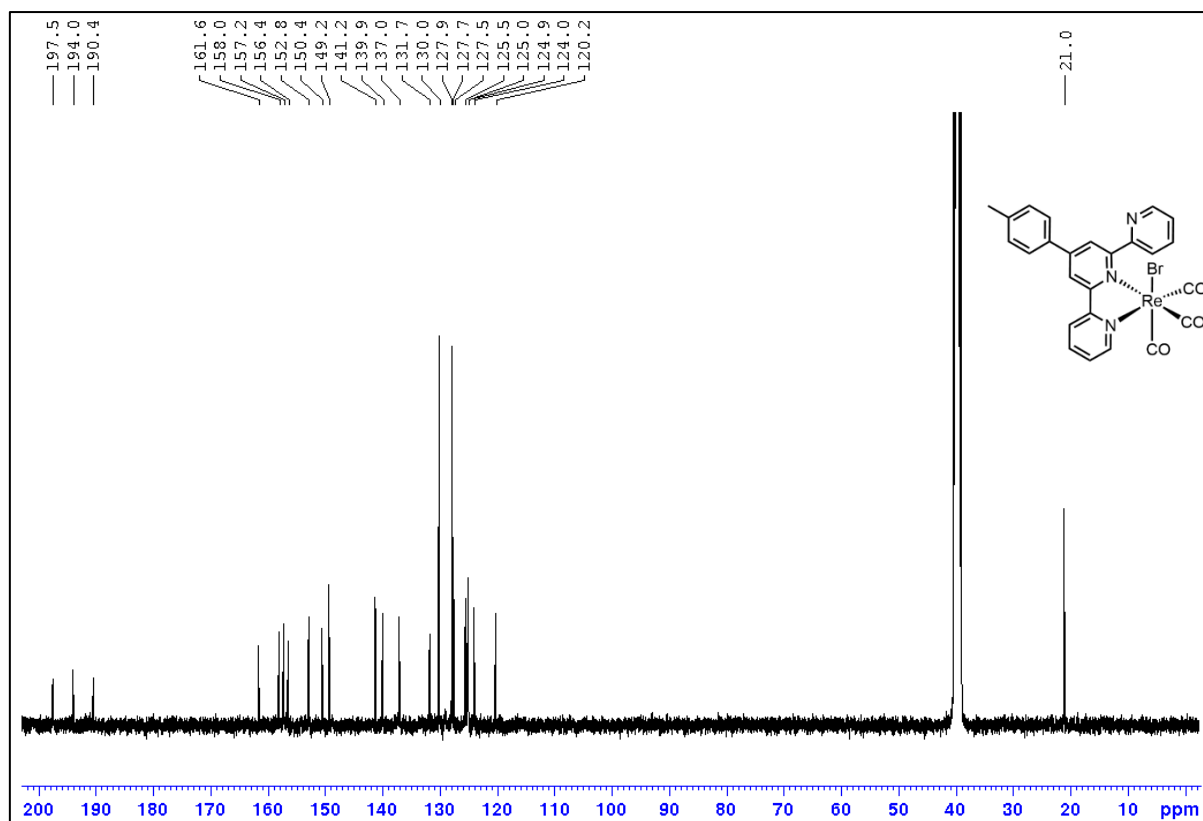


Figure S7c: $^{13}\text{C}\{^1\text{H}\}$ NMR spectrum of **Re3** (101 MHz, DMSO-d_6) with 13643 scans.

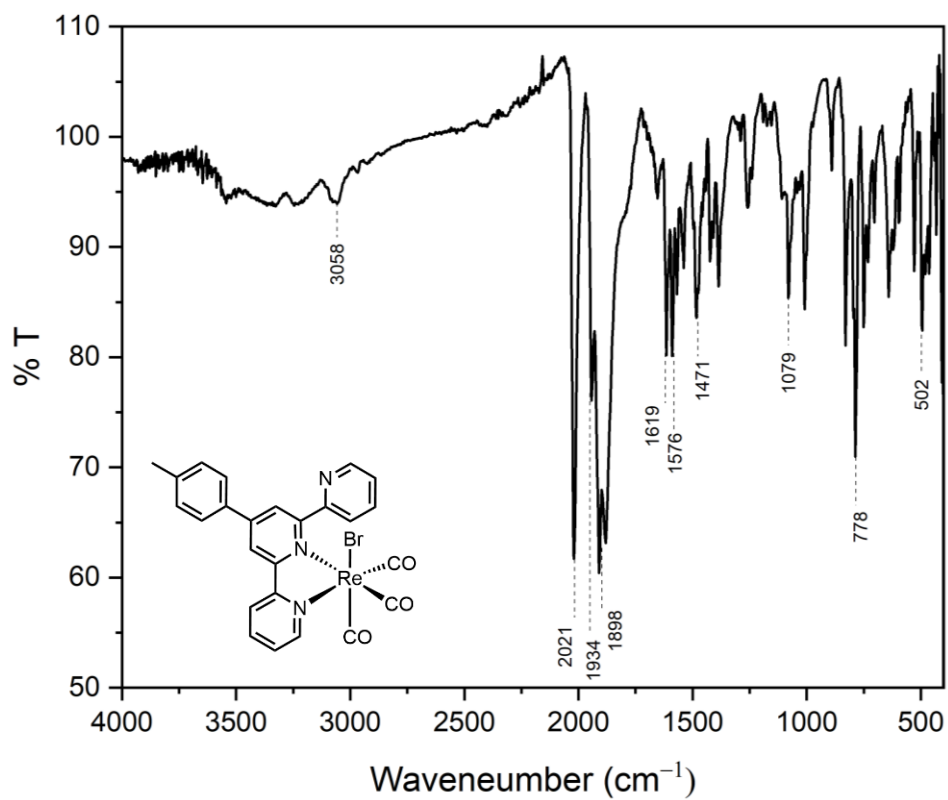


Figure S7d: ATR-IR spectrum of **Re3**.

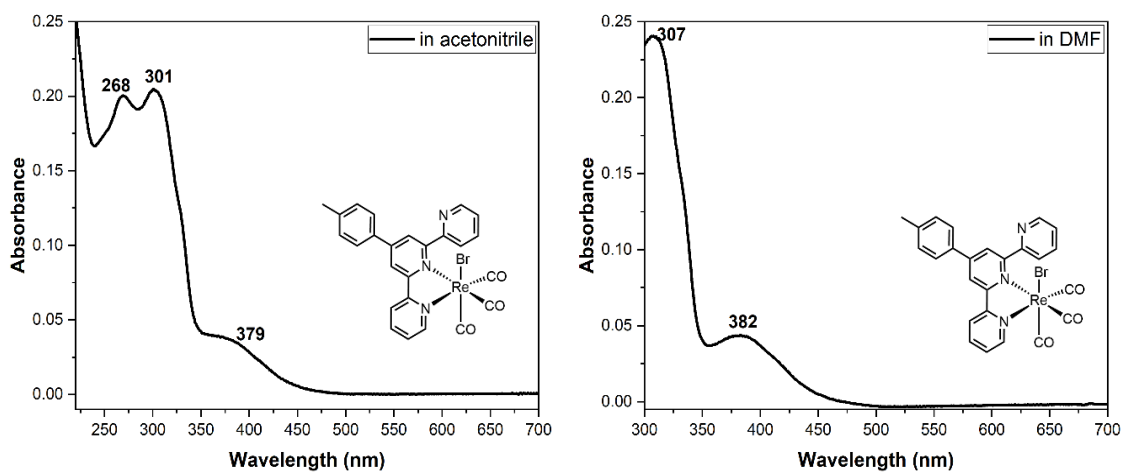


Figure S7e: Absorbance spectra of **Re3** (0.01 mM) in acetonitrile and DMF.

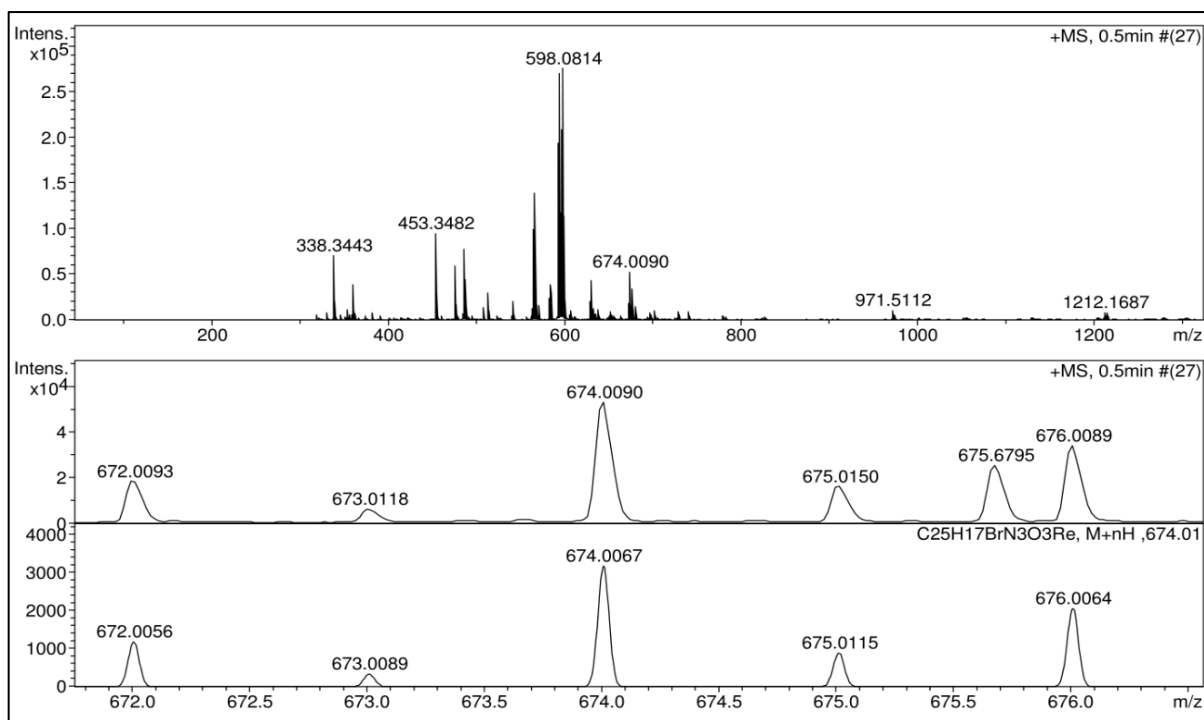


Figure S7f: HRMS for **Re3** [$C_{25}H_{17}BrN_3O_3Re = M$]; Calcd for $[M+H]^+$ $m/z = 674.0055$ ($C_{25}H_{18}^{79}BrN_3O_3Re$) found $m/z = 674.0090$; Calcd for $[(M-CO-Br)^+ + MeOH]$ $m/z = 598.1112$ found $m/z = 598.0814$.

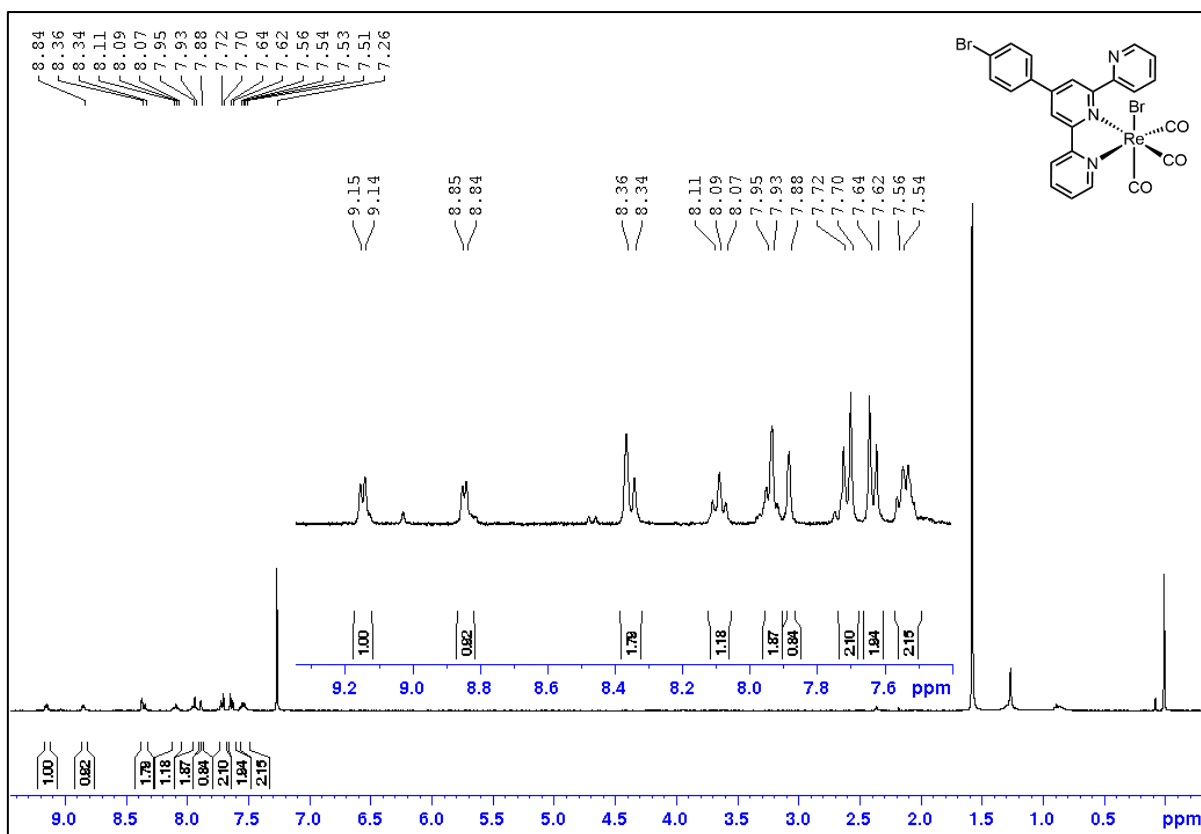


Figure S8a: ^1H NMR spectrum of **Re4** (500 MHz, CDCl_3) (water peak at 1.6 ppm).

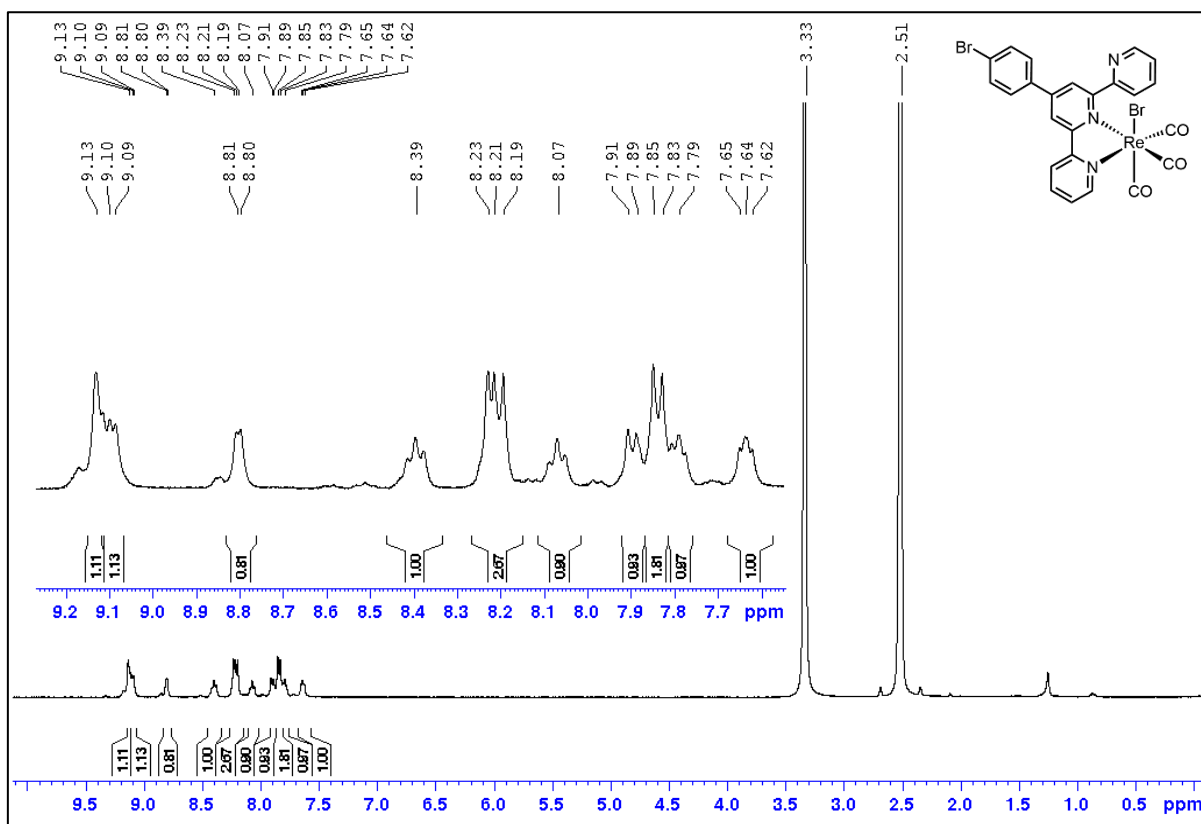


Figure S8b: ^1H NMR spectrum of **Re4** (400 MHz, $\text{DMSO}-d_6$) (water peak at 3.33 ppm).

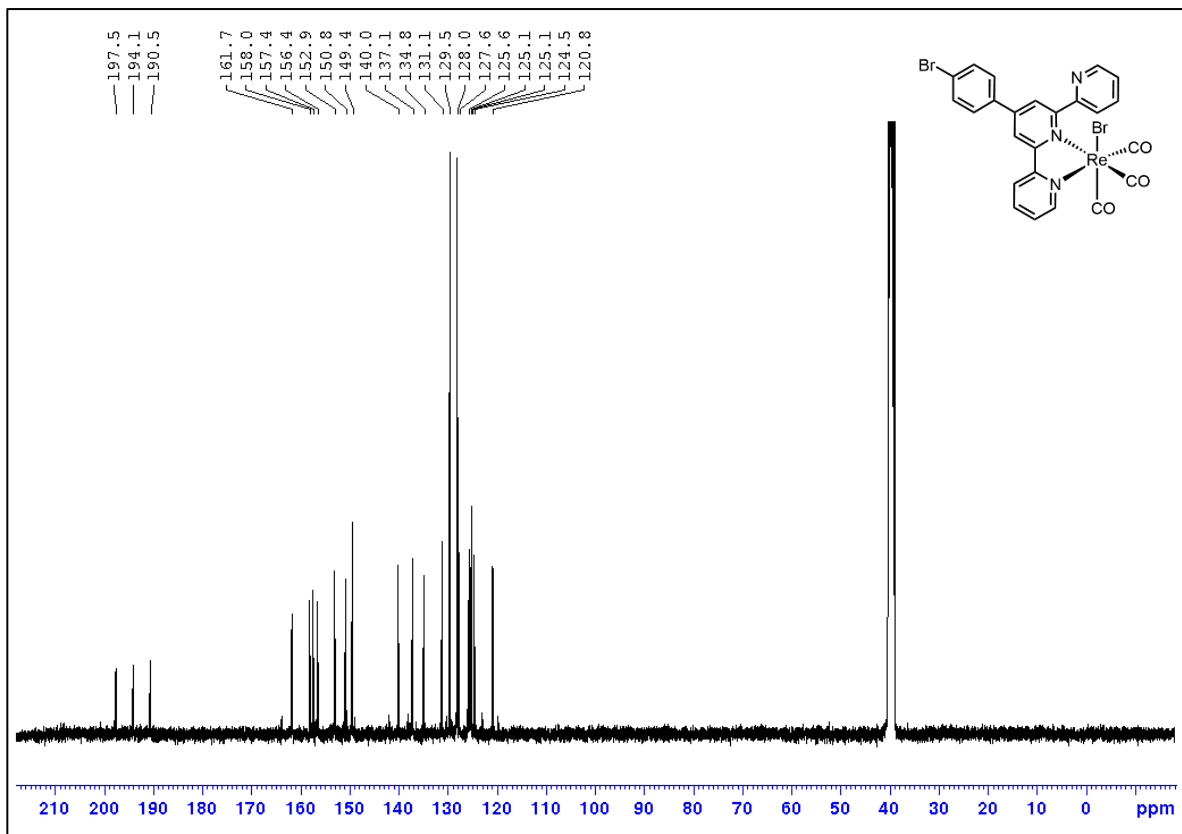


Figure S8c: $^{13}\text{C}\{^1\text{H}\}$ NMR spectrum of **Re4** (101 MHz, $\text{DMSO-}d_6$) with 11100 scans.

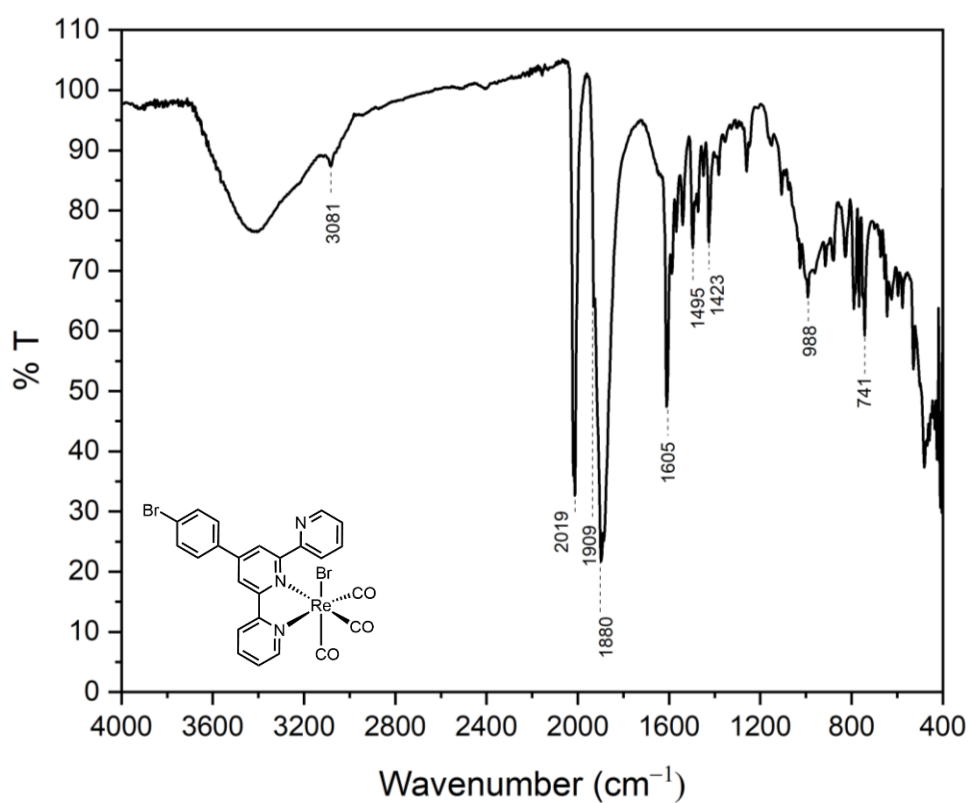


Figure S8d: ATR-IR spectrum of **Re4**.

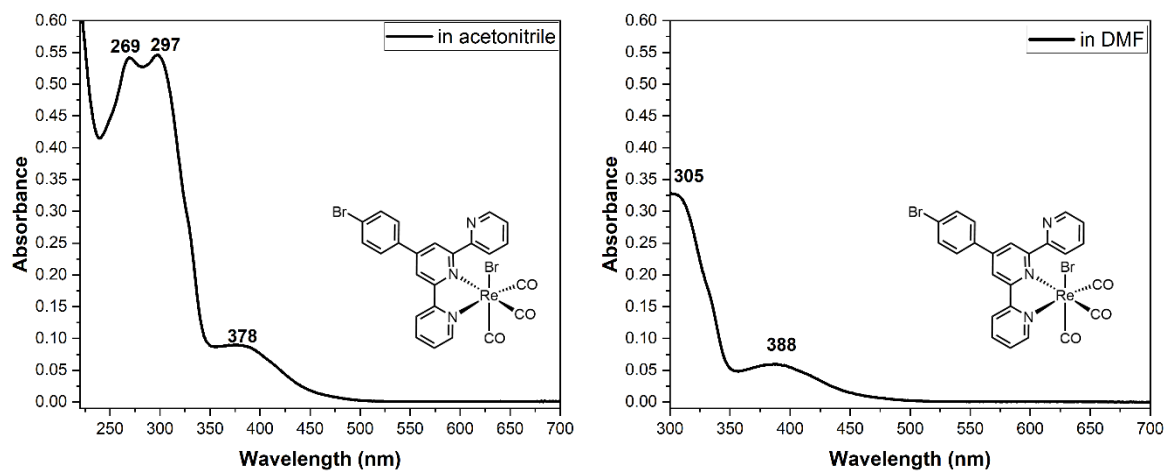


Figure S8e: Absorbance spectra of **Re4** (0.01 mM) in acetonitrile and DMF.

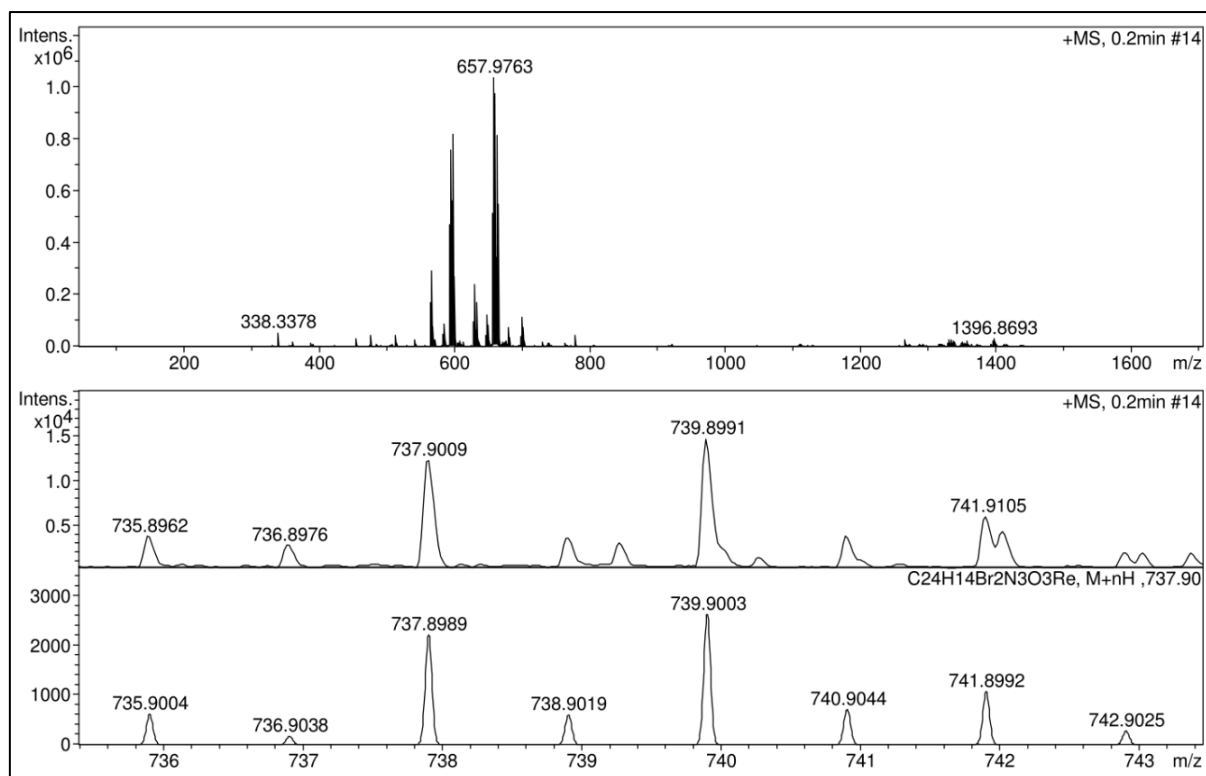


Figure S8f: HRMS for **Re4** [$C_{24}H_{14}Br_2N_3O_3Re = M$] Calcd for $[M+H]^+$ $m/z = 739.9004$ ($C_{25}H_{18}^{81}Br_2N_3O_3Re$) found $m/z = 739.8991$; Calcd for $[(M-Br)^+]$ $m/z = 657.9748$ found $m/z = 657.9763$.

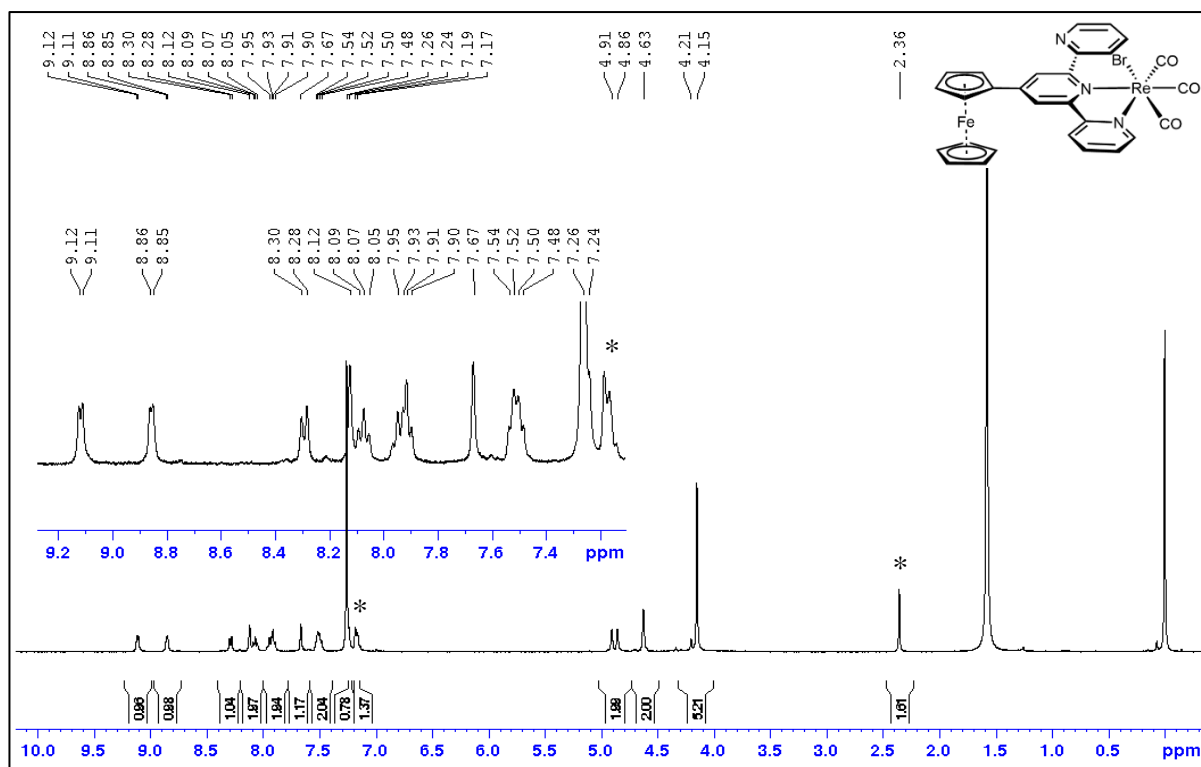


Figure S9a: ^1H NMR spectrum of **Re5** (400 MHz, CDCl_3) (water peak at 1.6 ppm) toluene peaks marked with *; observed at 7.24, 7.18 & 2.36 ppm; reported³ at 7.25, 7.17 & 2.36 ppm.

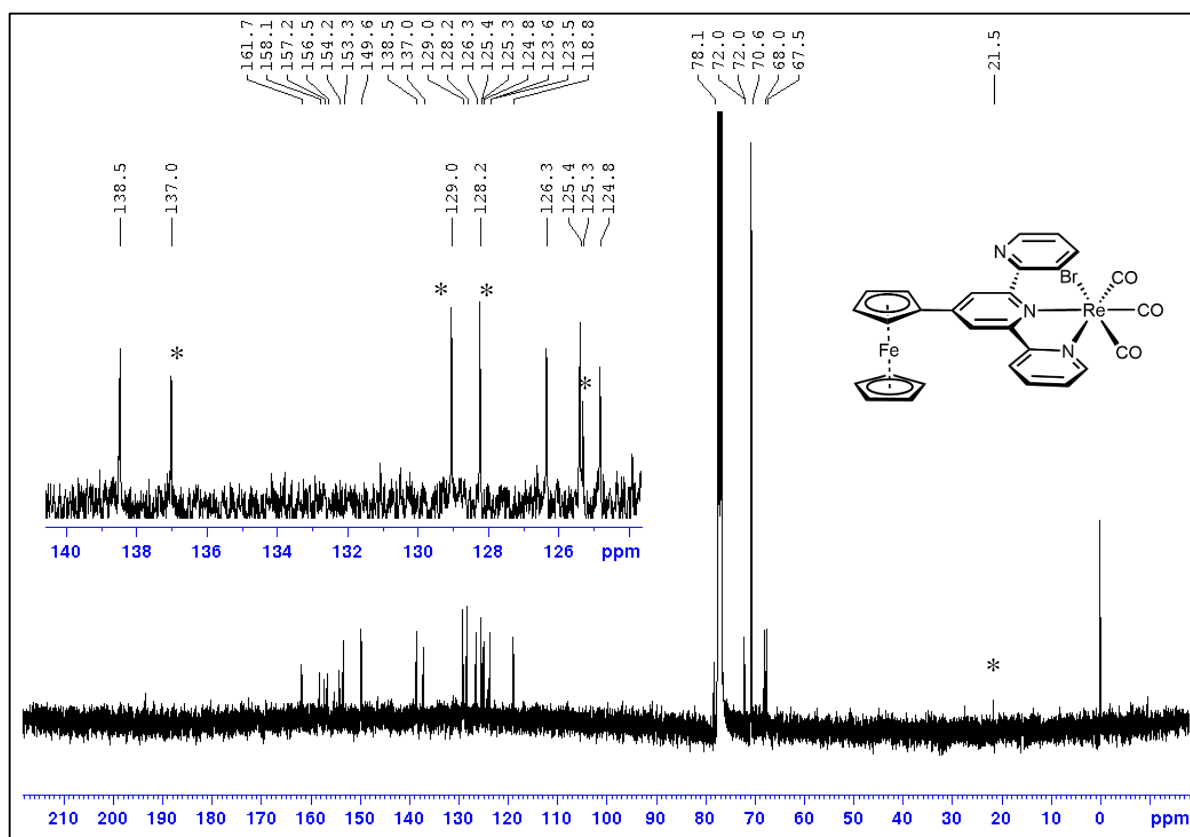


Figure S9b: $^{13}\text{C}\{^1\text{H}\}$ NMR spectrum of **Re5** (101 MHz, CDCl_3), with 15879 scans. The ^{13}C peaks for CO were not observed even with longer scans; toluene peaks marked with *; observed at 137.9, 129.1, 128.3, 125.3 & 21.5 ppm; reported³ at 137.0, 129.0, 128.2, 125.3 & 21.5 ppm.

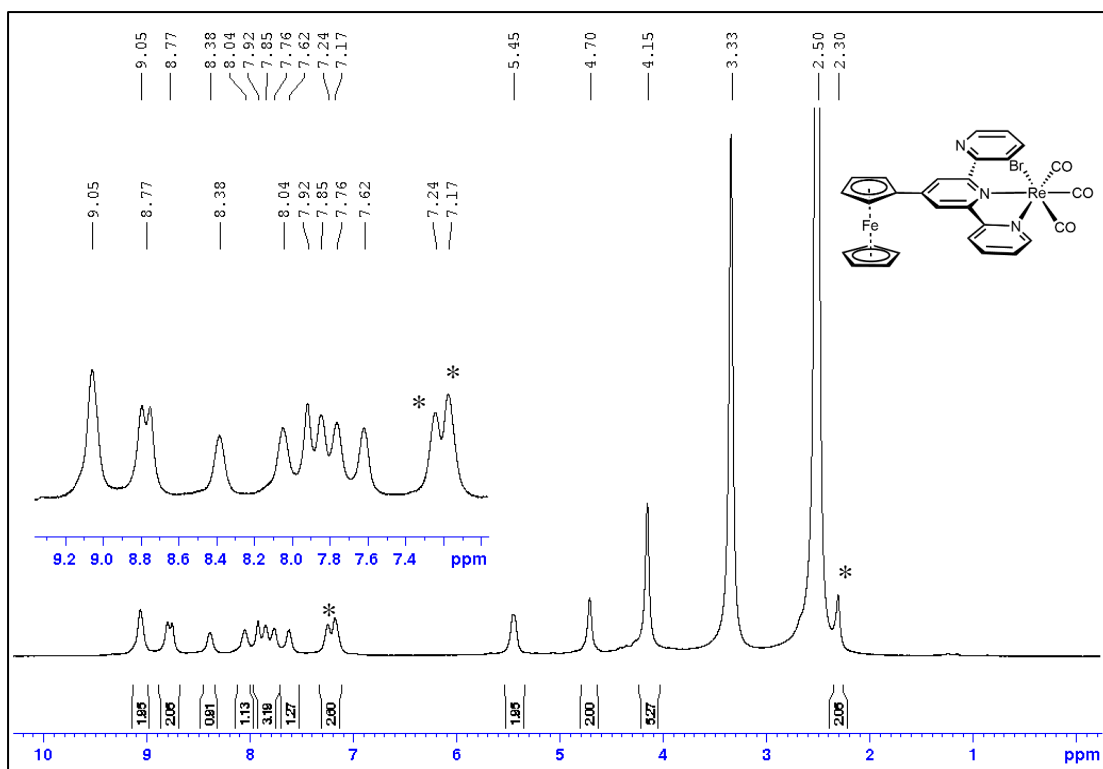


Figure S9c: ^1H NMR spectrum of **Re5** (400 MHz, DMSO-d_6) (water peak at 3.33 ppm); toluene peaks marked with *; observed at 7.24, 7.17 & 2.30 ppm; reported³ at 7.25, 7.18 & 2.30 ppm.

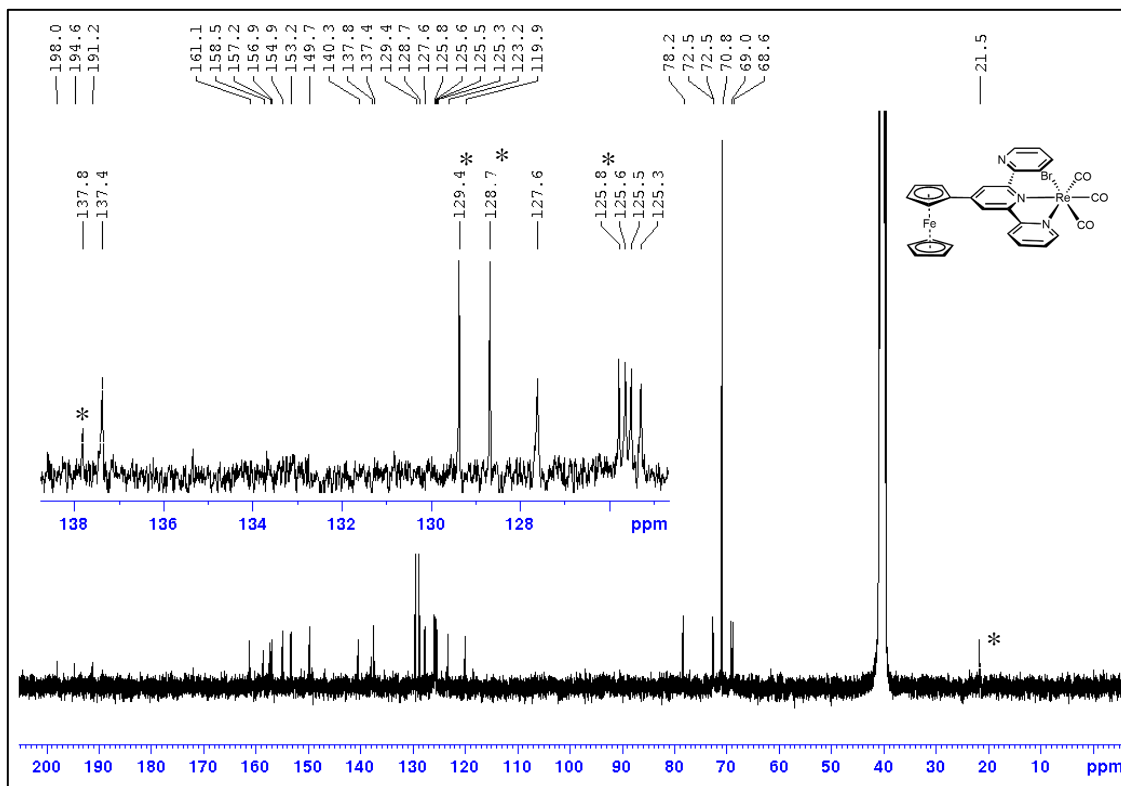


Figure S9d: $^{13}\text{C}\{^1\text{H}\}$ NMR spectrum of **Re5** (101 MHz, DMSO-d_6) with 1024 scans; toluene peaks marked with *; observed at 137.8, 129.4, 128.7, 125.8 & 21.5 ppm; reported³ at 137.4, 128.9, 128.2, 125.3 & 21.0 ppm.

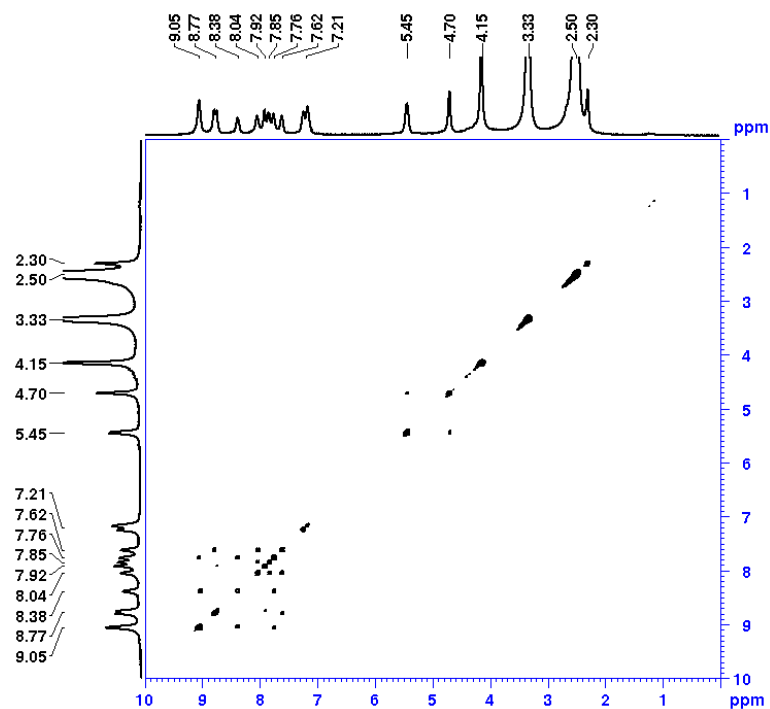


Figure S9e: COSY spectra of *Re5* (DMSO-*d*₆).

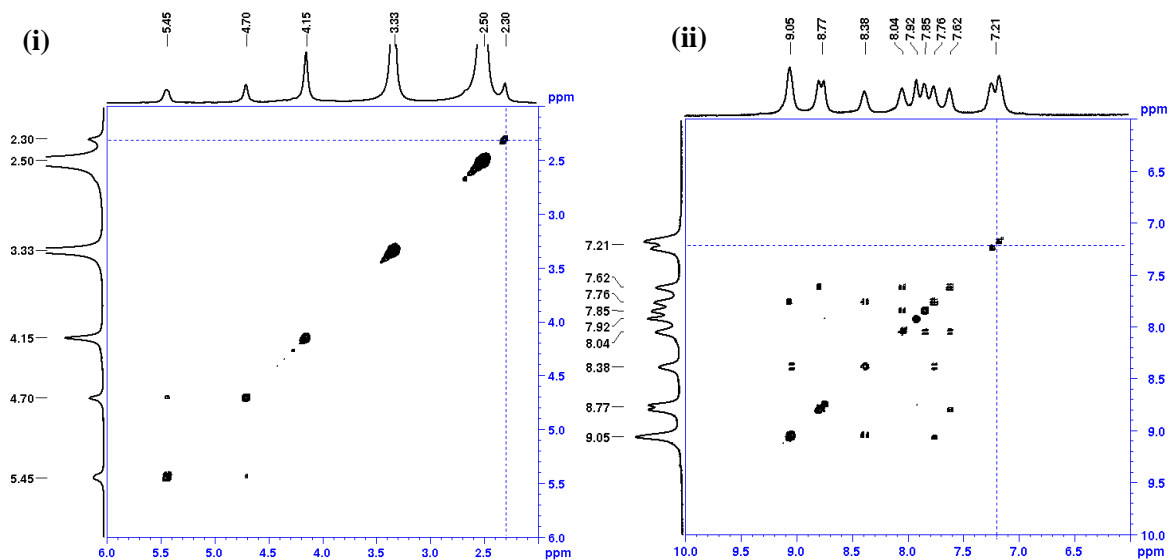


Figure S9f: (i) Section of COSY spectra (0-6 ppm) shows the -CH₃ peak of toluene, with no correlation to any other protons; (ii) Section of COSY spectra (6-10 ppm) shows the aromatic protons of toluene, having no correlation with any other aromatic peaks of the complex.

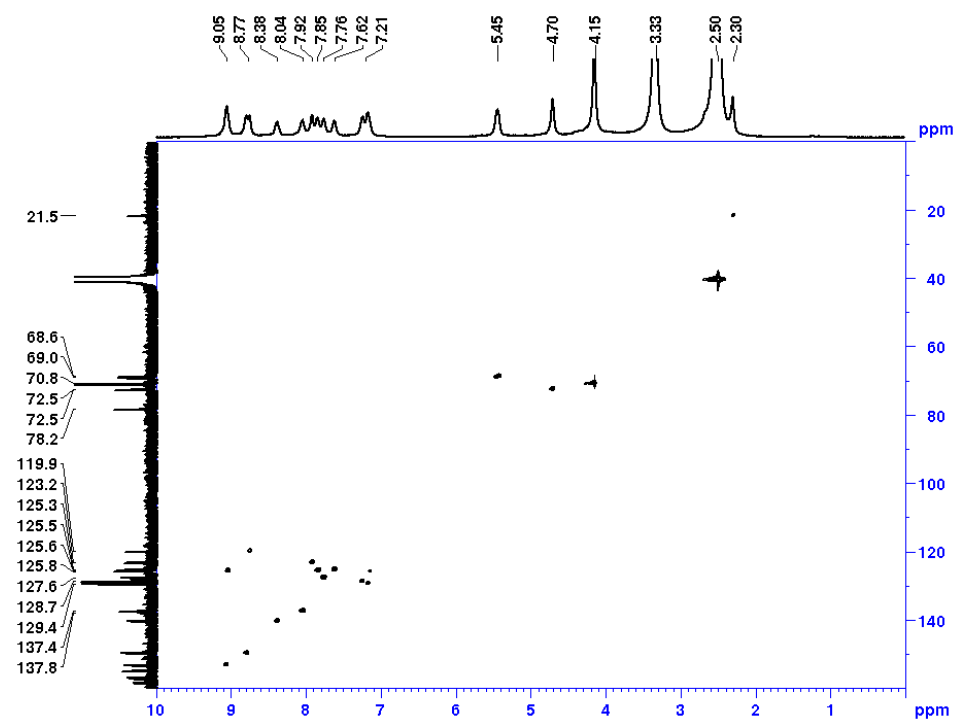


Figure S9g: HSQC spectra of **Re5** (DMSO- d_6).

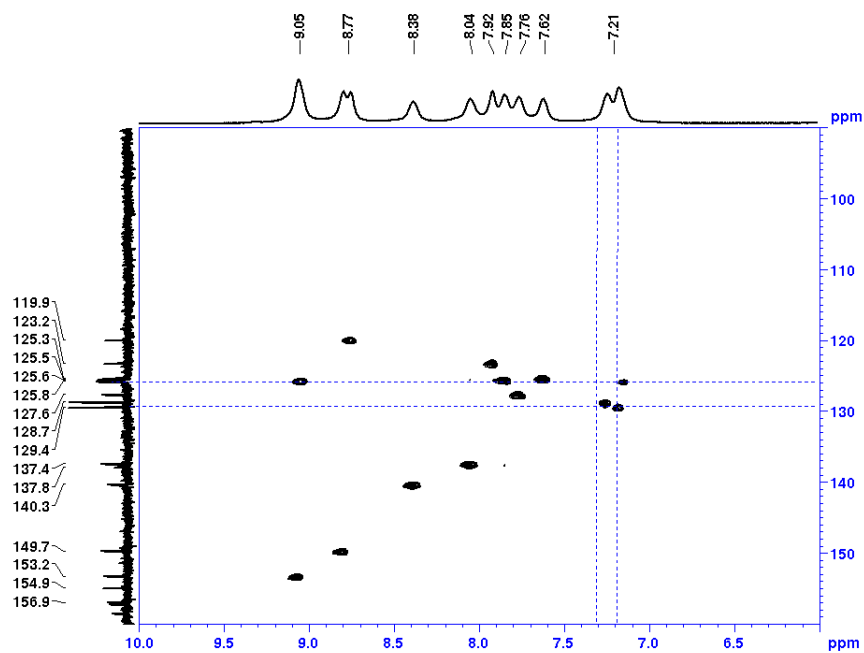


Figure S9h: HSQC spectra of the aromatic region shows three ^{13}C correlated with the protons at 7.21 ppm, which are characteristic of toluene³.

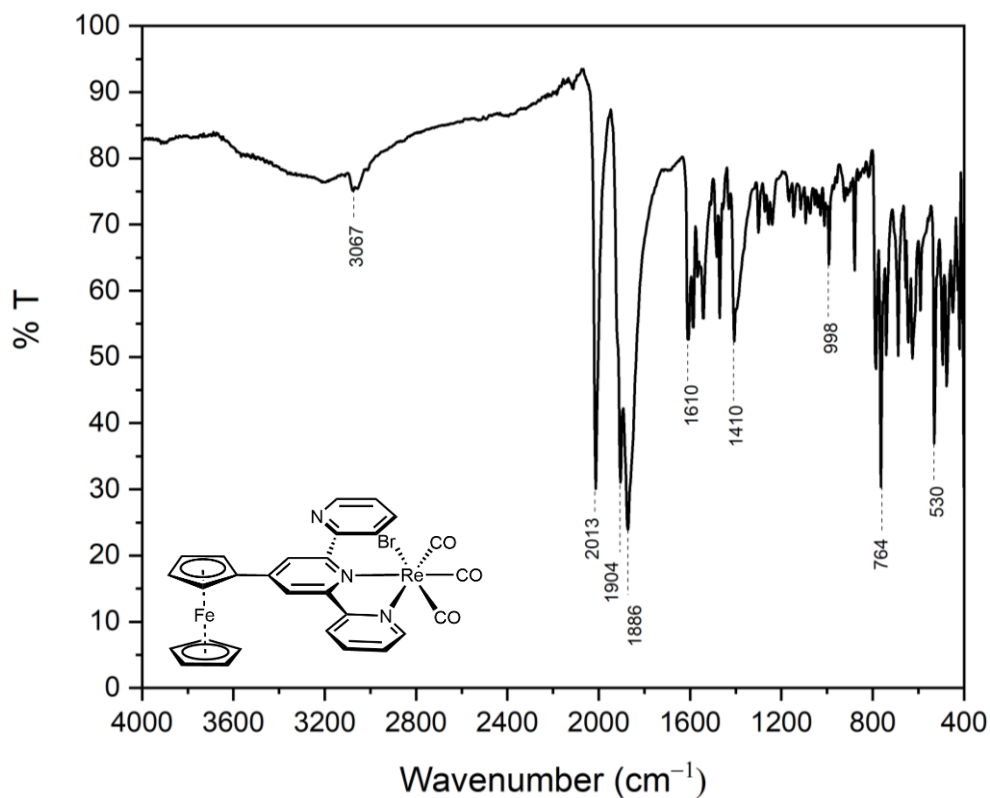


Figure S9i: ATR-IR spectrum of **Re5**.

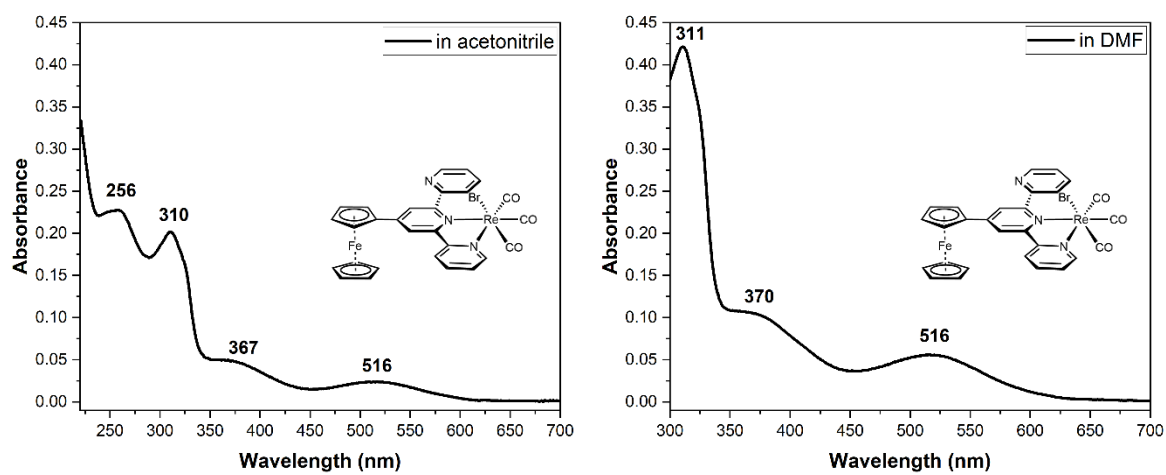


Figure S9j: Absorbance spectra of **Re5** (0.01 mM) in acetonitrile and DMF.

<Sample Information>

Sample Name : Re5
 Sample ID : Re5
 Data Filename : Re5_27-03-2023_003.lcd
 Method Filename : C_95_D_5_10_min_0.2ml_min.lcm
 Batch Filename : 27032023.lcb
 Vial # : 1-93
 Injection Volume : 0.5 uL
 Date Acquired : 3/27/2023 10:22:05 AM
 Date Processed : 3/27/2023 10:32:10 AM
 Sample Type : Unknown
 Acquired by : IIT GOA
 Processed by : IIT GOA

<Chromatogram>

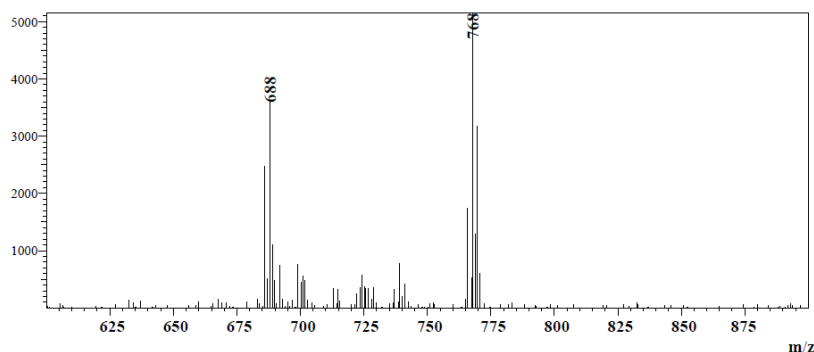
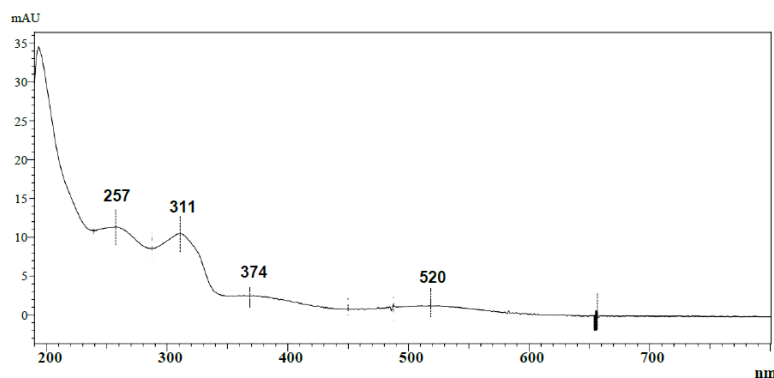
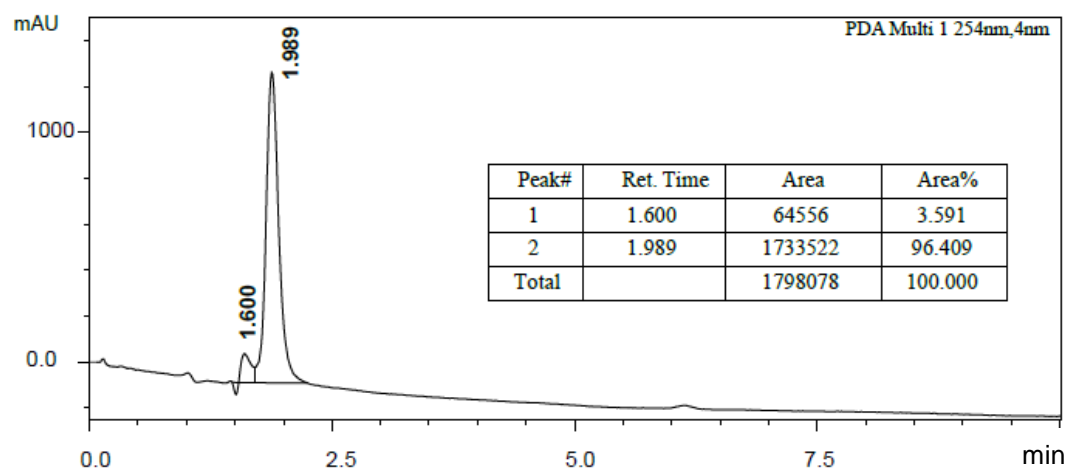


Figure S9k: RP-HPLC-MS and corresponding UV-Vis spectra of **Re5** at $t_R = 1.989$ min; HPLC purity 96.4%; m/z values for $t_R =$ for 1.600 & 1.989 min shows same m/z ; Mass fragmentation pattern at 1.989 min [$C_{28}H_{19}BrFeN_3O_3Re = M$], $m/z = 768$ [$M+H$]⁺ ($C_{28}H_{20}BrFeN_3O_3Re$), $m/z = 688$ [$M-Br$]⁺ ($C_{28}H_{19}N_3O_3Re$).

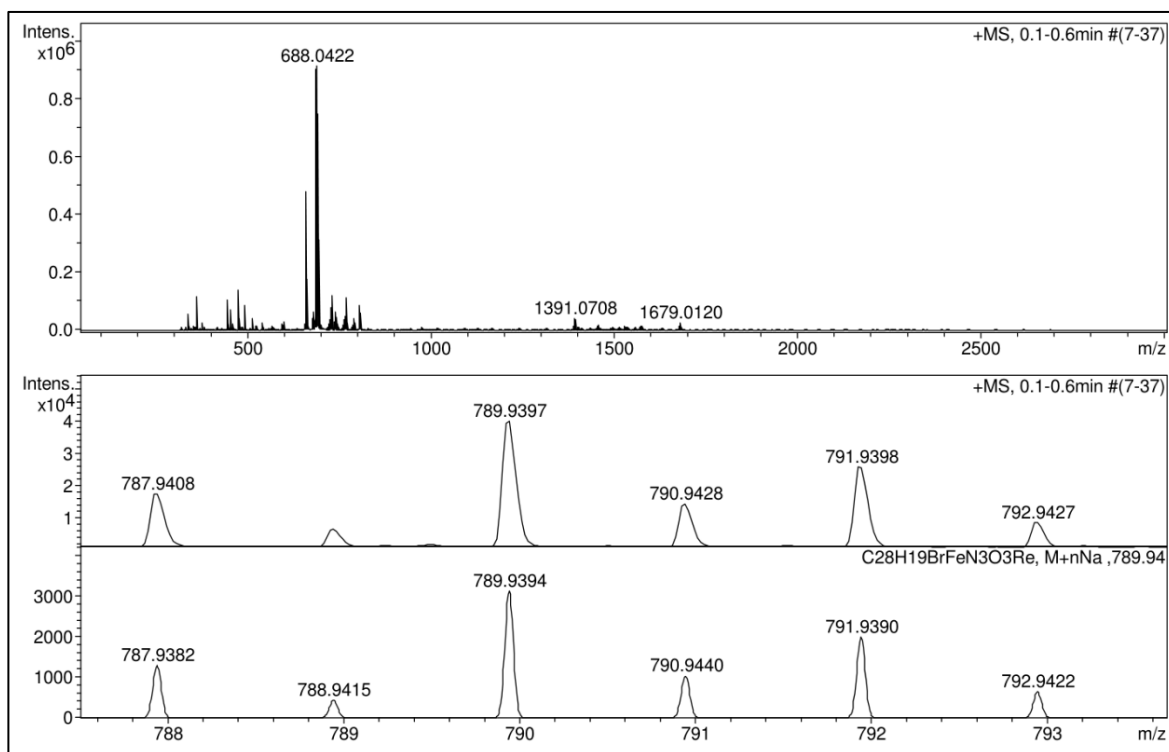
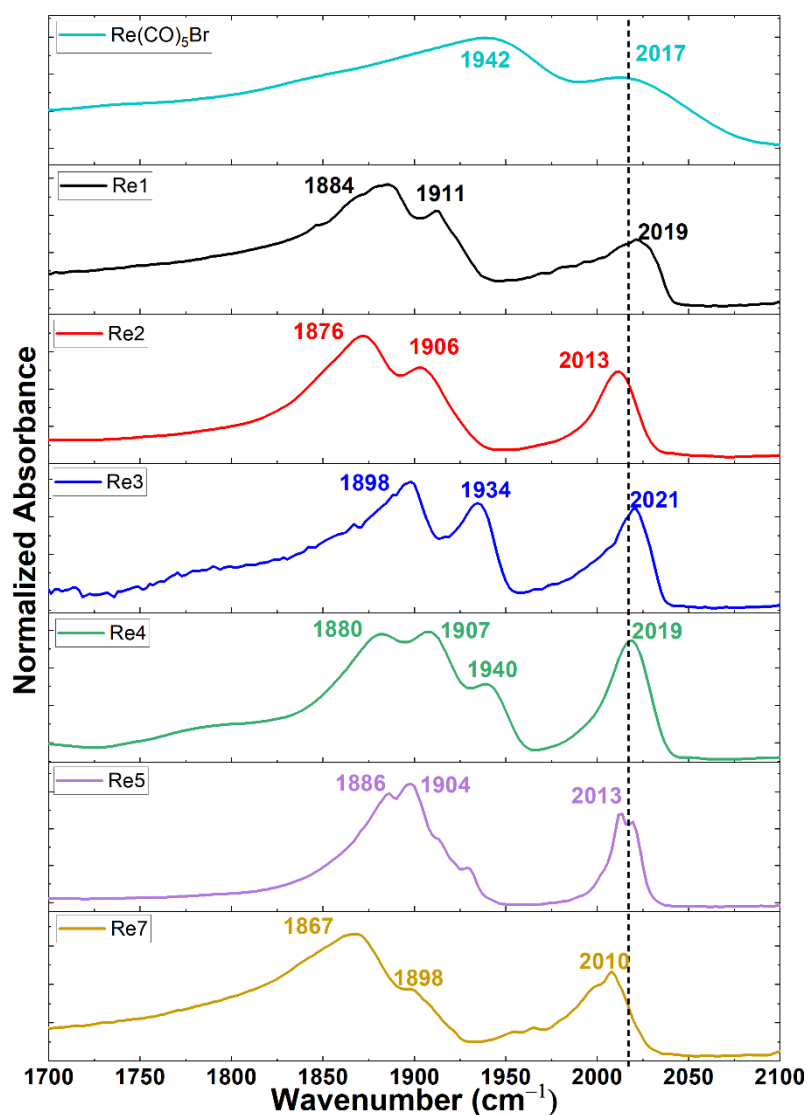


Figure S9i: HRMS for Re5 [$C_{28}H_{19}BrFeN_3O_3Re = M$] Calcd for $[M+Na]^+$ $m/z = 789.9394$ ($C_{28}H_{19}^{79}BrFeN_3O_3ReNa$) found $m/z = 789.9397$ $[M+Na]^+$; Calcd for $[(M-Br)^+]$ $m/z = 688.0352$ found $m/z = 688.0422$.



<i>Re(I) complexes</i>	$\nu_{\text{str}(\text{C}=\text{O})} (\text{cm}^{-1})$		
<i>Re(CO)₅Br</i>	2017	1942	
<i>Re1</i>	2019	1911	1884
<i>Re2</i>	2013 (2018) ¹	1906 (1909)	1876 (1878)
<i>Re3</i>	2021	1934	1898
<i>Re4</i>	2019	1940 & 1907	1880
<i>Re5</i>	2013	1904	1886
<i>Re(bpy)(CO)₃Br/Re7</i>	2010(2011) ²	1898 (1903)	1867 (1880)

Figure S10: Comparisons of infrared spectra for all *Re(I)* complexes and *Re(CO)₅Br*, the starting precursor. In the parenthesis, previously reported values are shown.

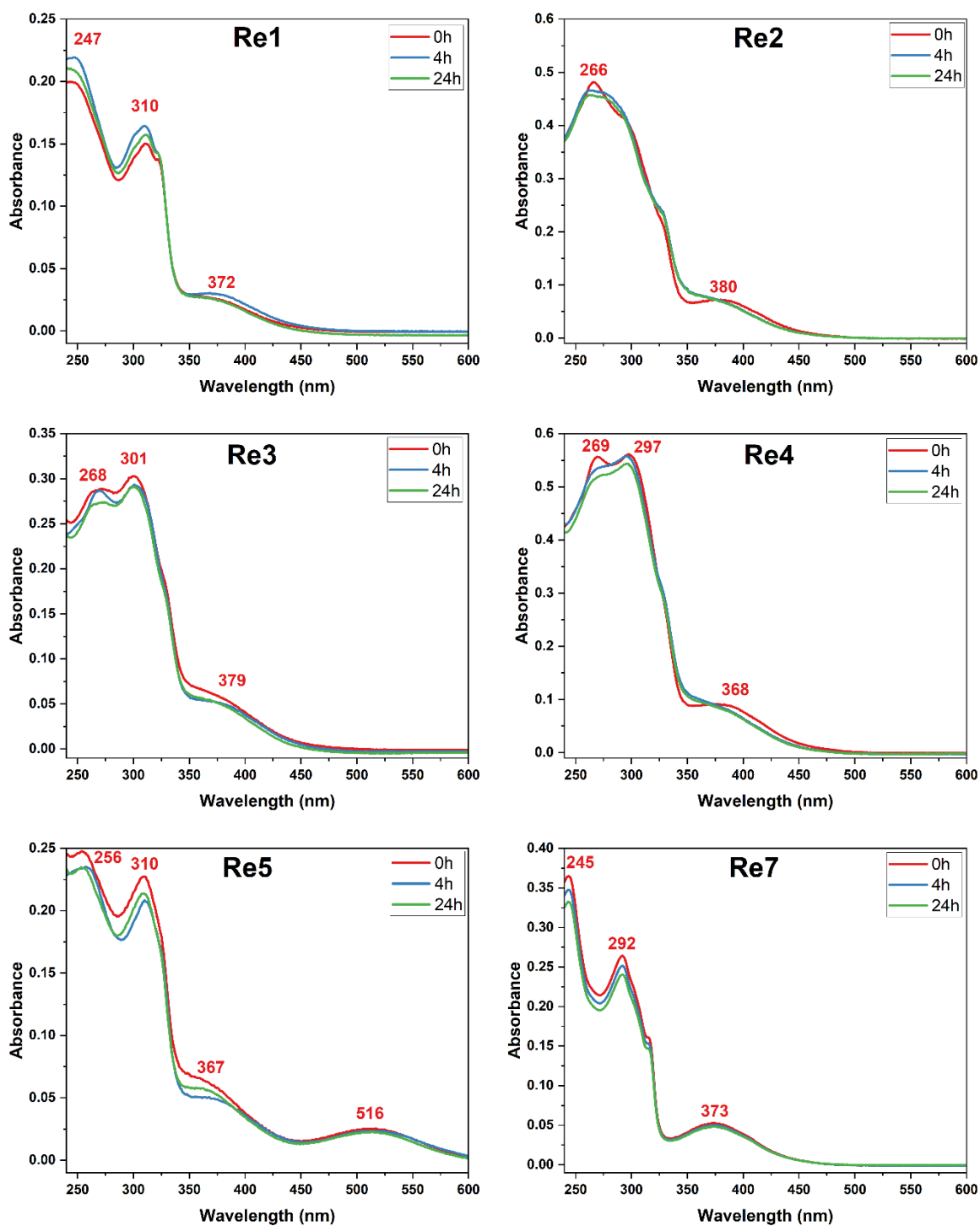
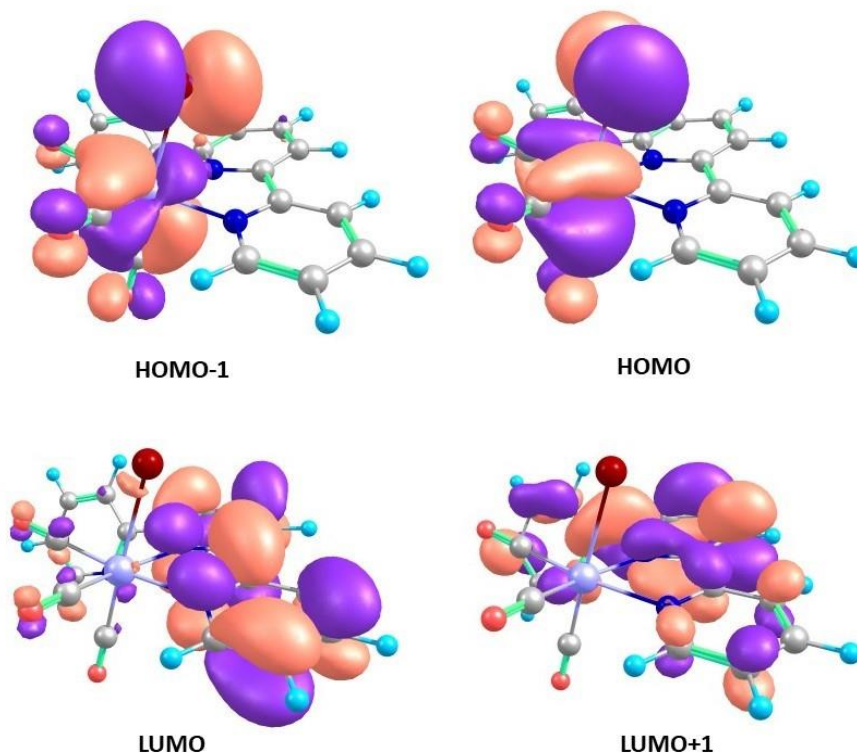


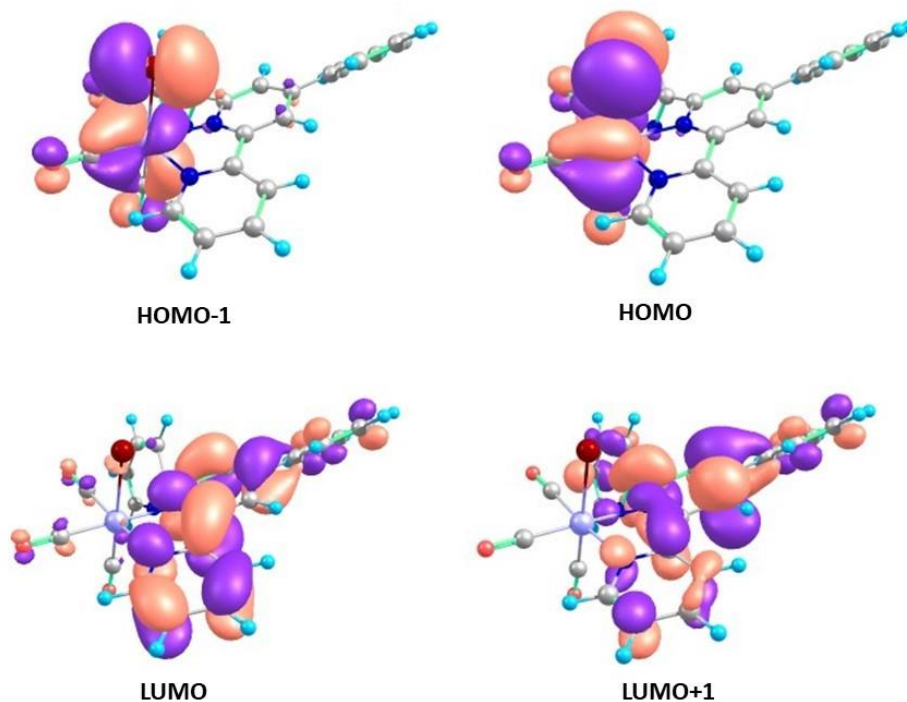
Figure S11.: UV-Vis spectral changes in Re(I) complexes (0.01 mM in acetonitrile, obtained from diluting a stock solution of 0.3 mM in acetonitrile) shown at certain time intervals 0 h, 4 h and 24 h. The sample was kept at ambient condition.



<i>Transition Wavelength(nm)</i>	<i>Oscillator Strength</i>	<i>Excitations</i>	<i>Nature</i>
249	0.180	$\pi(tpy) \rightarrow \pi^*(tpy)$ $p_x(Br) \rightarrow \pi^*(tpy)$	ILCT
256	0.146	$\pi(tpy) \rightarrow \pi^*(tpy)$ $p_y(Br) \rightarrow \pi^*(tpy)$	ILCT
303	0.393	$\pi(tpy) \rightarrow \pi^*(tpy)$ $\pi_{yz}(Re-Br) \rightarrow \pi^*(tpy)$	Combination of MLCT and ILCT
431	0.056	$5d_{yz}(Re), 4p_y(Br) \rightarrow \pi^*(tpy)$	MLCT

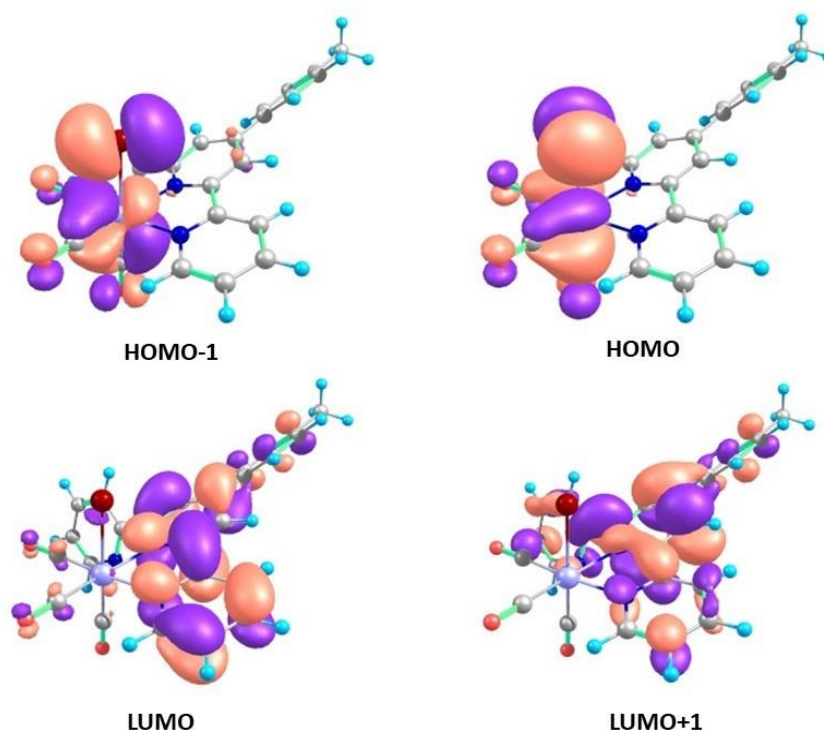
tpy=terpyridine

Figure S12: Frontier Molecular Orbitals of complex **ReI**; with TDDFT data calculated at B3LYP/Def2-TZVP level of theory using acetonitrile as implicit solvent.



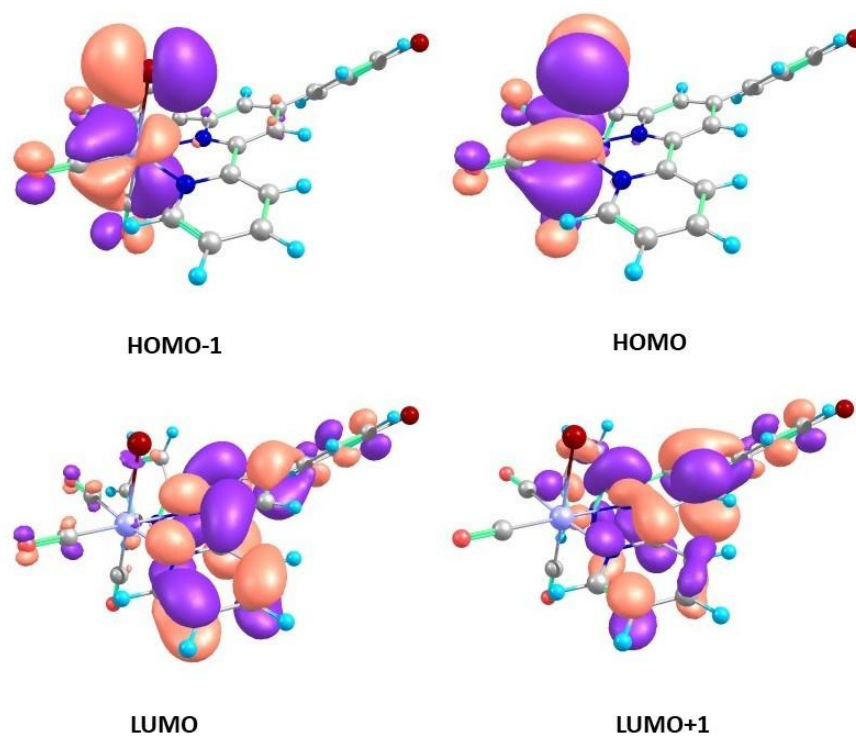
<i>Transition Wavelength(nm)</i>	<i>Oscillator Strength</i>	<i>Excitations</i>	<i>Nature</i>
281	0.355	$\pi(tpy) \rightarrow \pi^*(tpy)$ $p_y(Br) \rightarrow \pi^*(tpy)$	<i>ILCT</i>
309	0.287	$\pi(tpy) \rightarrow \pi^*(tpy)$ $\pi_{yz}(Re-Br) \rightarrow \pi^*(tpy)$	<i>Combination of MLCT and ILCT</i>
438	0.088	$5d_{yz}(Re), 4p_y(Br) \rightarrow \pi^*(tpy)$	<i>MLCT</i>

Figure S13: Frontier Molecular Orbitals of complex **Re2**; with TDDFT data calculated at B3LYP/Def2-TZVP level of theory using acetonitrile as implicit solvent.



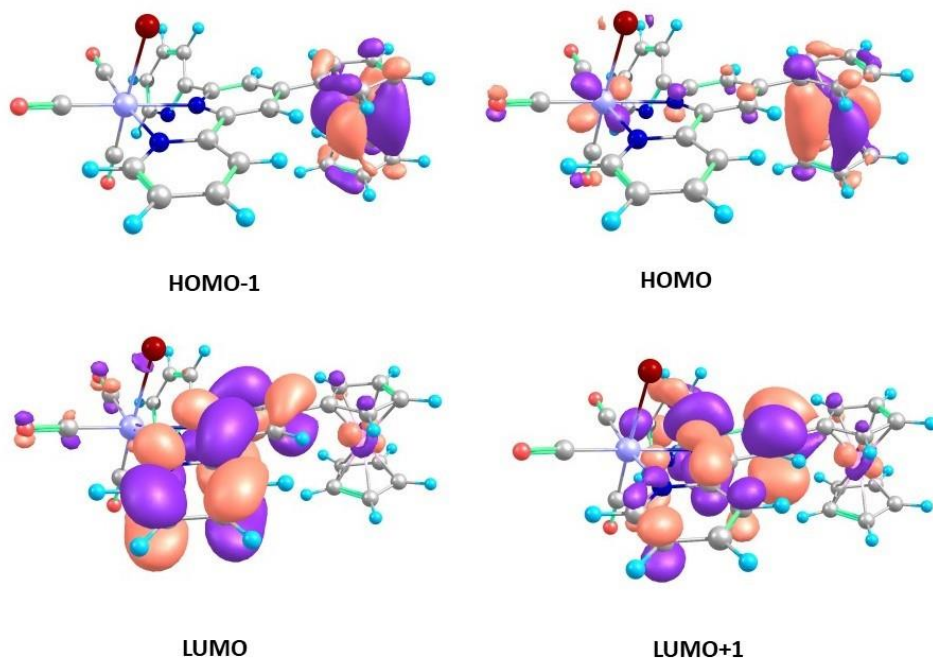
<i>Transition Wavelength(nm)</i>	<i>Oscillator Strength</i>	<i>Excitations</i>	<i>Nature</i>
287	0.328	$\pi(tpy) \rightarrow \pi^*(tpy)$ $p_y(Br) \rightarrow \pi^*(tpy)$	ILCT
309	0.227	$\pi(tpy) \rightarrow \pi^*(tpy)$ $\pi_{yz}(Re-Br) \rightarrow \pi^*(tpy)$	Combination of MLCT and ILCT
436	0.098	$5d_{yz}(Re), 4p_y(Br) \rightarrow \pi^*(tpy)$	MLCT

Figure S14: Frontier Molecular Orbitals of complex **Re3**; with TDDFT data calculated at B3LYP/Def2-TZVP level of theory using acetonitrile as implicit solvent.



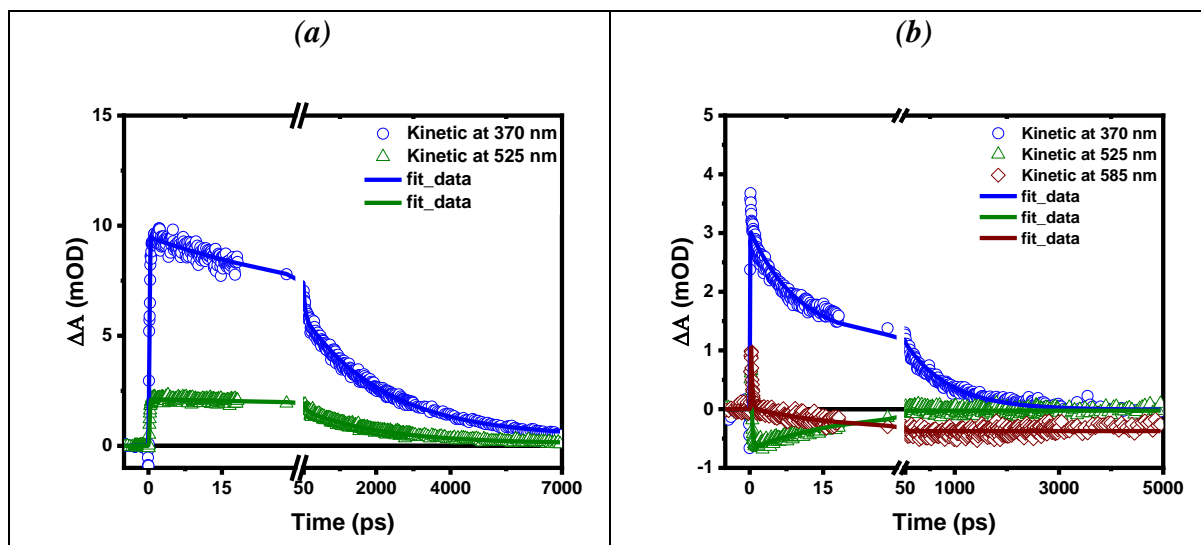
<i>Transition Wavelength(nm)</i>	<i>Oscillator Strength</i>	<i>Excitations</i>	<i>Nature</i>
285	0.437	$\pi(tpy) \rightarrow \pi^*(tpy)$ $p_y(Br) \rightarrow \pi^*(tpy)$	ILCT
310	0.211	$\pi(tpy) \rightarrow \pi^*(tpy)$ $\pi_{yz}(Re-Br) \rightarrow \pi^*(tpy)$	Combination of MLCT and ILCT
441	0.095	$5d_{yz}(Re), 4p_y(Br) \rightarrow \pi^*(tpy)$	MLCT

Figure S15: Frontier Molecular Orbitals of complex **Re4**; with TDDFT data calculated at B3LYP/Def2-TZVP level of theory using acetonitrile as implicit solvent.



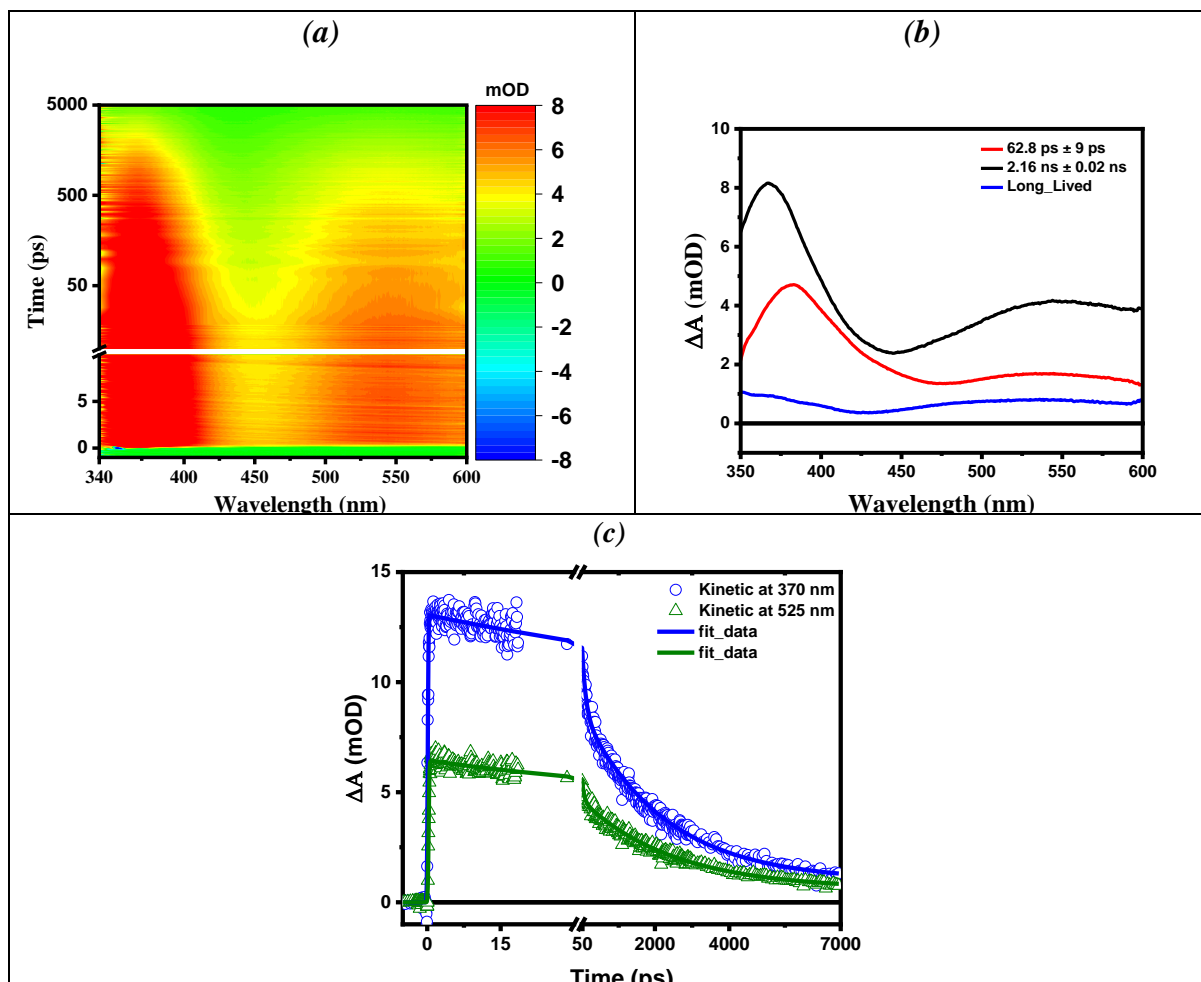
<i>Transition Wavelength(nm)</i>	<i>Oscillator Strength</i>	<i>Excitations</i>	<i>Nature</i>
282	0.260	$\pi(tpy) \rightarrow \pi^*(tpy)$ $p_y(Br) \rightarrow \pi^*(tpy)$	ILCT
309	0.197	$\pi(tpy) \rightarrow \pi^*(tpy)$ $\pi_{yz}(Re-Br) \rightarrow \pi^*(tpy)$	Combination of MLCT and ILCT
438	0.098	$3d_{xy}(Fe) \rightarrow \pi^*(tpy)$ $5d_{yz}(Re), 4p_y(Br) \rightarrow \pi^*(tpy)$	MLCT
516	0.008	$3d_{x^2-y^2}(Fe) \rightarrow 3d_{xz}(Fe)$ $3d_{z^2}(Fe) \rightarrow 3d_{yz}(Fe)$	d-d transition
602	0.013	$3d_{x^2-y^2}(Fe) \rightarrow 3d_{xz}(Fe)$ $3d_{xy}(Fe) \rightarrow 3d_{yz}(Fe)$	d-d transition

Figure S16: Frontier Molecular Orbitals of complex **Re5**; with TDDFT data calculated at B3LYP/Def2-TZVP level of theory using acetonitrile as implicit solvent.



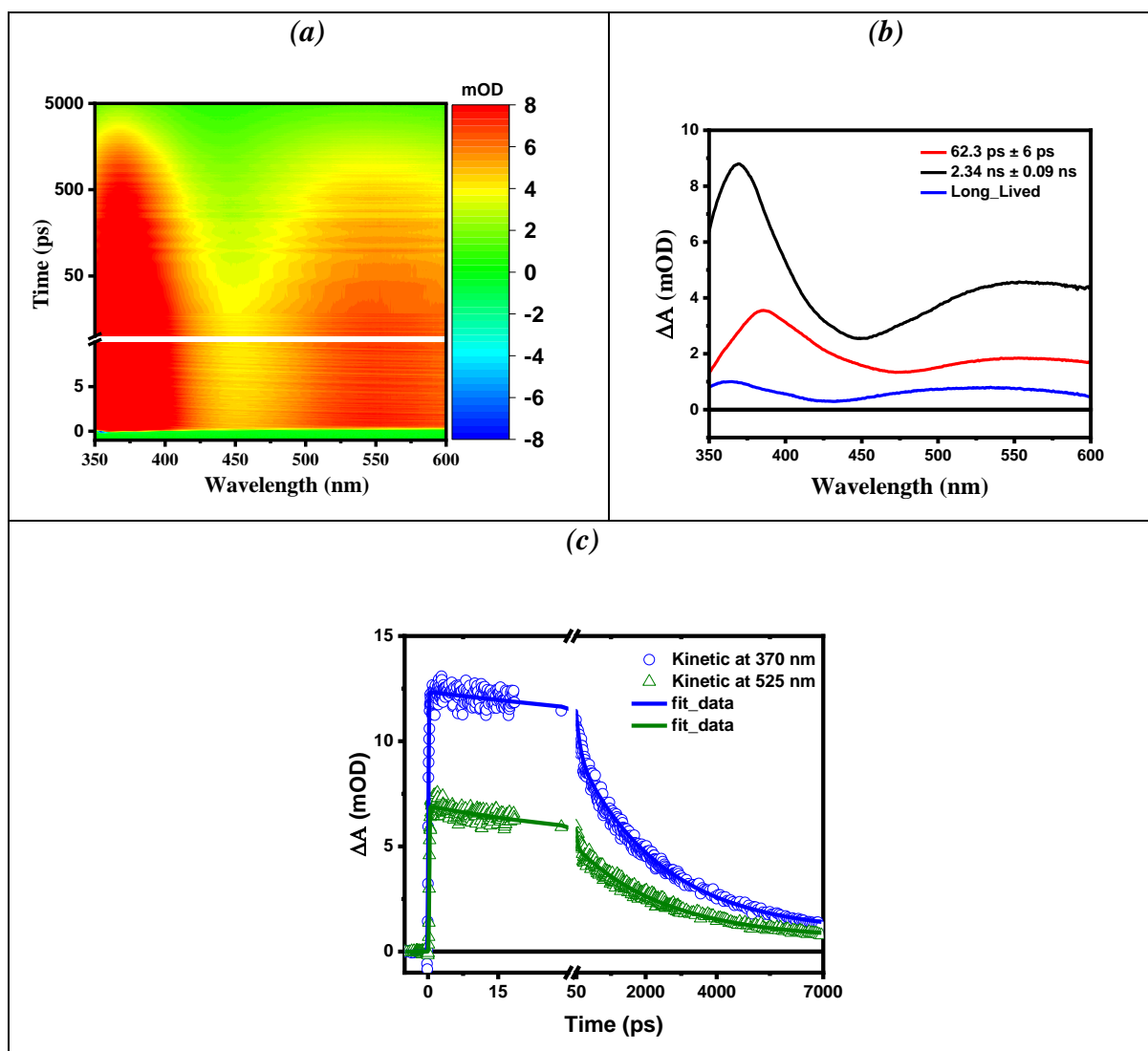
<i>Compound</i>	<i>Wavelength (nm)</i>	τ_1 (ps)	τ_2 (ps)	<i>Standard Deviation</i>
Re1	370	46 ± 5 (0.0034 ± 0.0001) 0.38	2212 ± 149 (0.0055 ± 0.0001) 0.62	0.0002
	525	97 ± 25 (0.0005 ± 0.00001) 0.25	2212 ± 164 (0.0015 ± 0.00003) 0.75	0.0001
	370 nm	10 ± 0.7 0.0018 ± 0.00001 0.60	855.0 0.0012 ± 0.0001 0.40	0.0001
Re5	525 nm		19 ± 3 -0.0006 ± 0.00003	0.00001
	585 nm	-	18 ± 3 0.0003 ± 0.00002	0.00001

Figure S17: Kinetic traces at 370 nm and 525 nm for **Re1** (a) and 370 nm, 525nm, and 585 nm for **Re5** (b), with the kinetic fitting parameters in the table.



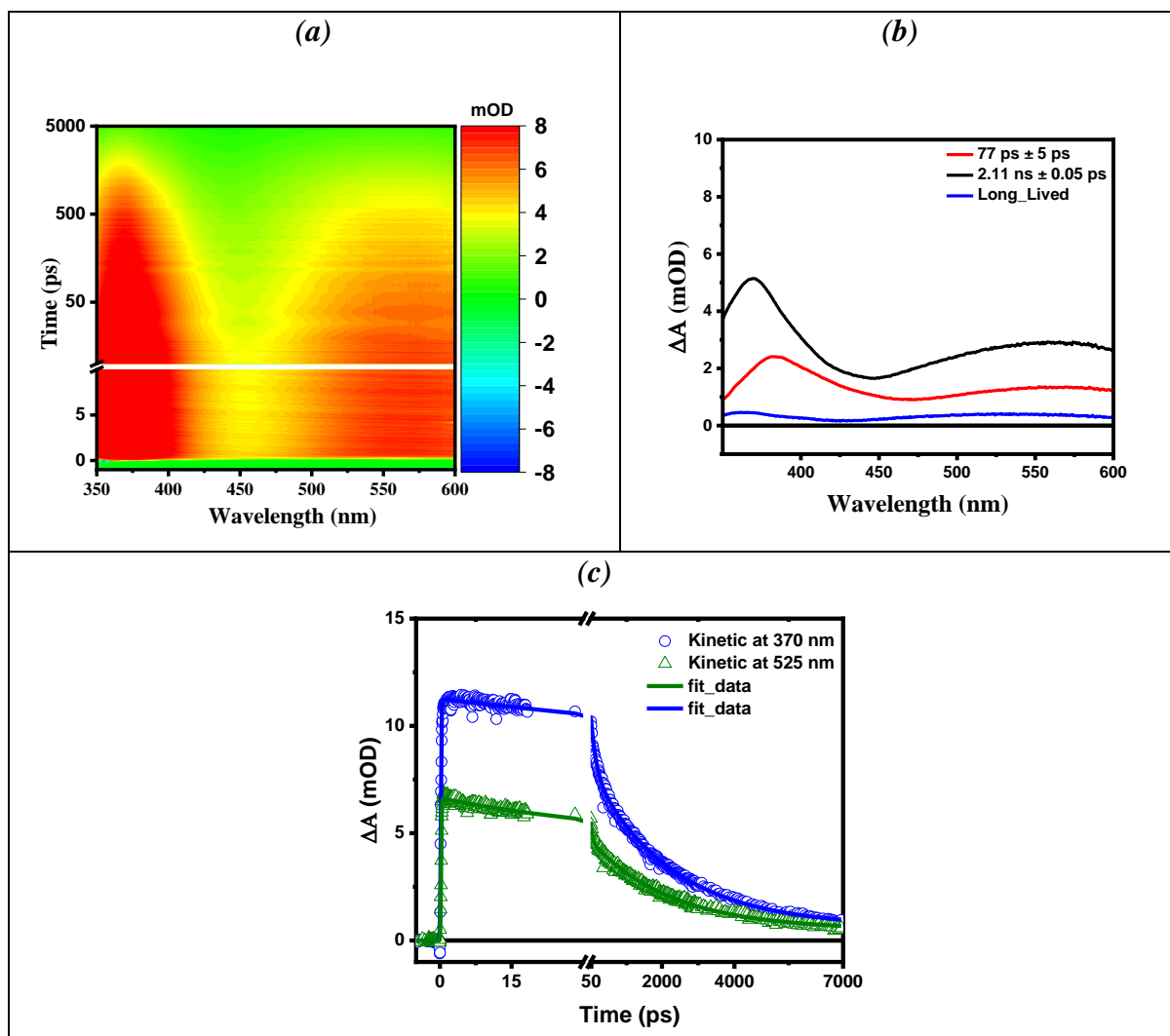
<i>Compound</i>	<i>Wavelength (nm)</i>	τ_1 (ps)	τ_2 (ps)	<i>Standard Deviation</i>
<i>Re2</i>	370	100 ± 18	2213 ± 210	0.0003
		(0.0042 ± 0.0002)	(0.007 ± 0.0002)	
	525	0.37	0.63	0.0002
		58 ± 11	2466 ± 200	
		(0.0020 ± 0.0001)	(0.0040 ± 0.0001)	
		0.29	0.71	

Figure S18: (a) 2D plots of *Re2*, (b) global lifetime analysis, (c) Kinetic traces at 370 nm and 525 nm; with the kinetic fitting parameters in the table.



<i>Compound</i>	<i>Wavelength (nm)</i>	τ_1 (ps)	τ_2 (ps)	<i>Standard Deviation</i>
<i>Re3</i>	370	118 ± 25	2438 ± 180	0.0002
		(0.0028 ± 0.0002)	(0.0086 ± 0.0001)	
	525	0.19	0.81	0.0002
		46 ± 8	2585 ± 206	
		(0.0018 ± 0.0001)	(0.0044 ± 0.0001)	
		0.29	0.71	

Figure S19: (a) 2D plots of *Re3*, (b) global lifetime analysis, (c) Kinetic traces at 370 nm and 525 nm; with the kinetic fitting parameters in the table.



<i>Compound</i>	<i>Wavelength (nm)</i>	τ_1 (ps)	τ_2 (ps)	<i>Standard Deviation</i>
<i>Re4</i>	370	141 ± 19	2210 ± 130	0.0001
		(0.0021 ± 0.0001)	(0.0049 ± 0.0001)	
	525	45 ± 4	2226 ± 95	0.0001
		(0.0012 ± 0.0001)	(0.0028 ± 0.0001)	
		0.30	0.70	

Figure S20: (a) 2D plots of *Re4*, (b) global lifetime analysis, (c) Kinetic traces at 370 nm and 525 nm; with the kinetic fitting parameters in the table.

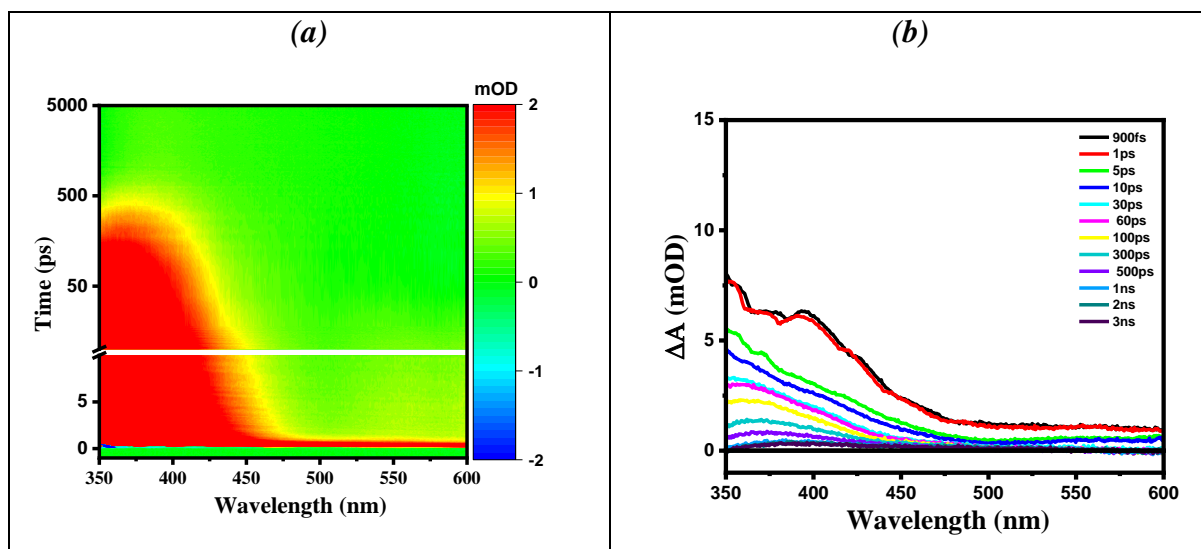


Figure S21: (a) 2D plots of *L5*, (b) transient absorption spectra at different delay times.

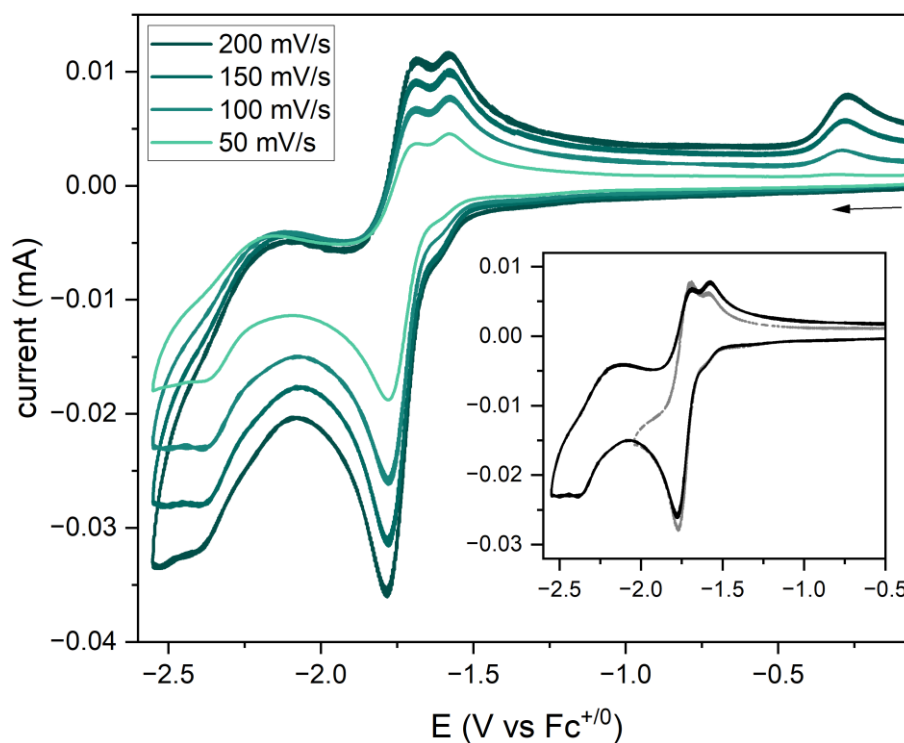


Figure S22: Scan rate dependent cyclic voltammograms of 1 mM *ReI* in N_2 saturated acetonitrile containing 0.1 M $n\text{-Bu}_4\text{NBF}_4$ as the supporting electrolyte. The inset figure shows the voltammogram of *ReI* when the scan is reversed before the second reduction.

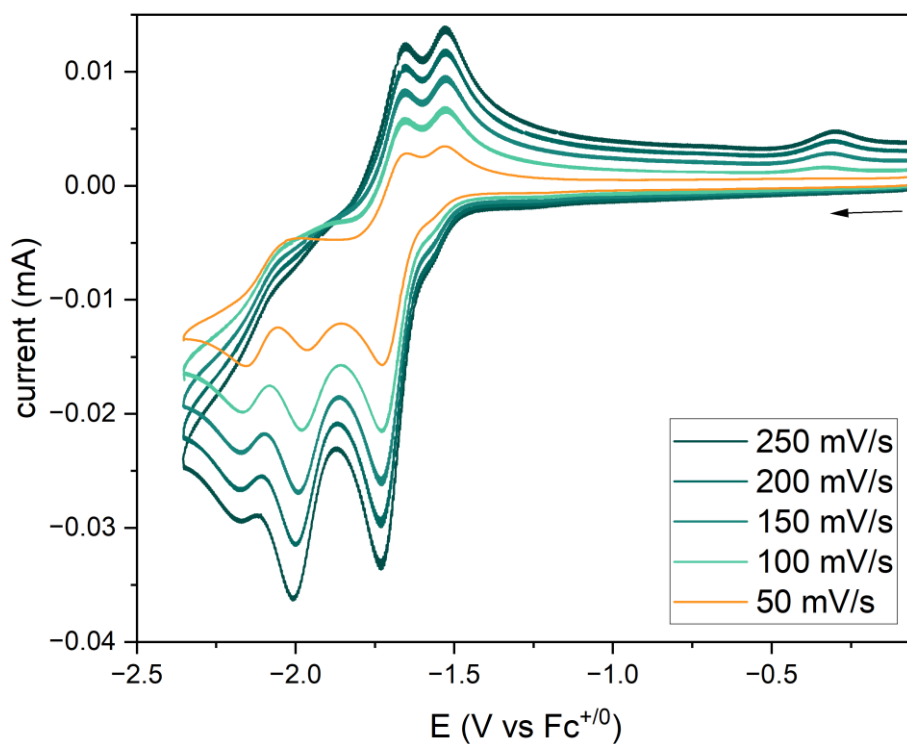


Figure S23: Scan rate dependent cyclic voltammograms of 1 mM **Re2** in N_2 saturated acetonitrile containing 0.1 M $n\text{-Bu}_4\text{NBF}_4$ as the supporting electrolyte.

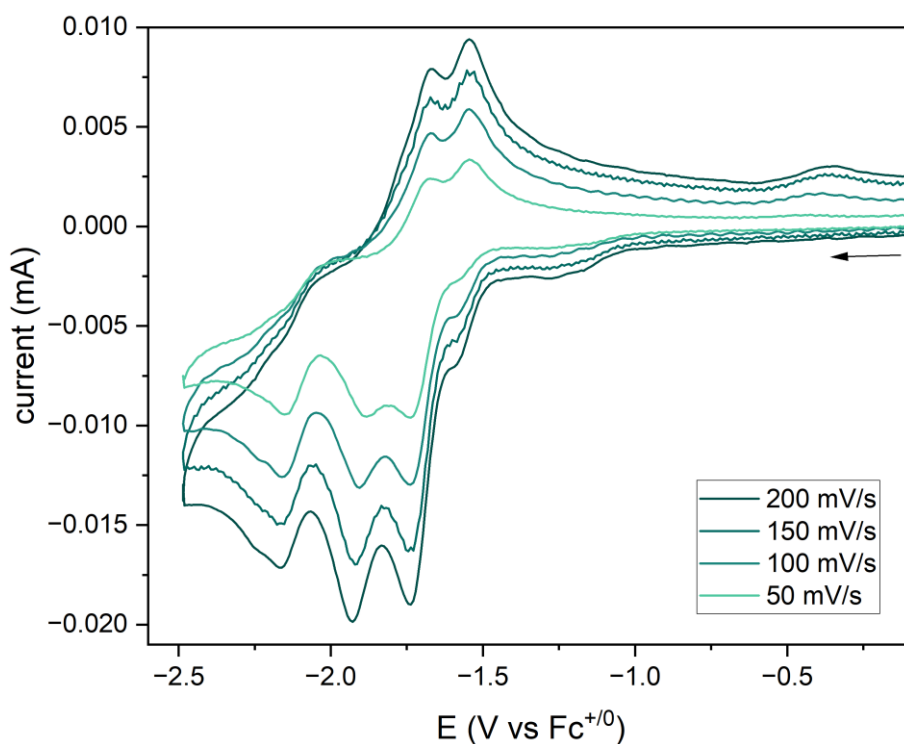


Figure S24: Scan rate dependent cyclic voltammograms of 0.6 mM **Re3** in N_2 saturated acetonitrile containing 0.1 M $n\text{-Bu}_4\text{NBF}_4$ as the supporting electrolyte.

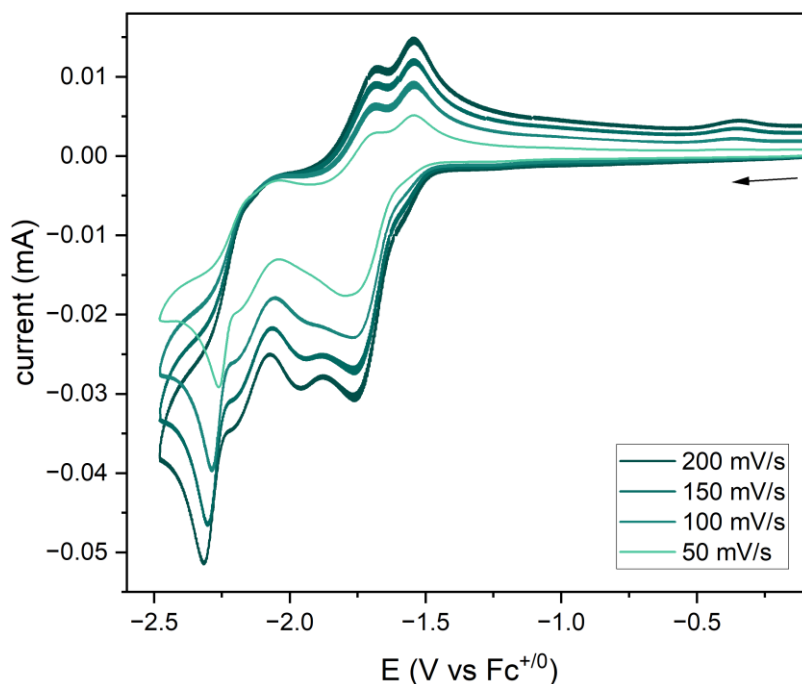


Figure S25: Scan rate dependent cyclic voltammograms of 1 mM **Re4** in N_2 saturated acetonitrile containing 0.1 M $n\text{-Bu}_4\text{NBF}_4$ as the supporting electrolyte.

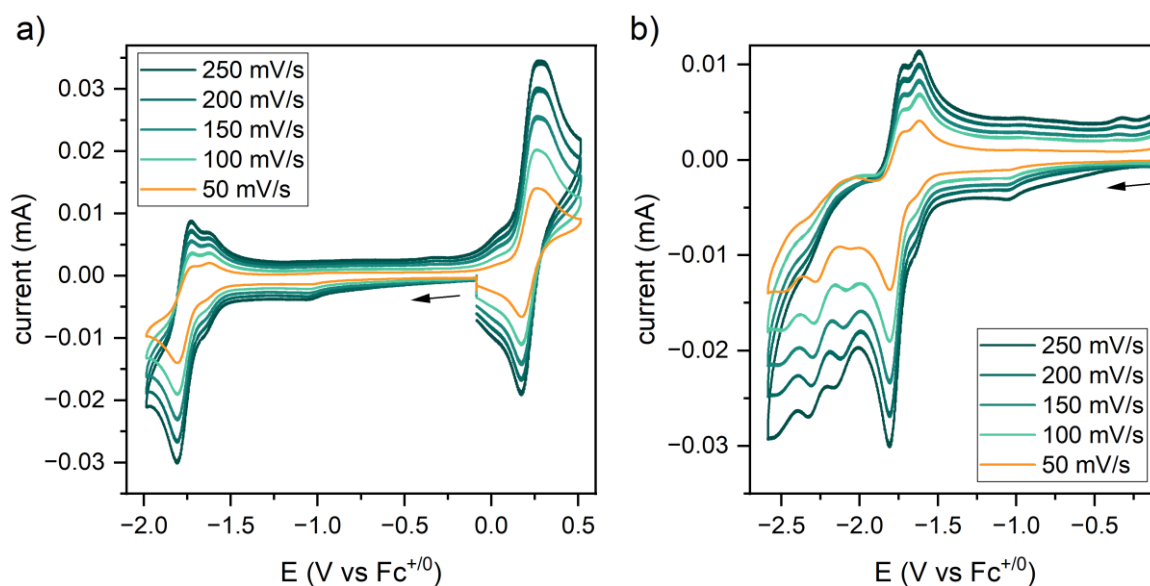


Figure S26: Scan rate dependent cyclic voltammograms of 1 mM **Re5** in N_2 saturated acetonitrile containing 0.1 M $n\text{-Bu}_4\text{NBF}_4$ as the supporting electrolyte. Figure (a) shows oxidative event(s) and the first reduction event. Figure (b) shows the reduction processes occurring before -2.5 V.

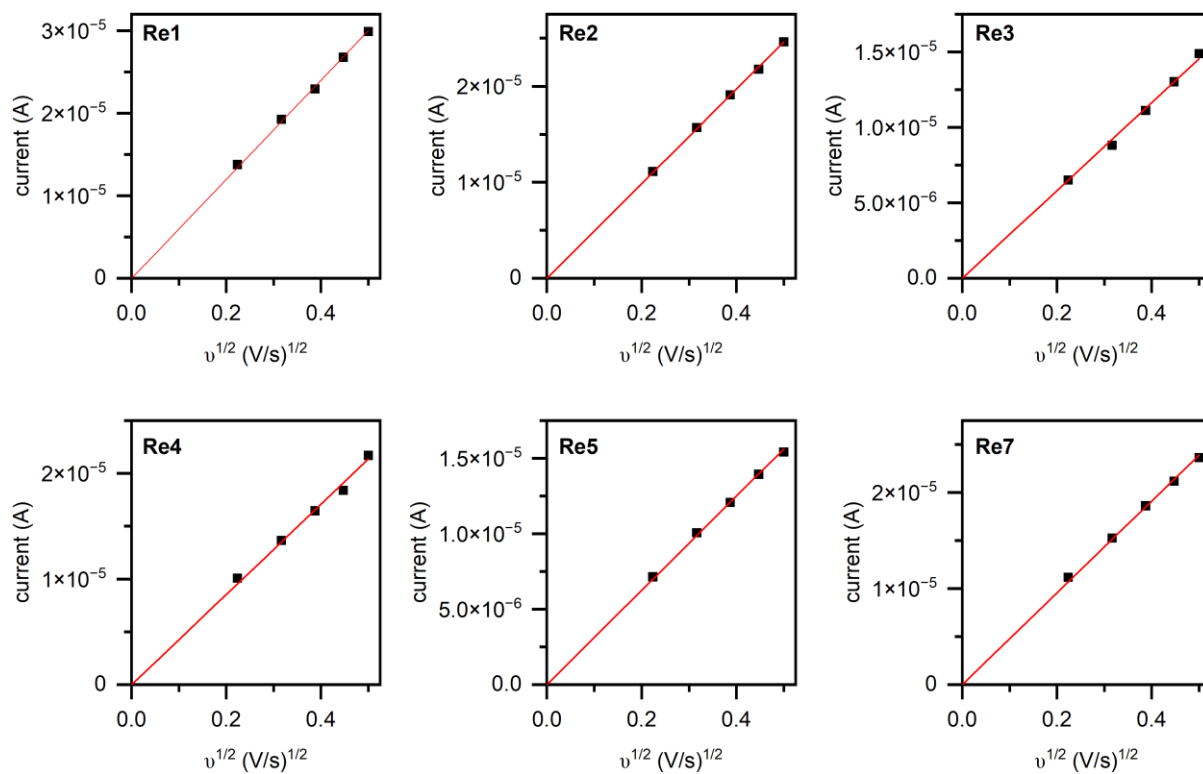


Figure S27: Determination of diffusion coefficients from scan rate dependent CVs shown in **Figure S22-26**. Peak currents for the first reductive step (~ -1.8 V) vs the square root of the scan rate for **Re1-5** and **Re7**.

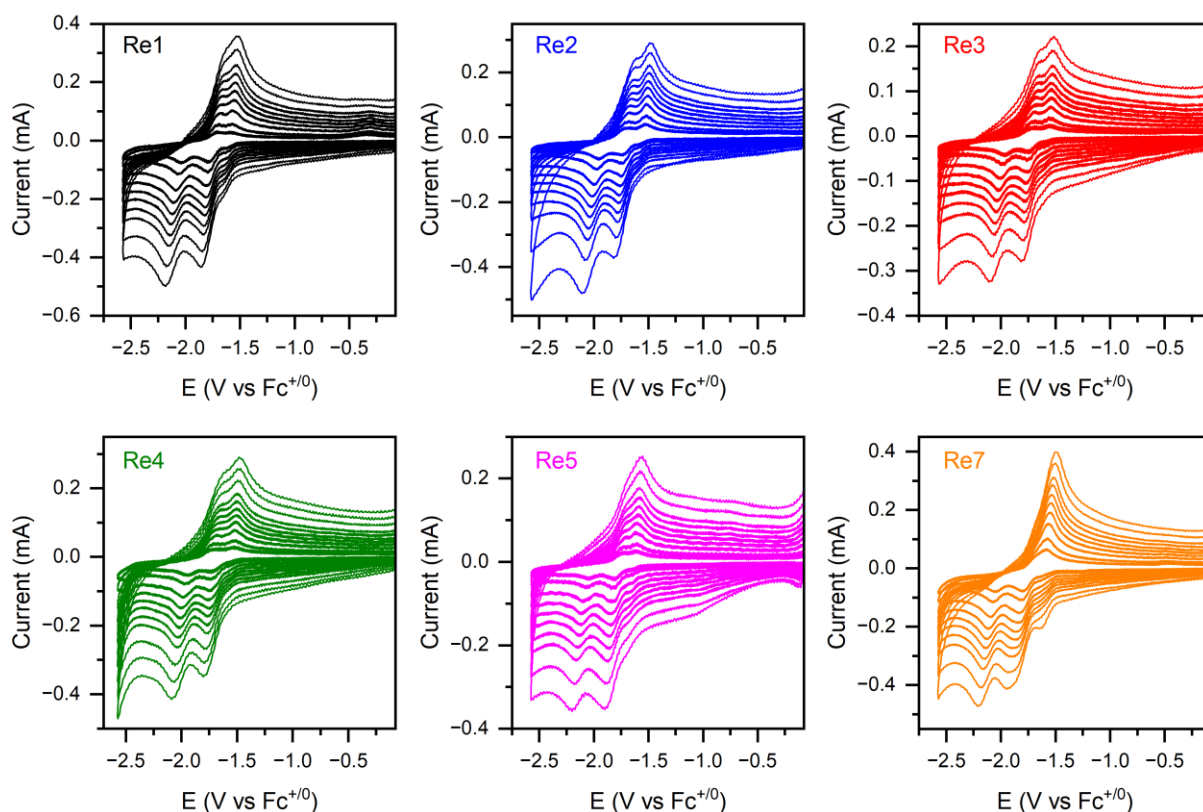


Figure S28: Scan rate dependent cyclic voltammograms of **Re1-5** and **Re7** at fast scan rates (25, 20, 15, 12.5, 10, 8, 6, 4, 2, 1 $V s^{-1}$) in N_2 saturated acetonitrile containing 0.1 M $n-Bu_4NBF_4$ as the supporting electrolyte.

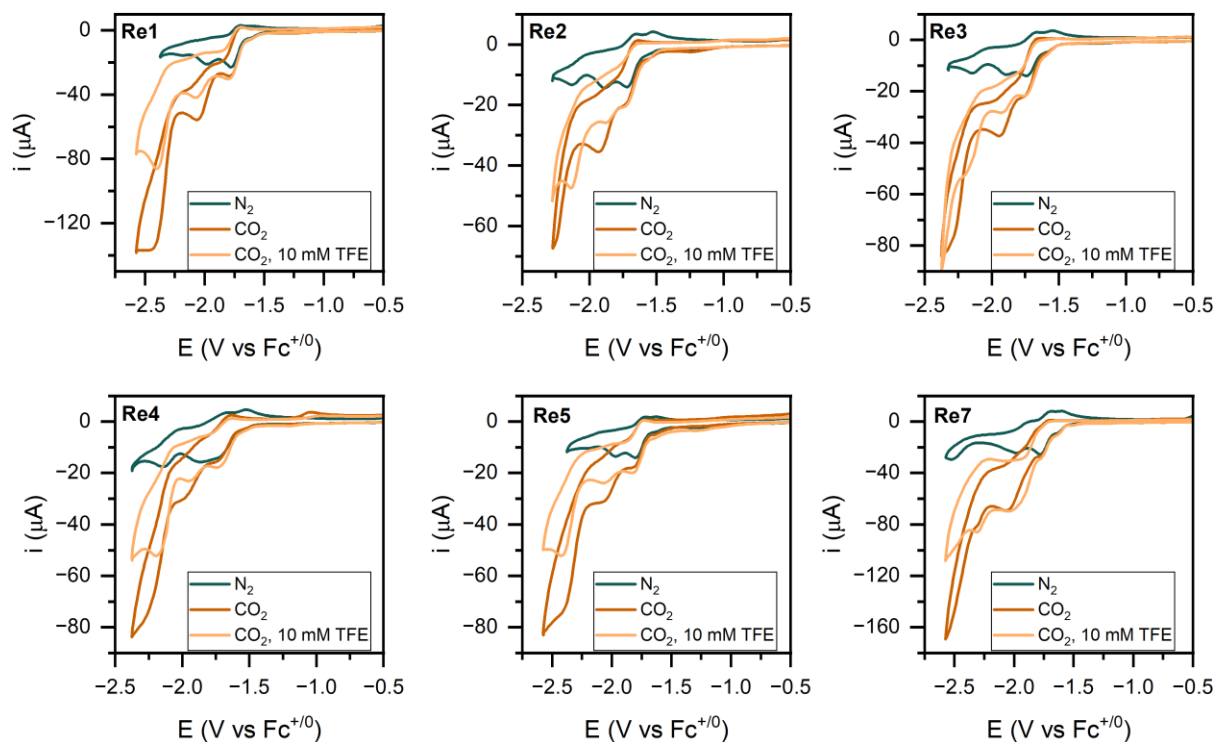


Figure S29: Catalytic cyclic voltammograms of **Re1-5** and **Re7** recorded in acetonitrile under N_2 and CO_2 in the absence or presence of 10 mM trifluoroethanol (TFE). Voltammograms were recorded at 100 $mV s^{-1}$ using 0.1 M $n-Bu_4NBF_4$ as the supporting electrolyte.

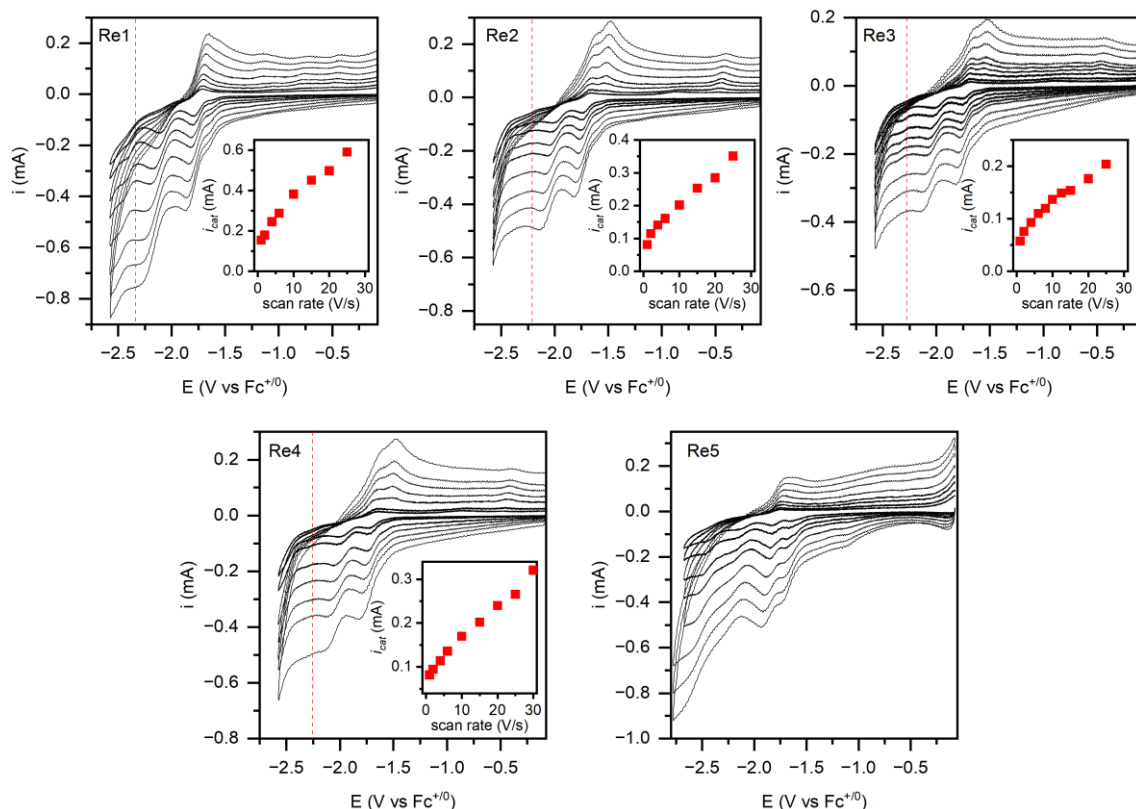


Figure S30: Cyclic voltammograms of **Re1-5** at fast scan rates (25, 20, 15, 12.5, 10, 8, 6, 4, 2, 1 $V s^{-1}$) in CO_2 saturated acetonitrile containing 0.1 M $n-Bu_4NBF_4$ as the supporting electrolyte. The inset figures present the scan rate dependence of the plateau catalytic current (i_{cat}). The corresponding potential is shown by the red dashed line.

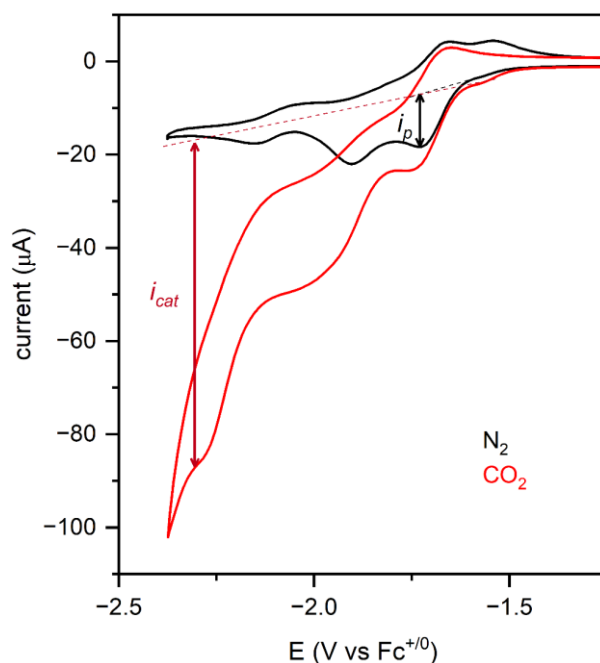


Figure S31: Representative cyclic voltammograms of **Re2** (~ 1 mM) under N_2 and CO_2 saturated acetonitrile to demonstrate the determination of i_{cat} and i_p . Conditions: supporting electrolyte 0.1 M $n-Bu_4NBF_4$, scan rate 100 $mV s^{-1}$.

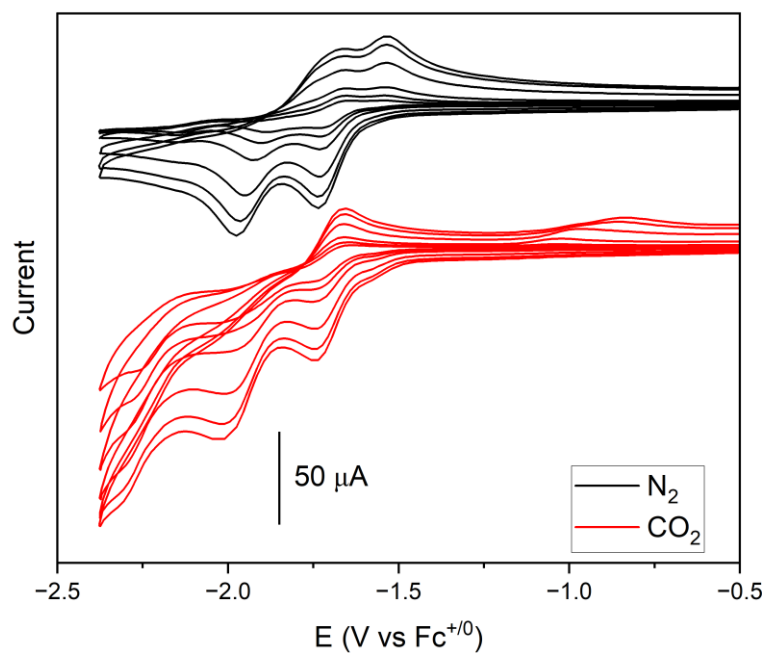


Figure S32: Cyclic voltammograms of **Re2** (~ 1 mM) under N_2 and CO_2 saturated acetonitrile at different scan rates (1, 0.8, 0.5, 0.2, 0.1, 0.05 $V s^{-1}$). Conditions: supporting electrolyte 0.1 M $n-Bu_4NBF_4$.

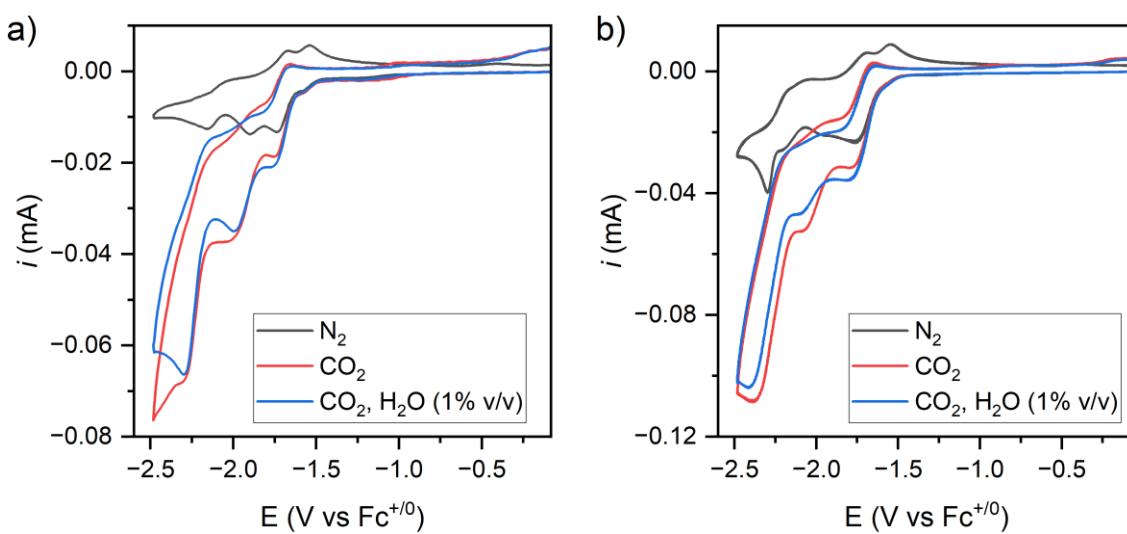


Figure S33: Cyclic voltammograms of (a) **Re3** (0.6 mM) and (b) **Re4** (1 mM) under N_2 and CO_2 in neat acetonitrile and in acetonitrile/water mixture (99:1 v/v), demonstrating minimal effect of water on electrocatalysis. Condition: 0.1 M $n-Bu_4NBF_4$ supporting electrolyte, 0.1 $V s^{-1}$ scan rate.

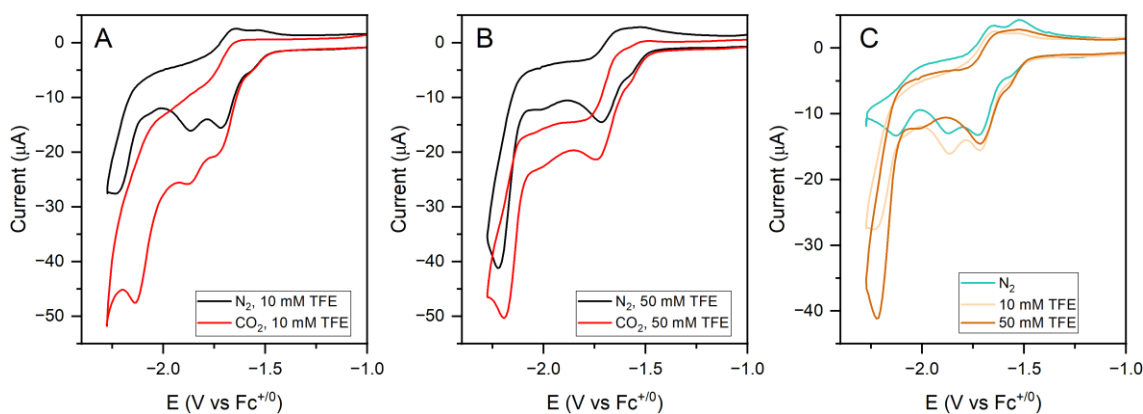


Figure S34: Cyclic voltammograms of **Re2** under N_2 and CO_2 in the presence of varying concentration of TFE. Figure A and B show the voltametric response in the presence of 10 mM and 50 mM TFE, respectively, under N_2 and CO_2 . Figure C shows the difference in response under N_2 without TFE and in the presence of TFE (10 and 50 mM). Condition: 0.1 M $n-Bu_4NBF_4$ supporting electrolyte, $0.1 V s^{-1}$ scan rate.

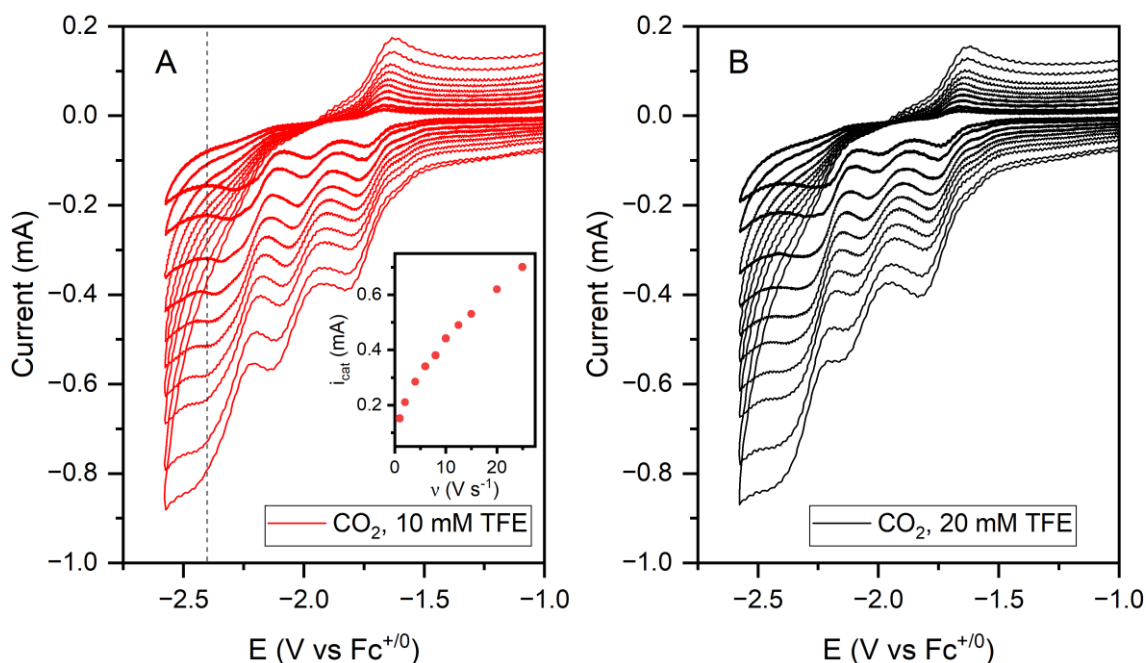


Figure S35: Cyclic voltammograms of **Re2** (~ 0.6 mM) at fast scan rates (25, 20, 15, 12.5, 10, 8, 6, 4, 2, $1 V s^{-1}$) in CO_2 saturated acetonitrile containing (A) 10 mM TFE and (B) 20 mM TFE. 0.1 M $n-Bu_4NBF_4$ was used as the supporting electrolyte. Inset figure (A) shows the dependence of i_{cat} on scan rate.

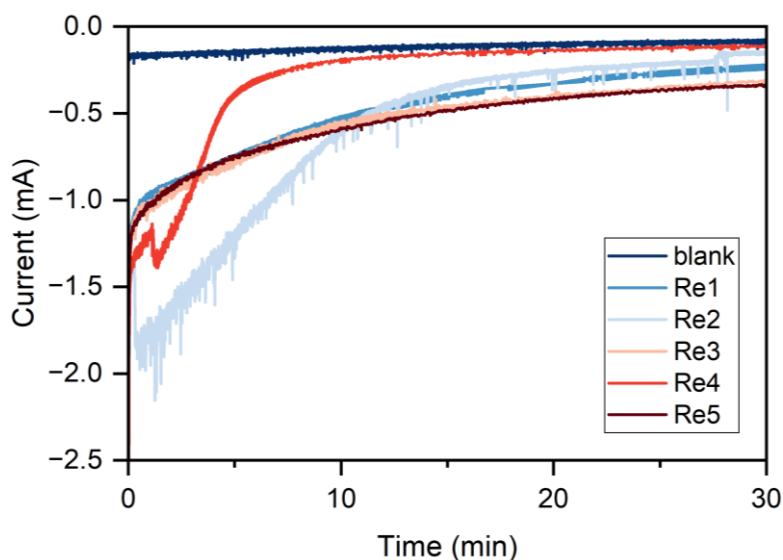


Figure S36: Current versus time plots for controlled potential electrolyses of **Re1-5** in CO_2 saturated 0.5% (v/v) water/acetonitrile mixture $-2.3 \text{ V vs } \text{Fc}^{+/0}$. Blank trace shows current in the absence of any catalyst. Electrolyses were performed using a glassy carbon plate working electrode ($A \sim 2 \text{ cm}^2$) and $0.1 \text{ M } n\text{-Bu}_4\text{NBF}_4$ electrolyte.

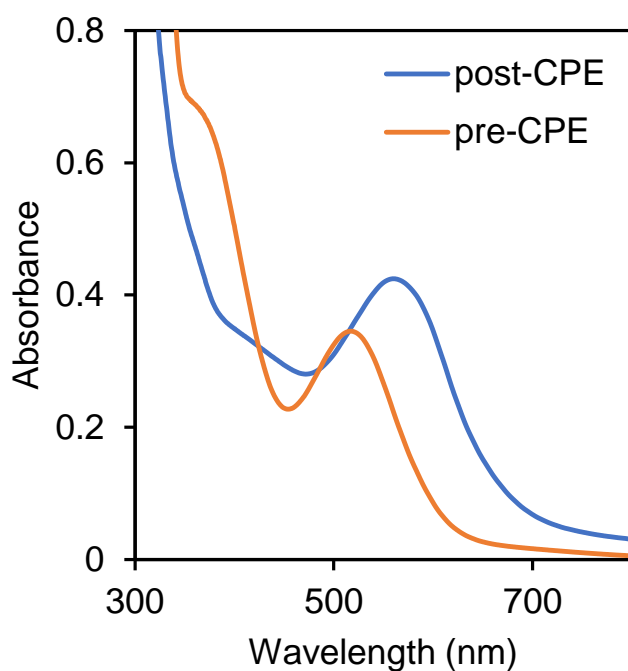


Figure S37: UV-vis spectra of **Re5** before and after 1 h electrolysis in CO_2 saturated 0.5% water/acetonitrile mixture.

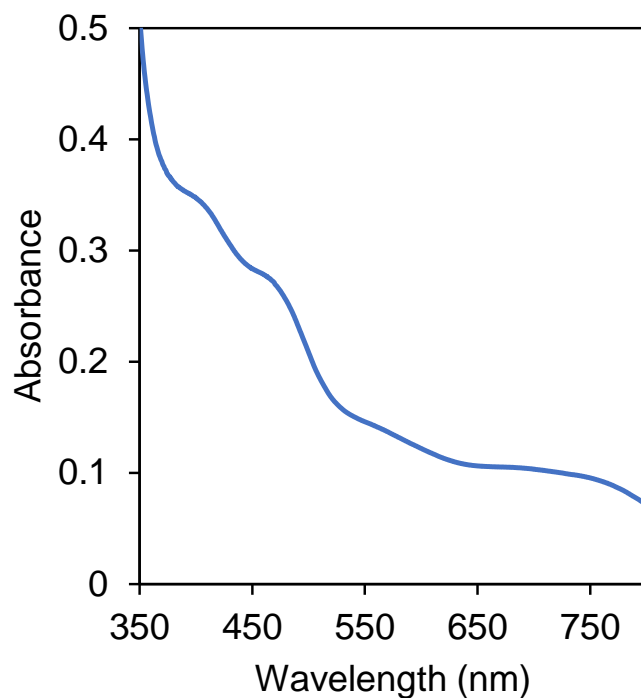


Figure S38: UV-vis spectrum of **Re1** after 1 h electrolysis in CO_2 saturated 0.5% water/acetonitrile mixture. The pre-CPE concentration of **Re1** in the electrolyte (0.1 M Bu_4NBF_4) was 0.25 mM.

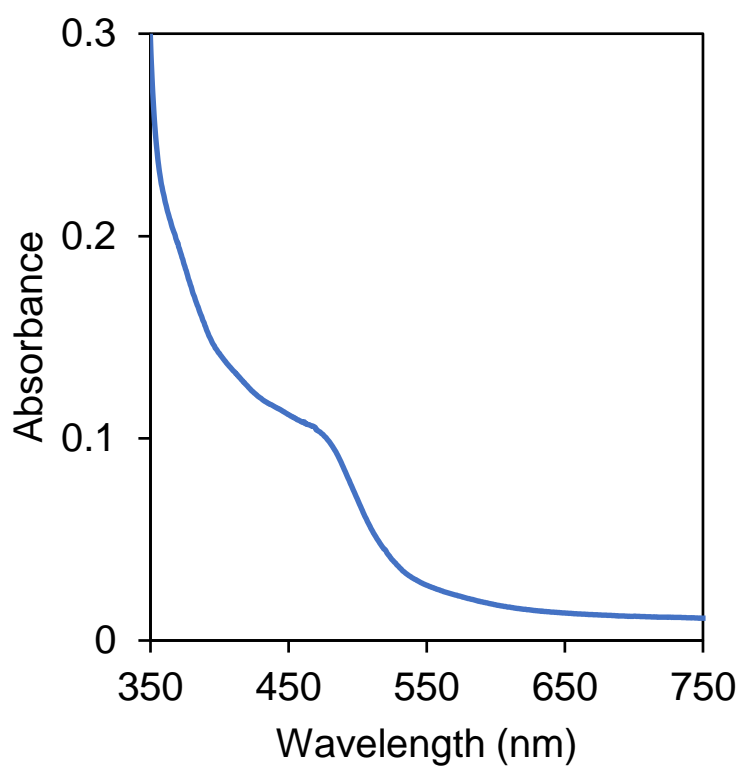


Figure S39: UV-vis spectrum of **Re2** after 1 h electrolysis in CO_2 saturated 0.5% water/acetonitrile mixture. The pre-CPE concentration of **Re2** in the electrolyte (0.1 M Bu_4NBF_4) was 0.25 mM.

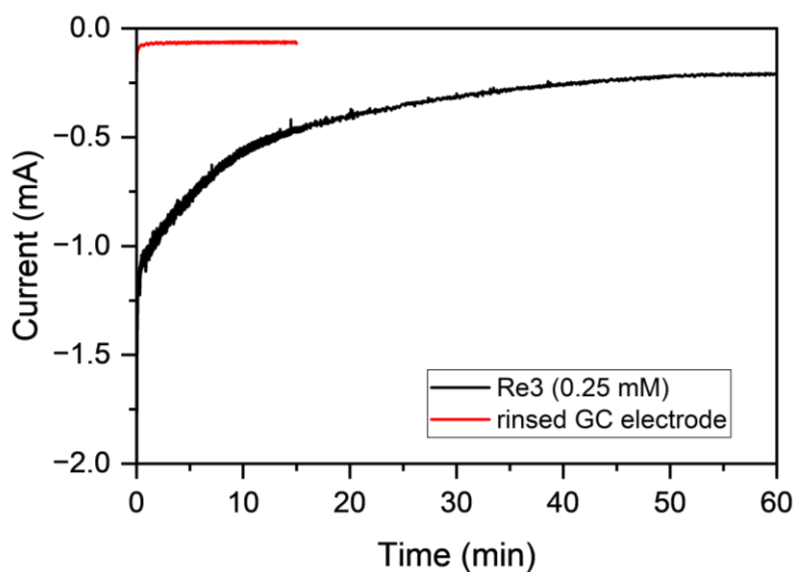


Figure S40: Current vs. time plot for a ‘Rinse test’ to exclude catalytically active deposit formation on electrode. Black trace shows the current vs. time plot for electrolysis of **Re3**. After electrolysis, the glassy carbon working electrode was removed, rinsed with acetonitrile and reused for a 15-min controlled potential electrolysis without any catalyst (red trace). A very low current demonstrates that the catalysis is homogeneous in nature.

References:

- 1 S. A. Moya, R. Pastene, H. Le Bozec, P. J. Baricelli, A. J. Pardey and J. Gimeno, *Inorganica Chim. Acta*, 2001, **312**, 7–14.
- 2 R. Kia and F. Safari, *Inorganica Chim. Acta*, 2016, **453**, 357–368.
- 3 G. R. Fulmer, A. J. M. Miller, N. H. Sherden, H. E. Gottlieb, A. Nudelman, B. M. Stoltz, J. E. Bercaw, and K. I. Goldberg, *Organomet.*, 2010, **29**, 2176–2179.

Cartesian Coordinates

1. L1

$E = -742.316928619992$ au

0 imaginary frequencies

N	2.189845000000	0.125053000000	-0.363231000000
N	-0.289042000000	1.444332000000	-0.391820000000
N	-2.662767000000	0.303166000000	-1.311087000000
C	3.320650000000	-0.508778000000	-0.673542000000
H	3.339100000000	-1.577767000000	-0.485821000000
C	4.436100000000	0.127146000000	-1.206461000000
H	5.327723000000	-0.438846000000	-1.442853000000
C	4.365858000000	1.496480000000	-1.424177000000
H	5.205761000000	2.034981000000	-1.845481000000
C	3.195660000000	2.168464000000	-1.099796000000
H	3.111206000000	3.232424000000	-1.274674000000
C	2.121253000000	1.448379000000	-0.569336000000
C	0.842396000000	2.133532000000	-0.215100000000
C	-1.460564000000	2.011473000000	-0.086846000000
C	-2.691737000000	1.196507000000	-0.311804000000
C	-3.749520000000	-0.434006000000	-1.538451000000
C	-1.542377000000	3.314542000000	0.413506000000
C	0.843401000000	3.439254000000	0.283993000000
C	-0.370200000000	4.031068000000	0.599699000000
H	-0.402237000000	5.042010000000	0.986548000000
H	1.771168000000	3.972966000000	0.437149000000
H	-2.500204000000	3.763970000000	0.635444000000
C	-4.916678000000	-0.332386000000	-0.790056000000
C	-3.822914000000	1.363219000000	0.493175000000
C	-4.947449000000	0.587388000000	0.249413000000
H	-3.687531000000	-1.140231000000	-2.360537000000
H	-5.769651000000	-0.957973000000	-1.018603000000
H	-3.818822000000	2.074727000000	1.307399000000
H	-5.830346000000	0.697184000000	0.866908000000

2. L2

$E = -973.313988510752$ au

0 imaginary frequencies

N	2.136872000000	0.434943000000	-0.514697000000
N	-0.378926000000	1.607386000000	-0.162857000000
N	-2.828116000000	0.530311000000	-1.013177000000
C	3.260568000000	-0.103674000000	-0.987389000000
H	3.335452000000	-1.185132000000	-0.931150000000
C	4.301787000000	0.642748000000	-1.526760000000
H	5.191717000000	0.151848000000	-1.898464000000
C	4.159537000000	2.022905000000	-1.574284000000
H	4.938840000000	2.646683000000	-1.994360000000

C	2.995855000000	2.595516000000	-1.080371000000
H	2.856391000000	3.667153000000	-1.121917000000
C	1.999877000000	1.767958000000	-0.553507000000
C	0.729956000000	2.338519000000	-0.012434000000
C	-1.533060000000	2.086377000000	0.310967000000
C	-2.750084000000	1.242073000000	0.120177000000
C	-3.905676000000	-0.227922000000	-1.215232000000
C	-1.621296000000	3.321298000000	0.953610000000
C	0.722572000000	3.581894000000	0.620016000000
C	-0.474269000000	4.099213000000	1.118035000000
H	1.640255000000	4.143221000000	0.722228000000
H	-2.575032000000	3.671857000000	1.321655000000
C	-4.954019000000	-0.328665000000	-0.307862000000
C	-3.757135000000	1.199802000000	1.088507000000
C	-4.871181000000	0.401388000000	0.870126000000
H	-3.935427000000	-0.781701000000	-2.148308000000
H	-5.804515000000	-0.962395000000	-0.522690000000
H	-3.662825000000	1.766620000000	2.004792000000
H	-5.658206000000	0.347848000000	1.612201000000
C	-0.524423000000	5.420253000000	1.790486000000
C	-1.635094000000	6.259970000000	1.637119000000
C	0.537061000000	5.858142000000	2.592714000000
C	-1.680338000000	7.500188000000	2.262680000000
C	0.487207000000	7.095591000000	3.223729000000
C	-0.620480000000	7.922300000000	3.059875000000
H	-2.460566000000	5.951354000000	1.008041000000
H	1.399056000000	5.219759000000	2.740543000000
H	-2.543799000000	8.139278000000	2.123044000000
H	1.313942000000	7.412194000000	3.848128000000
H	-0.657231000000	8.887969000000	3.549167000000

3. L3

$E = -1012.617136712920$ au

0 imaginary frequencies

N	2.144839000000	0.444352000000	-0.478228000000
N	-0.382655000000	1.606841000000	-0.162536000000
N	-2.825170000000	0.511465000000	-1.008025000000
C	3.273706000000	-0.095136000000	-0.937743000000
H	3.357622000000	-1.174449000000	-0.857531000000
C	4.309330000000	0.647899000000	-1.492312000000
H	5.203887000000	0.156474000000	-1.852075000000
C	4.155472000000	2.025525000000	-1.570268000000
H	4.930233000000	2.646342000000	-2.003041000000
C	2.986448000000	2.599102000000	-1.090293000000
H	2.837447000000	3.668330000000	-1.155258000000
C	1.996791000000	1.774909000000	-0.546423000000
C	0.721733000000	2.346287000000	-0.017767000000

C	-1.539968000000	2.086799000000	0.303331000000
C	-2.752693000000	1.234654000000	0.118518000000
C	-3.898826000000	-0.253802000000	-1.204553000000
C	-1.635586000000	3.327594000000	0.932876000000
C	0.706197000000	3.597711000000	0.597853000000
C	-0.493585000000	4.115709000000	1.089963000000
H	1.621740000000	4.164025000000	0.691768000000
H	-2.592218000000	3.674574000000	1.296674000000
C	-4.948361000000	-0.350857000000	-0.298147000000
C	-3.761561000000	1.197121000000	1.085189000000
C	-4.871379000000	0.391198000000	0.872741000000
H	-3.924215000000	-0.816713000000	-2.132325000000
H	-5.795246000000	-0.991050000000	-0.508163000000
H	-3.671744000000	1.773887000000	1.995705000000
H	-5.659554000000	0.341144000000	1.613878000000
C	-0.551294000000	5.442291000000	1.747549000000
C	-1.677474000000	6.262750000000	1.623399000000
C	0.521635000000	5.917029000000	2.514583000000
C	-1.726340000000	7.508831000000	2.238040000000
C	0.464024000000	7.158124000000	3.131365000000
C	-0.659894000000	7.981308000000	3.004444000000
H	-2.518960000000	5.938294000000	1.023838000000
H	1.402585000000	5.301513000000	2.648320000000
H	-2.608930000000	8.126163000000	2.114505000000
H	1.305969000000	7.493359000000	3.727168000000
C	-0.707574000000	9.328743000000	3.672129000000
H	-1.660128000000	9.828265000000	3.491414000000
H	-0.571768000000	9.238417000000	4.753284000000
H	0.090805000000	9.979190000000	3.303976000000

4. L4

E = -3546.759084658975 au

0 imaginary frequencies

N	2.138119000000	0.436426000000	-0.508972000000
N	-0.376481000000	1.612040000000	-0.166316000000
N	-2.824321000000	0.525132000000	-1.008137000000
C	3.261594000000	-0.106037000000	-0.977613000000
H	3.335576000000	-1.187185000000	-0.914665000000
C	4.303750000000	0.636274000000	-1.520940000000
H	5.193474000000	0.142339000000	-1.889116000000
C	4.162794000000	2.016210000000	-1.576855000000
H	4.942922000000	2.636700000000	-2.000245000000
C	2.999348000000	2.592923000000	-1.086967000000
H	2.860980000000	3.664456000000	-1.134948000000
C	2.002479000000	1.769287000000	-0.555923000000
C	0.732531000000	2.343399000000	-0.018703000000
C	-1.531091000000	2.091974000000	0.304991000000
C	-2.747652000000	1.246054000000	0.119402000000
C	-3.901765000000	-0.234601000000	-1.205046000000
C	-1.619840000000	3.329413000000	0.942540000000

C	0.725237000000	3.589163000000	0.609377000000
C	-0.472376000000	4.106483000000	1.104749000000
H	1.642847000000	4.150867000000	0.710758000000
H	-2.573405000000	3.681260000000	1.309710000000
C	-4.951120000000	-0.327674000000	-0.297975000000
C	-3.755537000000	1.211770000000	1.087148000000
C	-4.869489000000	0.411837000000	0.874138000000
H	-3.930593000000	-0.796172000000	-2.133458000000
H	-5.801493000000	-0.962992000000	-0.508508000000
H	-3.662099000000	1.785783000000	1.999009000000
H	-5.657259000000	0.364511000000	1.615842000000
C	-0.524689000000	5.426140000000	1.778214000000
C	-1.635796000000	6.264125000000	1.628563000000
C	0.532013000000	5.864555000000	2.584421000000
C	-1.695973000000	7.499850000000	2.260052000000
C	0.482973000000	7.094629000000	3.228244000000
C	-0.634115000000	7.900815000000	3.058831000000
H	-2.461416000000	5.963252000000	0.996572000000
H	1.399025000000	5.233903000000	2.733400000000
H	-2.560335000000	8.135266000000	2.122406000000
H	1.305331000000	7.409590000000	3.856178000000
Br	-0.710778000000	9.599376000000	3.944836000000

5. L5

$E = -2391.766938733877$ au

0 imaginary frequencies

N	2.138271000000	0.444137000000	-0.709081000000
N	-0.393384000000	1.599335000000	-0.374721000000
N	-2.836872000000	0.567435000000	-1.303494000000
C	3.274154000000	-0.074086000000	-1.175992000000
H	3.355714000000	-1.156173000000	-1.148532000000
C	4.319989000000	0.693429000000	-1.675146000000
H	5.220034000000	0.218852000000	-2.043649000000
C	4.168988000000	2.073520000000	-1.687967000000
H	4.951714000000	2.713099000000	-2.076881000000
C	2.992643000000	2.624723000000	-1.200227000000
H	2.844733000000	3.695889000000	-1.214543000000
C	1.993096000000	1.776813000000	-0.713589000000
C	0.711219000000	2.327502000000	-0.179376000000
C	-1.554177000000	2.065375000000	0.099723000000
C	-2.770113000000	1.231649000000	-0.140939000000
C	-3.913098000000	-0.180441000000	-1.547882000000
C	-1.653989000000	3.276337000000	0.781714000000
C	0.694189000000	3.546779000000	0.496189000000
C	-0.510784000000	4.052696000000	0.990346000000
H	1.616848000000	4.086253000000	0.652041000000
H	-2.619228000000	3.618899000000	1.125400000000
C	-4.971327000000	-0.316568000000	-0.656995000000
C	-3.788288000000	1.151653000000	0.813577000000

C	-4.900833000000	0.364898000000	0.550685000000
H	-3.933525000000	-0.695287000000	-2.503265000000
H	-5.819972000000	-0.939977000000	-0.906610000000
H	-3.701879000000	1.681297000000	1.752700000000
H	-5.696445000000	0.282331000000	1.280857000000
Fe	-1.041702000000	7.201111000000	0.916372000000
C	0.517729000000	6.249921000000	1.905807000000
C	-0.342106000000	7.928813000000	-0.906066000000
C	-0.566773000000	5.330355000000	1.713230000000
C	0.049553000000	7.339416000000	2.686346000000
C	-0.838717000000	9.000815000000	-0.109983000000
C	-1.411183000000	7.014440000000	-1.125939000000
C	-1.710256000000	5.888016000000	2.377623000000
C	-1.325832000000	7.115876000000	2.978012000000
C	-2.213552000000	8.747402000000	0.162164000000
C	-2.567621000000	7.518268000000	-0.465293000000
H	1.518347000000	6.143117000000	1.518848000000
H	0.669868000000	7.820063000000	-1.264020000000
H	0.630601000000	8.198526000000	2.983540000000
H	-0.268183000000	9.846068000000	0.242660000000
H	-1.349788000000	6.088099000000	-1.675971000000
H	-2.695722000000	5.452766000000	2.418743000000
H	-1.971676000000	7.773832000000	3.538340000000
H	-2.866151000000	9.367211000000	0.757230000000
H	-3.536301000000	7.044243000000	-0.431991000000

6. Rel

$E = -3734.835146463211$ au

0 imaginary frequencies

Re	0.274653000000	-0.879752000000	-0.076046000000
Br	0.813799000000	-0.272336000000	2.495956000000
O	-2.385549000000	-2.185616000000	0.786550000000
O	1.433536000000	-3.700067000000	0.310963000000
O	-0.301282000000	-1.591578000000	-3.007923000000
N	2.169979000000	0.138151000000	-0.555618000000
N	-0.227075000000	1.335982000000	-0.239063000000
N	-2.852761000000	0.480544000000	-1.410382000000
C	-1.414477000000	-1.659726000000	0.454208000000
C	0.999103000000	-2.638924000000	0.163904000000
C	-0.092650000000	-1.297773000000	-1.907592000000
C	3.312022000000	-0.508401000000	-0.836072000000
H	3.268001000000	-1.587321000000	-0.844327000000
C	4.496225000000	0.151365000000	-1.107673000000
H	5.387343000000	-0.419411000000	-1.329561000000
C	4.502666000000	1.539443000000	-1.091883000000
H	5.407835000000	2.093183000000	-1.304608000000
C	3.326588000000	2.211694000000	-0.806221000000
H	3.312435000000	3.290510000000	-0.805815000000
C	2.165281000000	1.488023000000	-0.537177000000
C	0.868668000000	2.136993000000	-0.261911000000

C	-1.440029000000	1.908982000000	-0.084022000000
C	-2.689647000000	1.109285000000	-0.240100000000
C	-4.000425000000	-0.163250000000	-1.623805000000
C	-1.578130000000	3.273384000000	0.157935000000
C	0.779755000000	3.509153000000	-0.046300000000
C	-0.455699000000	4.081683000000	0.191401000000
H	-0.543319000000	5.143942000000	0.378321000000
H	1.667293000000	4.122400000000	-0.049713000000
H	-2.566876000000	3.689168000000	0.290600000000
C	-5.031460000000	-0.214542000000	-0.692186000000
C	-3.669435000000	1.118112000000	0.751760000000
C	-4.857800000000	0.438266000000	0.520206000000
H	-4.103637000000	-0.657193000000	-2.584441000000
H	-5.943402000000	-0.751710000000	-0.918037000000
H	-3.498658000000	1.638787000000	1.684725000000
H	-5.633181000000	0.419839000000	1.275936000000

7. Re2

$E = -3965.832843722565$ au

0 imaginary frequencies

Re	0.254279000000	-0.716825000000	-0.341322000000
Br	1.082775000000	-0.642060000000	2.227088000000
O	-2.273687000000	-2.274559000000	0.499850000000
O	1.490448000000	-3.512536000000	-0.660113000000
O	-0.656264000000	-0.852047000000	-3.270981000000
N	2.071939000000	0.443214000000	-0.808184000000
N	-0.277529000000	1.462845000000	0.017525000000
N	-3.001867000000	0.843371000000	-1.058099000000
C	-1.354200000000	-1.651124000000	0.189436000000
C	1.024413000000	-2.461223000000	-0.544039000000
C	-0.319213000000	-0.772481000000	-2.165989000000
C	3.171081000000	-0.090021000000	-1.363311000000
H	3.130892000000	-1.142761000000	-1.601193000000
C	4.306448000000	0.651447000000	-1.632355000000
H	5.164069000000	0.171923000000	-2.083526000000
C	4.306661000000	2.003424000000	-1.317759000000
H	5.172719000000	2.620396000000	-1.518845000000
C	3.173887000000	2.559750000000	-0.748413000000
H	3.154212000000	3.614113000000	-0.519372000000
C	2.061614000000	1.756917000000	-0.496748000000
C	0.802420000000	2.283619000000	0.068237000000
C	-1.466736000000	1.962159000000	0.416295000000
C	-2.723587000000	1.185439000000	0.205662000000
C	-4.161994000000	0.234077000000	-1.303838000000
C	-1.583624000000	3.229517000000	0.973088000000
C	0.733042000000	3.561552000000	0.605272000000
C	-0.469643000000	4.057336000000	1.103714000000
H	1.618521000000	4.176263000000	0.637967000000
H	-2.558512000000	3.559719000000	1.301397000000
C	-5.092720000000	-0.062743000000	-0.314244000000

C	-3.595600000000	0.931049000000	1.263193000000
C	-4.798655000000	0.291357000000	0.995189000000
H	-4.359995000000	-0.024185000000	-2.339021000000
H	-6.020820000000	-0.557094000000	-0.570159000000
H	-3.332690000000	1.222887000000	2.271343000000
H	-5.492728000000	0.073993000000	1.797407000000
C	-0.560146000000	5.399578000000	1.718915000000
C	-1.717995000000	6.176443000000	1.582533000000
C	0.511545000000	5.918201000000	2.457576000000
C	-1.798449000000	7.435755000000	2.163718000000
C	0.424854000000	7.173591000000	3.046104000000
C	-0.728915000000	7.938187000000	2.899294000000
H	-2.552905000000	5.806388000000	1.001091000000
H	1.409226000000	5.328269000000	2.593481000000
H	-2.697307000000	8.026935000000	2.038282000000
H	1.258898000000	7.552719000000	3.623954000000
H	-0.794225000000	8.918429000000	3.355395000000

8. Re3

E = -4005.136265536305 au

0 imaginary frequencies

Re	0.254032000000	-0.712366000000	-0.333985000000
Br	1.074575000000	-0.624302000000	2.237161000000
O	-2.279174000000	-2.263251000000	0.503684000000
O	1.492559000000	-3.509727000000	-0.628718000000
O	-0.643231000000	-0.865467000000	-3.266952000000
N	2.074056000000	0.444578000000	-0.800781000000
N	-0.277967000000	1.469648000000	0.010010000000
N	-3.001230000000	0.843478000000	-1.062074000000
C	-1.357591000000	-1.642147000000	0.194595000000
C	1.024459000000	-2.458285000000	-0.521923000000
C	-0.310845000000	-0.779150000000	-2.160977000000
C	3.175569000000	-0.093099000000	-1.346901000000
H	3.136658000000	-1.147951000000	-1.575375000000
C	4.311686000000	0.646296000000	-1.618131000000
H	5.171420000000	0.162976000000	-2.061097000000
C	4.309841000000	2.001182000000	-1.316206000000
H	5.176201000000	2.616829000000	-1.519919000000
C	3.174700000000	2.562031000000	-0.756090000000
H	3.153600000000	3.618429000000	-0.536964000000
C	2.061969000000	1.760969000000	-0.500707000000
C	0.801293000000	2.291606000000	0.057851000000
C	-1.467058000000	1.971321000000	0.407159000000
C	-2.724272000000	1.194428000000	0.199618000000
C	-4.161563000000	0.233551000000	-1.305108000000
C	-1.583282000000	3.239486000000	0.960922000000
C	0.731679000000	3.572080000000	0.588009000000
C	-0.470283000000	4.070612000000	1.088357000000
H	1.617361000000	4.186505000000	0.614893000000

H	-2.557762000000	3.569232000000	1.290312000000
C	-5.094119000000	-0.055368000000	-0.314908000000
C	-3.598166000000	0.947853000000	1.257572000000
C	-4.801519000000	0.307615000000	0.992416000000
H	-4.358234000000	-0.031980000000	-2.338689000000
H	-6.022316000000	-0.550571000000	-0.568709000000
H	-3.336387000000	1.246060000000	2.264115000000
H	-5.496879000000	0.096585000000	1.795183000000
C	-0.562292000000	5.411111000000	1.702192000000
C	-1.737535000000	6.166571000000	1.621345000000
C	0.525319000000	5.961693000000	2.395494000000
C	-1.819172000000	7.423292000000	2.208173000000
C	0.433435000000	7.212098000000	2.986478000000
C	-0.739585000000	7.970308000000	2.903940000000
H	-2.592245000000	5.784553000000	1.077426000000
H	1.443561000000	5.396895000000	2.497386000000
H	-2.738940000000	7.990113000000	2.120410000000
H	1.286254000000	7.605883000000	3.528183000000
C	-0.824883000000	9.327717000000	3.545464000000
H	-1.815956000000	9.765039000000	3.420403000000
H	-0.610243000000	9.270723000000	4.615973000000
H	-0.093475000000	10.014664000000	3.110426000000

9. Re4

$E = -6539.277625232964$ au

0 imaginary frequencies

Re	0.255110000000	-0.714429000000	-0.336620000000
Br	1.079574000000	-0.624375000000	2.232384000000
O	-2.274909000000	-2.267214000000	0.507410000000
O	1.498322000000	-3.509291000000	-0.633067000000
O	-0.648590000000	-0.868397000000	-3.267703000000
N	2.072659000000	0.444428000000	-0.807479000000
N	-0.278919000000	1.467609000000	0.010128000000
N	-3.001184000000	0.836501000000	-1.060966000000
C	-1.354535000000	-1.645811000000	0.195685000000
C	1.027964000000	-2.459058000000	-0.525766000000
C	-0.313710000000	-0.781979000000	-2.162624000000
C	3.172553000000	-0.090237000000	-1.359540000000
H	3.134352000000	-1.144593000000	-1.590428000000
C	4.306382000000	0.651792000000	-1.633919000000
H	5.164835000000	0.170859000000	-2.081956000000
C	4.304038000000	2.005908000000	-1.328856000000
H	5.168516000000	2.623334000000	-1.535169000000
C	3.170452000000	2.563717000000	-0.762395000000
H	3.148014000000	3.619647000000	-0.540891000000
C	2.060424000000	1.760016000000	-0.504298000000
C	0.801125000000	2.288113000000	0.058983000000
C	-1.468473000000	1.967328000000	0.407262000000
C	-2.724919000000	1.189310000000	0.200237000000

C	-4.160644000000	0.224593000000	-1.303030000000
C	-1.585319000000	3.235679000000	0.962160000000
C	0.732609000000	3.566508000000	0.595256000000
C	-0.470315000000	4.061543000000	1.092848000000
H	1.618469000000	4.180707000000	0.628957000000
H	-2.559870000000	3.566507000000	1.290873000000
C	-5.092489000000	-0.064566000000	-0.312144000000
C	-3.598097000000	0.943196000000	1.258823000000
C	-4.800409000000	0.300549000000	0.994676000000
H	-4.357147000000	-0.042537000000	-2.336212000000
H	-6.019926000000	-0.561613000000	-0.565140000000
H	-3.336571000000	1.243250000000	2.264902000000
H	-5.495277000000	0.089397000000	1.797835000000
C	-0.559664000000	5.401144000000	1.712766000000
C	-1.712647000000	6.183354000000	1.577285000000
C	0.507652000000	5.912888000000	2.460249000000
C	-1.801847000000	7.438008000000	2.165720000000
C	0.428326000000	7.161187000000	3.062626000000
C	-0.728540000000	7.912638000000	2.907472000000
H	-2.548213000000	5.825955000000	0.989487000000
H	1.405901000000	5.325071000000	2.598856000000
H	-2.697256000000	8.031312000000	2.039774000000
H	1.258334000000	7.533091000000	3.647604000000
Br	-0.844089000000	9.636236000000	3.736055000000

10.Re5

$E = -5384.286714240699$ au

0 imaginary frequencies

Re	0.258215000000	-0.742999000000	-0.329794000000
Br	1.045967000000	-0.636532000000	2.251553000000
O	-2.287587000000	-2.284880000000	0.486267000000
O	1.490537000000	-3.547121000000	-0.587500000000
O	-0.590122000000	-0.916129000000	-3.276143000000
N	2.084636000000	0.411677000000	-0.776613000000
N	-0.281107000000	1.439616000000	-0.010738000000
N	-2.990660000000	0.808696000000	-1.112527000000
C	-1.360741000000	-1.668167000000	0.183711000000
C	1.028099000000	-2.491686000000	-0.494507000000
C	-0.277785000000	-0.822278000000	-2.164764000000
C	3.196121000000	-0.129610000000	-1.298714000000
H	3.161585000000	-1.186127000000	-1.520204000000
C	4.336999000000	0.608041000000	-1.553793000000
H	5.205076000000	0.121816000000	-1.976910000000
C	4.329196000000	1.965193000000	-1.261557000000
H	5.199241000000	2.579587000000	-1.453111000000
C	3.183631000000	2.529643000000	-0.727129000000
H	3.158052000000	3.587655000000	-0.516077000000
C	2.066582000000	1.729996000000	-0.485950000000
C	0.796090000000	2.264012000000	0.046746000000

C	-1.474900000000	1.944099000000	0.372892000000
C	-2.729888000000	1.167389000000	0.150648000000
C	-4.147793000000	0.198571000000	-1.367658000000
C	-1.599341000000	3.213405000000	0.918578000000
C	0.721206000000	3.545061000000	0.571781000000
C	-0.487313000000	4.047809000000	1.054951000000
H	1.613034000000	4.147586000000	0.631285000000
H	-2.581784000000	3.550424000000	1.214583000000
C	-5.094459000000	-0.082947000000	-0.388815000000
C	-3.618907000000	0.927899000000	1.197803000000
C	-4.819429000000	0.287715000000	0.920212000000
H	-4.330543000000	-0.073365000000	-2.402155000000
H	-6.019675000000	-0.578683000000	-0.652374000000
H	-3.370496000000	1.231765000000	2.206053000000
H	-5.526077000000	0.082512000000	1.714641000000
Fe	-1.077046000000	7.176431000000	0.767728000000
C	0.488963000000	6.318271000000	1.827879000000
C	-0.372149000000	7.830518000000	-1.080651000000
C	-0.577500000000	5.367488000000	1.679684000000
C	-0.009127000000	7.439277000000	2.539425000000
C	-0.894984000000	8.928651000000	-0.338967000000
C	-1.423074000000	6.888555000000	-1.267995000000
C	-1.740338000000	5.941412000000	2.297702000000
C	-1.383582000000	7.206628000000	2.829621000000
C	-2.267584000000	8.663722000000	-0.068303000000
C	-2.594389000000	7.401340000000	-0.641828000000
H	1.497096000000	6.207783000000	1.462137000000
H	0.645031000000	7.723465000000	-1.424044000000
H	0.551884000000	8.325273000000	2.792701000000
H	-0.342249000000	9.797656000000	-0.017070000000
H	-1.340788000000	5.940541000000	-1.777028000000
H	-2.717662000000	5.490140000000	2.356320000000
H	-2.047363000000	7.884287000000	3.343505000000
H	-2.936535000000	9.298283000000	0.492159000000
H	-3.555042000000	6.912367000000	-0.595221000000